

# **Reciprocating Compressor Performance with Nanorefrigerant in a Vapour Compression System**

*Thesis submitted towards the partial fulfillment  
of the requirements for the award of degree of*

**Master of Engineering  
in  
Thermal Engineering**

Submitted By:

**Shailendra Kumar  
Roll No. 801483023**

Under the guidance of

**Mr. Kundan Lal  
Assistant Professor, MED  
Thapar University, Patiala**



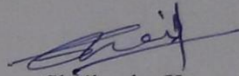
**MECHANICAL ENGINEERING DEPARTMENT  
THAPAR UNIVERSITY, PATIALA – 147004, PUNJAB, INDIA**

**July 2016**


## CERTIFICATE

I hereby declare that the thesis entitled "Reciprocating Compressor Performance with Nanorefrigerant in a Vapour Compression System" is an authentic record of my work carried out as requirements for the award of the degree of Master of Engineering in Thermal Engineering at Thapar University, Patiala under the supervision of Mr. Kundan Lal, Assistant Professor, Mechanical Engineering Department, Thapar University, Patiala during July, 2014 to July, 2016. No part of the matter embodied in this report has been submitted to any other university or institute for the award of any degree.

Date: 15/07/2016

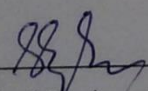
  
Shailendra Kumar

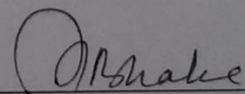
It is certified that the above statement made by the student is correct to the best of my/our knowledge and belief.



Mr. Kundan Lal  
Mechanical Engineering Department  
Thapar University, Patiala – 147004

Countersigned by

  
Head, Mechanical Engineering Department  
Thapar University, Patiala – 147004

  
Dean of Academic Affairs  
Thapar University, Patiala – 147004

## *Dedication*

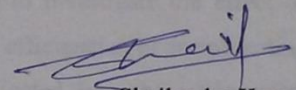
*I dedicate this thesis to my beloved father Ashok Kumar and my mother Asha Devi, who are an ever supporting and encouraging with their great patience. I also dedicate this to my family and to all my dearest friends.*

## ACKNOWLEDGEMENT

I would like to express my deepest gratitude to my supervisor, Mr. Kundan Lal for their excellent guidance, caring, patience, constant encouragement and providing me with an excellent atmosphere for doing research. The opportunity, support, exposure and atmosphere provided by the Thapar University, Patiala, to carry out my studies are highly appreciated.

A special debt of gratitude is owed to the authors whose work I have consulted and quoted in this work. I would also like to thank all my friends who have assisted me at all moments of need. I am forever grateful to my parents and family for their unconditional support and best wishes.

Above all, I express my indebtedness to the "ALMIGHTY" for all his blessing and kindness.



Shailendra Kumar

## ABSTRACT

In the present era, refrigeration systems play a vital role to fulfill the human comfort and industrial needs. In the refrigeration systems main energy consuming devices are compressors. The various researches are being carried out in order to reduce energy consumption and improve the performance of these compressors. In the presented work, an attempt has been made to improve the performance of such system. In this study, an experimental investigation into the performance of a reciprocating compressor using pure refrigerant (R134a) and nanorefrigerant (R134a+Al<sub>2</sub>O<sub>3</sub>) in a vapor compression refrigeration system has been presented. A standard experimental setup was built up and made to function under varying evaporating temperature conditions. The performance of the refrigeration system depends upon the various factors such as; individual component's performance, nature and properties of the refrigerant being used and environmental conditions. The experiments have been conducted to investigate the effect of nanoparticles on the COP of the refrigeration system and various efficiencies of reciprocating compressor. The nanoparticles along with the refrigerant are injected into the refrigeration system for the investigations. Aluminium Oxide (Al<sub>2</sub>O<sub>3</sub>) nanoparticles of 20 nm diameter are used with two different weight fractions (0.4 and 0.8%) in base refrigerant R134a. Experiments have been conducted with three refrigerant volume flow rates (6, 8 and 11 LPH) and four evaporator heat fluxes (at 20 °C, 25 °C, 30 °C and 35 °C). The coefficient of performance (COP) of vapour compression refrigeration system is found to be improved for both weight fractions. At a 0.8 % weight fraction COP is found to be maximum. The results show that while working at high volume flow rates and lower evaporator heat fluxes COP decreases. The adiabatic efficiency of reciprocating compressor is improved by using of nanorefrigerant and the results also show that the adiabatic efficiency of reciprocating compressor is improved by working at higher volume flow rates, higher evaporator heat fluxes and with higher weight fractions of nanoparticles. The electromechanical efficiency of reciprocating compressor is found to be improved for both weight fractions of nanorefrigerant and the results also show that by working at high volume flow rates and higher evaporator heat fluxes reciprocating compressor gives higher values of the electromechanical efficiency. It has been also found that the overall efficiency of reciprocating compressor is improved by using of nanorefrigerant and the results also show that the overall efficiency of reciprocating compressor is improved by working at

higher volume flow rates, higher evaporator heat fluxes and higher weight fractions of nanoparticles. Thus, using aluminium oxide nanoparticles along with refrigerant in refrigeration system is feasible and within the investigated limits it gives a significant improvement in performance of the reciprocating compressor and refrigeration system.

**Keywords:** Aluminum oxide nanoparticles, nanorefrigerant, COP, energy consumption, adiabatic efficiency, electromechanical efficiency, overall efficiency

# CONTENTS

<b>List of Figures</b>	ix
<b>List of Tables</b>	xiii
<b>Nomenclature</b>	xiv
<b>Chapter-1 Introduction</b>	<b>1</b>
1.1 Introduction To Vapor Compression Refrigeration System	1
1.1.1 Refrigerant	1
1.1.2 Nanorefrigerant	2
1.2 Compressor	2
1.2.1 Reciprocating Compressor	2
1.3 Introduction to Nanofluids	3
1.3.1 Properties of Nanofluid	4
1.3.2 Particle Volume Fraction	5
1.3.3 Nanofluids Thermal Conductivity	5
1.3.4 Particle Material	5
1.3.5 Base Fluid	6
1.3.6 Particle Shape	6
1.3.7 Particle Size	6
<b>Chapter-2 Literature Review</b>	<b>7</b>
2.1 Literature Review	7
<b>Chapter-3 Gaps Study and Research Objectives</b>	<b>15</b>
3.1 Gaps Study	15
3.2 Research Objectives	15
<b>Chapter- 4 Experimental Setup And Methodology</b>	<b>17</b>
4.1 Experimental Setup	17
4.2 Components of Setup	18
4.2.1 Refrigeration Compressor	18
4.2.2 Refrigerant Flow Device	19
4.2.3 Condenser	20

4.2.4	Evaporator	22
4.2.5	Heating Element	23
4.2.6	Filter	23
4.2.7	Pressure Gauge	24
4.2.8	Refrigerant	25
4.2.9	Rotameter	26
4.2.10	Voltmeter	26
4.2.11	Ammeter	27
4.2.12	Energy-Meter	27
4.2.13	Digital Temperature Controller	28
4.2.14	Hand Shut Off Valve	29
4.2.15	Temperature Gauge (Digital Panel Meter)	30
4.2.16	Flexible Charging Line	30
4.2.17	Vacuum Compressor	31
4.3	Test Procedure and Methodology	31
4.3.1	Parameters To Be Varied	32
4.3.2	Performance Parameters To Be Studied	32
4.3.3	Methodology	33
4.4	Properties of Base Refrigerant R134a	33
4.5	Properties of Alumina ( $\text{Al}_2\text{O}_3$ ) Nanoparticles	35
4.5.1	XRD And TEM Of $\text{Al}_2\text{O}_3$ Nanoparticles	36
<b>Chapter 5 Results and Discussions</b>		<b>38</b>
5.1	Coefficient of Performance (C.O.P.)	38
5.1.1	C.O.P. Comparison According To Constant Volume Flow	38
5.1.2	C.O.P. Comparison According To Constant Heat Flux	43
5.2	Adiabatic Efficiency	47
5.2.1	Adiabatic Efficiency Comparison According To Constant Volume Flow	48
5.2.2	Adiabatic Efficiency Comparison According To Constant Heat Flux	53
5.3	Electromechanical Efficiency	58

5.3.1	Electromechanical Efficiency Comparison According To Constant Volume Flow	58
5.3.2	Electromechanical Efficiency Comparison According To Constant Heat Flux	63
5.4	Overall Efficiency	68
5.4.1	Overall Efficiency Comparison According To Constant Volume Flow	69
5.4.2	Overall Efficiency Comparison According To Constant Heat Flux	73
<b>Chapter 6 Conclusions and Future Scope</b>		<b>80</b>
6.1	Conclusion	80
6.2	Challenges with Nanofluids	82
6.3	Future Scope	83
<b>REFERENCES</b>		<b>84</b>

## LIST OF FIGURES

<b>Figure No.</b>	<b>Description</b>	<b>Page No.</b>
1.1	Reciprocating Compressor	3
4.1	Experimental Setup	17
4.2	Compressor of the Experimental Setup	19
4.3	Hand Operated Expansion Valve	20
4.4	Finned static condenser	21
4.5	Emersion Coil Type Evaporator	22
4.6	Heating Element	23
4.7	Filter	24
4.8	Pressure Gauge	24
4.9	R134a Refrigerant Can	25
4.10	Rotameter	25
4.11	Voltmeter	27
4.12	Ammeter	27
4.13	Energy meter	28
4.14	Digital Temperature Controller	29
4.15	Relay Switch	29
4.16	Hand Shut off Valve	29
4.17	Digital panel meter	30

4.18	Flexible Charging line	31
4.19	Vacuum Compressor	31
4.20	Molecular structure of R134a	34
4.21	Crystal structure and appearance of nanopowder	36
4.22	XRD and TEM of Al <sub>2</sub> O <sub>3</sub> (20nm) nanoparticles	37
5.1	C.O.P. comparison for at 10 LPH volume flow rate and heat flux at 20-21 <sup>0</sup> C, 25-26 <sup>0</sup> C, 30-31 <sup>0</sup> C and 35-36 <sup>0</sup> C	39
5.2	C.O.P. comparison for at 8 LPH volume flow rate and heat flux at 20-21 <sup>0</sup> C, 25-26 <sup>0</sup> C, 30-31 <sup>0</sup> C and 35-36 <sup>0</sup> C	40
5.3	C.O.P. comparison for at 6 LPH volume flow rate and heat flux at 20-21 <sup>0</sup> C, 25-26 <sup>0</sup> C, 30-31 <sup>0</sup> C and 35-36 <sup>0</sup> C	42
5.4	C.O.P. comparison for heat flux at 20-21 <sup>0</sup> C and volume flow rate 6LPH, 8LPH and 10 LPH	43
5.5	C.O.P. comparison for heat flux at 25-26 <sup>0</sup> C and volume flow rate 6LPH, 8LPH and 10 LPH	44
5.6	C.O.P. comparison for heat flux at 30-31 <sup>0</sup> C and volume flow rate 6LPH, 8LPH and 10 LPH	45
5.7	C.O.P. comparison for heat flux at 35-36 <sup>0</sup> C and volume flow rate 6LPH, 8LPH and 10 LPH	46
5.8	Adiabatic efficiency comparison for at 10 LPH volume flow rate and heat flux at 20-21 <sup>0</sup> C,25-26 <sup>0</sup> C, 30-31 <sup>0</sup> C and 35-36 <sup>0</sup> C	49
5.9	Adiabatic efficiency comparison for at 8 LPH volume flow rate and heat flux at 20-21 <sup>0</sup> C,25-26 <sup>0</sup> C, 30-31 <sup>0</sup> C and 35-36 <sup>0</sup> C	50

5.10	Adiabatic efficiency comparison for at 6 LPH volume flow rate and heat flux at 20-21 <sup>0</sup> C,25-26 <sup>0</sup> C, 30-31 <sup>0</sup> C and 35-36 <sup>0</sup> C	52
5.11	Adiabatic efficiency comparison for heat flux at 20-21 <sup>0</sup> C and volume flow rate 6LPH, 8LPH and 10 LPH	53
5.12	Adiabatic efficiency comparison for heat flux at 25-26 <sup>0</sup> C and volume flow rate 6LPH, 8LPH and 10 LPH	54
5.13	Adiabatic efficiency comparison for heat flux at 30-31 <sup>0</sup> C and volume flow rate 6LPH, 8LPH and 10 LPH	55
5.14	Adiabatic efficiency comparison for heat flux at 35-36 <sup>0</sup> C and volume flow rate 6LPH, 8LPH and 10 LPH	57
5.15	Electromechanical efficiency comparison for at 10 LPH volume flow rate and heat flux at 20-21 <sup>0</sup> C,25-26 <sup>0</sup> C, 30-31 <sup>0</sup> C and 35-36 <sup>0</sup> C	59
5.16	Electromechanical efficiency comparison for at 8 LPH volume flow rate and heat flux at 20-21 <sup>0</sup> C,25-26 <sup>0</sup> C, 30-31 <sup>0</sup> C and 35-36 <sup>0</sup> C	61
5.17	Electromechanical efficiency comparison for at 6 LPH volume flow rate and heat flux at 20-21 <sup>0</sup> C,25-26 <sup>0</sup> C, 30-31 <sup>0</sup> C and 35-36 <sup>0</sup> C	62
5.18	Electromechanical efficiency comparison for heat flux at 20-21 <sup>0</sup> C and volume flow rate 6LPH, 8LPH and 10 LPH	64
5.19	Electromechanical efficiency comparison for heat flux at 25-26 <sup>0</sup> C and volume flow rate 6LPH, 8LPH and 10 LPH	65
5.20	Electromechanical efficiency comparison for heat flux at 30-31 <sup>0</sup> C and volume flow rate 6LPH, 8LPH and 10 LPH	66
5.21	Electromechanical efficiency comparison for heat flux at 35-36 <sup>0</sup> C and volume flow rate 6LPH, 8LPH and 10 LPH	68
5.22	Overall efficiency comparison for at 10 LPH volume flow rate and heat flux at 20-21 <sup>0</sup> C,25-26 <sup>0</sup> C, 30-31 <sup>0</sup> C and 35-36 <sup>0</sup> C	70

5.23	Overall efficiency comparison for at 8 LPH volume flow rate and heat flux at 20-21 <sup>0</sup> C, 25-26 <sup>0</sup> C, 30-31 <sup>0</sup> C and 35-36 <sup>0</sup> C	71
5.24	Overall efficiency comparison for at 6 LPH volume flow rate and heat flux at 20-21 <sup>0</sup> C, 25-26 <sup>0</sup> C, 30-31 <sup>0</sup> C and 35-36 <sup>0</sup> C	73
5.25	Overall efficiency comparison for heat flux at 20-21 <sup>0</sup> C and volume flow rate 6LPH, 8LPH and 10 LPH	74
5.26	Overall efficiency comparison for heat flux at 25-26 <sup>0</sup> C and volume flow rate 6LPH, 8LPH and 10 LPH	75
5.27	Overall efficiency comparison for heat flux at 30-31 <sup>0</sup> C and volume flow rate 6LPH, 8LPH and 10 LPH	77
5.28	Overall efficiency comparison for heat flux at 35-36 <sup>0</sup> C and volume flow rate 6LPH, 8LPH and 10 LPH	78

## LIST OF TABLES

Figure No.	Description	Page No.
4.1	Components of Experimental Setup	18
4.2	Compressor Specifications	19
4.3	Condenser Specifications	21
4.4	Evaporator Specifications	22
4.5	Heater Specifications	23
4.6	Pressure gauge Specifications	24
4.7	Refrigerant Specifications	25
4.8	Voltage Specifications	26
4.9	Ammeter Specifications	27
4.10	Energy-meter Specifications	28
4.11	Digital Temperature Controller Specifications	29
4.12	Thermophysical properties of R134a	34
4.13	Chemical properties of $Al_2O_3$	35
4.14	Thermophysical properties of $Al_2O_3$	35

## NOMENCLATURE

COP	Coefficient of performance
Nm	Nanometer
CNT	Carbon nanotubes
LPH	Litre per hour
SEM	Scanning Electron Microscope
KW	Kilowatt
EG	Ethylene Glycol
POE	Polyesters
Psi	Pound square inch
Ppm	Parts per million
amp	Ampere
V	Volts
Kg	Kilogram
CC	Centimeter cube
PAG	Polyalkylene glycol
Hz	Frequency
Cp	Specific heat
K	Temperature in Kelvin
km/hr	Kilometer per hour
kWh	Kilowatt hour energy consumed
Kw	Power consumption
m <sup>3</sup> /kg	Specific volume
kg/m <sup>3</sup>	Density
wt%	Concentration by weight
vol%	Concentration by volume
$\eta_{\text{eleme}}$	Electromechanical Efficiency
$\eta_o$	Overall Efficiency
$T_{\text{dis(ideal)}}$	Ideal compressor discharge temperature
$T_{\text{dis(actual)}}$	Actual compressor discharge temperature

$T_{suc(actual)}$	Ideal compressor suction temperature
$c_{p(ideal)}$	Ideal isobaric specific heat capacity
$c_{p(actual)}$	Actual isobaric specific heat capacity
$c_{p(ideal)}$ (R134a)	Ideal isobaric specific heat capacity of R134a
$c_{p(Al_2O_3)}$	Isobaric specific heat capacity of $Al_2O_3$
$c_{p(ideal)}$ (nano+ref)	Isobaric specific heat capacity of R134 + $Al_2O_3$
$\varphi_{R134a}$	Mass fraction of R134a
$\varphi_{Al_2O_3}$	Mass fraction of $Al_2O_3$
$h_2$	Specific Enthalpy at compressor discharge
$h_1$	Specific Enthalpy at compressor suction
$W_{ele}$	Power consume by compressor
$\dot{m}_2$	Mass flow rate at compressor discharge
$\dot{m}_1$	Mass flow rate at compressor suction
$\dot{m}$	Mass flow rate
$\dot{v}$	Volume flow rate
$P$	Density
$\rho_{(R134a)}$	Density of R134a
$\rho_{(Al_2O_3)}$	Density of $Al_2O_3$
$\eta_{adia}$	Adiabatic Efficiency
$P_{dis(actual)}$	Compressor discharge pressure
$P_{suc(actual)}$	Compressor discharge pressure
$R$	Characteristics Gas constant

# Chapter-1

## Introduction

---

### 1.1 Introduction to Vapor Compression Refrigeration System

Demand for the refrigeration and air conditioning is increasing day by day. In industry as well as in the homes there is need for the comfort environment for human as well as for manmade systems. This can be achieved by the refrigeration and air conditioning. Vapor compression refrigeration is the system among all most used for this purpose. In this system, refrigerant is used as the working fluid which is the crucial part of the system. Its working involves four main processes i.e. compression, condensation, throttling and evaporation. The low pressure and low temperature vapor refrigerant enters into the compressor through inlet valve and discharges to high pressure and high temperature refrigerant. Then it enters into the condenser in which phase change of refrigerant occurs at constant pressure and temperature, where it rejects heat to the environment, now the refrigerant is throttled through throttle valve in which refrigerant temperature becomes low and it enters into evaporator through which it absorbs heat and the cycle continues. The main measuring parameter to check the performance of the system is COP which is defined as the ratio of cooling effect produced and work input.

#### 1.1.1 Refrigerant

Refrigerant is the fluid which is used in refrigeration and air conditioning systems for heat transfer purposes. The performance of the system mainly depends upon the properties of the refrigerant. There are different types of refrigerants available like HFC, HC, azeotropes etc. HFC refrigerants are mostly used due to their high performance characteristics. In automobile air conditioners and domestic refrigerator application HFC134a (1,1,1,2-Tetrafluoroethane ) is the most widely accepted as alternative refrigerant. The HFC 134a (R134a) have a little high greenhouse warming potential (GWP) compare to other refrigerant, in many countries R134a has been used as a long-run alternative refrigerant.

### **1.1.2 Nanorefrigerant**

Recently in order to improve the heat transfer characteristics of refrigerant some studies on the nanoparticles in refrigeration systems have been conducted. The nanoparticles used with refrigerant as a fluid are called nanorefrigerants. There is scope of using nanoparticles in the vapor compression refrigeration cycle. The nanoparticles can be either mixed with refrigerant or it can also be used as a nanolubricant in which nanoparticles mixed with lubricating oil. The results show that there is improvement in the system with the use of nanotechnology in the refrigeration system. Sheng-shan et al. [2007] investigated the performance of the refrigerator using R134a and POE oil as the base and then compared using R134a and mineral oil with nanoparticles of  $\text{TiO}_2$  which results in reduction in energy consumption. Jwo et al. [2009] studied the mixing of mineral lubricant with  $\text{Al}_2\text{O}_3$  nanoparticles to improve the lubrication and heat-transfer performance. This analysis showed that R-134a and 0.1 wt %  $\text{Al}_2\text{O}_3$  nanoparticles were optimal for better performance. Bi et al. [2011] used a domestic refrigerator with reciprocating compressor for experimental study in which  $\text{TiO}_2$ -R600a nanorefrigerant was used as working fluid. This investigation also showed positive impact on performance.

## **1.2 Compressor**

Compressor is an integral and important part of any refrigeration system. Its main work is to raise the pressure and temperature of the refrigerant across the pipe by giving some pumping power. There are different types of compressors like; reciprocating compressors, rotary screw compressors, centrifugal compressors, scroll compressors and hermetically sealed compressor which are commonly used in refrigeration systems depending upon the requirements.

### **1.2.1 Reciprocating Compressor**

Reciprocating compressors usually compress air but are also used in refrigeration where they compress a superheated vapour. In order to be practical there is a clearance between the piston crown and the top of the cylinder. Air 'trapped' in this clearance volume is never delivered, it expands as the piston moves back and limits the volume of fresh air which can be induced to a value less than the swept volume.

Reciprocating compressors generally, employ piston-cylinder arrangement where displacement of piston in cylinder causes rise in pressure. Reciprocating compressors are capable of giving large pressure ratios but the mass handling capacity is limited or small. Reciprocating compressors may also be single acting compressor or double acting compressor. Single acting compressor has one delivery stroke per revolution while in double acting there are two delivery strokes per revolution of crank shaft.

Reciprocating compressors have been the most widely used for industrial plant air systems. The two major types are single acting and double acting, both of which are available as one or two stage compressors. The Single acting cylinder performs compression on one side of the piston during one direction of the power stroke. Two stage compressions reach the final output pressure in two separate compression cycles, or stages, in series. The double acting compressor is configured to provide a compression stroke as the piston moves in either direction. This is accomplished by mounting a cross head on the crank arm which is then connected to a double acting piston by a piston rod. Distance pieces connect the cylinder to the crankcase. They are sealed to prevent mixing of crank shaft lubricant with the air, but vented so as to prevent pressure built up.

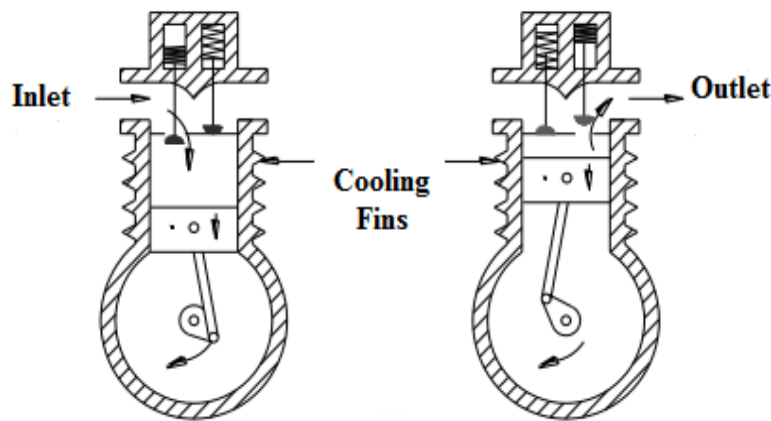


Figure 1.1: Reciprocating Compressor

### 1.3 Introduction to Nanofluids

In cooling as well as heating applications, thermo-physical properties of matter play an important role. It has been observed that the system performance mainly depends on thermal conductivity, viscosity, specific heat and density of gases and liquids which are used in system.

Conventional fluids have poor heat transfer properties and low thermal conductivity which limits its performance. Due to this, there is always a need to develop effective and efficient fluids which are able to meet with high heat transfer rate. Small solid additives usually in micrometer size are good option to enhance the thermal properties of fluids, but it has been found that these small solid additives also possess various problems like particle sedimentation, particle clogging, large pressure drop in the system, corrosion of components, etc. [Maxwell et al., 1873]. Investigations show that scattering of nanoparticles in conventional fluids is a good option and it also reduces the number of other problems because at nanometer the material behaves like colloidal solutions. It is possible to break down the limits of conventional solid particle suspensions by adopting the concept of nanoparticle-fluid suspensions. These nanoparticle-fluid suspensions are termed as nanofluids which is obtained by mixing nanometer sized particles in a base fluid like water, oil etc. In other words solid particles with size less than 100nm suspended in a fluid is known as nanofluid. Nanoparticles such as metallic oxides ( $\text{Al}_2\text{O}_3$ ,  $\text{CuO}$ ,  $\text{SiO}_2$ ), semiconductors ( $\text{TiO}_2$ ,  $\text{SiC}$ ), nitride ceramics ( $\text{AlN}$ ,  $\text{SiN}$ ), carbide ceramics ( $\text{SiC}$ ,  $\text{TiC}$ ), metals ( $\text{Cu}$ ,  $\text{Ag}$ ), single, double or multi walled carbon nanotubes are used. Even at very low concentrations the nanofluid shows a good enhancement in the performance and thermal conductivity [Choi et al., 2001]. With increase in temperature and concentration they show large improvement [Wang et al., 1999].

### **1.3.1 Properties of Nanofluid**

Like Conventional fluids, nanofluids have also number of properties which determine its behavior like particle size, particle shape, material, thermal conductivity etc. and also the stability of particles in base fluid, which is a major concern. The main reason which helps nanoparticles to make stable suspension is their high surface to volume ratio. As the thermal conductivity of nanoparticles is higher than that of base fluids therefore overall thermal conductivity of mixture increased. Due to the very small dimensions, the nanoparticles disperse easily in base fluids and behave like a suspended base fluid molecule, which helps to reduce problems like particle clogging, sedimentation, corrosion etc. Viscosity of nanofluids is also a major concern. If concentration of nanoparticles in base fluid increases beyond certain limit (5 %) then viscosity also increases this limits its performance & suitability for particular application.

### **1.3.2 Particle Volume Fraction**

Particle volume fraction determines the amount of nanoparticles in the base fluid. It plays an important role in the formation of base fluid. It affects the properties like thermal conductivity and viscosity of base fluid. There are many researches that have been performed to see the effect of particle volume fraction on the thermal conductivity and viscosity of nanofluids. For a volume fraction of about 4.3 % of  $\text{Al}_2\text{O}_3$  nanoparticles there is a 32.4 % improvement in thermal conductivity of nanofluid [Masuda et al., 1993]. Xing et al. [2015] analyses the thermal conductivity of nanofluid by mixing it with three different types of CNT at 0.48 % vol. fraction which results in 8.1 %, 16.2 % and 5 % enhancement in thermal conductivity for single walled nanotubes, long walled nanotubes and multi walled nanotubes. Xiaoke et al. [2015] studied the rheological behavior of ethylene glycol (EG) with SiC nanoparticles of 1.0 % vol. in which they found 16.21 % enhancement in thermal conductivity.

### **1.3.3 Nanofluids Thermal Conductivity**

The effect of nanoparticle depends mainly on the basis of improved value of thermal conductivity. There are various theoretical and practical models to explain the rise in the thermal conductivity of nanofluids. But researches are still going on to find the best way to explain the increased value of thermal conductivity. The improved value of thermal conductivity mainly depends upon the concentration of nanoparticles in the base fluid which shows superior results over base fluid. Shape, size, surface area all these factors plays a vital role in the enhancement of thermal conductivity. Higher the surface area caused more enhancements in thermal conductivity. Also phenomenon like boiling and convection are being studied by many researchers to find the coefficient of heat transfer so that improvement can be made.

### **1.3.4 Nano Material**

Another property which decides the thermal conductivity of nanofluids is the particle material like CuO has higher thermal conductivity than  $\text{Al}_2\text{O}_3$  due to the reason Cu is more conducting than Al. Rudyak k. et al. [2014] determines the dependency of particle material on viscosity of nanofluid. He used aluminium and lithium nanoparticles in lithium argon fluid and showed its effect on viscosity. Humnic et al. [2015] also showed that higher thermal conductivity in base

fluid water due to addition of FeC nanoparticles and found out that thermal conductivity and viscosity of nanofluid increases with the weight concentration of nanoparticles.

### **1.3.5 Base Fluids**

It is simply a fluid which can be used for various purposes like heat transfer, lubrication, cooling etc. Maxwell et al. [1873] determines that the less is the thermal conductivity of base fluid, more is the thermal conductivity ratio when nanoparticles will mixed into it. Since ethylene glycol (EG) has less thermal conductivity than water and engine based fluids therefore EG based nanofluids show high thermal conductivity ratio as compared to others and engine oil shows somewhat lower thermal conductivity ratio than ethylene glycol. Compatibility of the nanoparticles with the base fluid is also an important factor, it should carry nanoparticles without sedimentation. Some nanoparticles are not compatible with the base fluid so selection of base fluid and nanoparticles is an important factor for investigation.

### **1.3.6 Particle Shape**

Nanoparticles have different shapes like cylindrical, spherical, rectangular etc. Also the thermal conductivity varies with their shapes. Jeong et al. [2013] investigated ZnO nanofluids with nanoparticles of rectangular and spherical shape. The results show that viscosity and thermal conductivity of rectangular nanoparticles was dominant over spherical nanoparticles. Mare et al. [2015] also found out there is sharp rise in thermal conductivity by using CNT in water. CNT shows higher thermal conductivity due to heat transfer along the tube length but it also creates a menace of high pumping power due to increased value of viscosity.

### **1.3.7 Particle Size**

The Thermophysical properties of the nanofluid also depend upon the particle size of nanoparticles. Thermal conductivity and viscosity of nanofluids are the main properties which vary with the particle size. Smaller size particles have more surface area therefore causes more contact with base fluid and hence improved heat transfer rate. Larger the size of the nanoparticles more is the viscosity.

# Chapter-2

## Literature Review

---

### 2.1 Literature Review

**Gond R.K. et al. (2016)** conducted study on the conventional vapour compression refrigeration system taking different refrigerants as R152a, R290, R600, R13 and R717. The whole investigation was carried out theoretically and the results obtained are compared to the R134a for evaporating temperature ranging from 248K to 283K, the refrigerant R600, R600a, R717 and R152a are found to have more efficiency and COP as compare to R134a. The condensation temperature is set to at 318K. The super heating and sub cooling are set at 10K and 5K respectively. The study carried out suggested that R600 would be a better replacement among other refrigerant.

**Coumaressin T. et al. (2014)** conducted an experiment in which effect of R134a based CuO nanofluid on evaporating heat transfer coefficient was evaluated with the help of CFD heat transfer analysis through FLUENT. The heat flux was varied from 10 to 40 kW/m<sup>2</sup>, particle size (CuO) from 10 to 70 nm and concentration from 0.05 % to 1 %. In this study it was found that by using CuO nanoparticles in combination with R134a evaporating heat transfer coefficient increases upto 0.55 % concentration and then decreases, this trend was followed with all heat fluxes. At 0.55 % concentration heat transfer coefficient of evaporation was found to be highest for all values of heat fluxes.

**Bhaskarn A. et al. (2012)** conducted analysis to study the performance of vapour compression refrigeration system for different refrigerants as HFC152a, HFC32, HC290, HC1270, HC6000a and RE170. The results obtained for these alternative refrigerants are compared with refrigerant R134a. The refrigerants HFC152a, HFC32, HC290, HC1270, HC6000a and R170 found to be more system COP than refrigerant R134a. The results are obtained for evaporating temperature taking in range of -30°C to 10°C and condensation temperature is set to be 50°C. The alternative refrigerant RE170 is found to be a suitable replacement of refrigerant R134a among other

available alternates of refrigerant. The effect of super heating, sub cooling and volumetric refrigeration capacity is also studied for different evaporating temperature.

**Kumar S.P.A. et al. (2012)** carried out the investigation to study the effect of different parameters like evaporating temperature, condensation temperature and mass flow rate of refrigerant on the performance of vapour compression refrigeration system. The study is conducted for different refrigerants as R290, R600A, R290/R600A and R134a. The results show in form of graphically by making mathematical modeling and the effect of various parameters is analyzed on the performance of vapour compression refrigeration system. The refrigeration effect and COP the mixture of selected refrigerants is found to be more than that of R134a.

**Kumar S.D. et al. (2012)** conducted an experimental investigation on domestic refrigerator of refrigerating capacity 125L based on refrigerant R134a. The experimental setup was consist of hermetically sealed compressor, fan cooled condenser, expansion device (capillary tube) and an evaporator section (loaded with water). Service ports were provided at the inlet of expansion device and compressor for charging the refrigerant. The ambient temperature was  $\pm 1.5^{\circ}\text{C}$  and air flow velocity was less than 0.35m/s.  $\text{Al}_2\text{O}_3$  nanoparticles of 40-50 nm in diameter were dispersed in PAG oil (compressor lubricant) and solution stability was achieved by magnetic stirrer and ultrasonic homogenizer. Nanolubricant with 0.2 % concentration was fed to the experimental setup and the tests were conducted under the same conditions. Performance tests were also conducted with charged masses of 150gm., 180 gm. and 200gm. Mixing of  $\text{Al}_2\text{O}_3$  nanoparticles in R134a showed enhancement in the COP of the refrigerator. Use for Nanolubricant reduced capillary tube length and found cost effective. With capillary length of 10.5 m, the maximum COP of around 3.5 was achieved. Moreover system consumed 10.32 % less energy than pure lubricant and R134a combination. Therefore the results showed improvement in heat transfer characteristics with the use of lubricant based nanofluid with  $\text{Al}_2\text{O}_3$ nanoparticles. Thus use of  $\text{Al}_2\text{O}_3$  nanoparticles in refrigerator compressor lubricating oil was found feasible.

**Bi S. et al. (2011)** carried out an experimental study on domestic refrigerator using nanoparticles in the working fluid and reliability and performance of was investigated. Mineral oil was used as lubricant instead of Polyester (POE) and R134a (1,1,1,2-tetrafluoroethane) was taken as refrigerant.  $\text{TiO}_2$  nanoparticles were dispersed in mineral oil. After conducting compatibility

study, the performance of domestic refrigerator with nanolubricat was investigated with the help of energy consumption and freeze capacity tests. In this study it had been found that R134a and nanolubricant (mineral oil+TiO<sub>2</sub> nanoparticles) worked normally in the refrigerator. The performance of refrigeration system was found better than the R134a + POE oil system, with 26.1 % reduction in energy consumption when 0.1 % mass fraction of TiO<sub>2</sub> nanoparticles was dispersed in mineral oil. Nanoparticles also increased the solubility of R134a and mineral oil. Thus use of nanoparticles in domestic refrigerators was found useful to reduce energy consumption.

**Jwo C.S. et al. (2011)** conducted an experimental study on a vapour compression refrigeration system in which refrigerant R-134a and polyester lubricating oil had been replaced with a hydrocarbon refrigerant and mineral oil lubricant. Al<sub>2</sub>O<sub>3</sub> nanoparticles were dispersed in mineral lubricant to improve the heat-transfer characteristics and lubrication properties. In this study 60 gm R-134a and 0.1 wt % Al<sub>2</sub>O<sub>3</sub> nanoparticles were found optimal. With above conditions, there was 2.4 % reduction in power consumption and the coefficient of performance (COP) was increased by 4.4 %.

**Subramani N. et al. (2011)** done experimental study on a test rig consists of a compressor (hermetically sealed), air-cooled condenser (forced convection), thermostatic expansion valve and an evaporator. Evaporator was immersed in water. Al<sub>2</sub>O<sub>3</sub> nanoparticles with average size <50nm were dispersed in lubricating oil (SUNISO 3GS – a mineral oil) by two step method. 0.06 % mass fraction of nanoparticles in the nanoparticle–lubricant mixture and it made stable with an ultrasonic vibrator. Dispersion of Al<sub>2</sub>O<sub>3</sub> nanoparticles found stable for 3 days without coagulation or deposition. R134a was used as refrigerant. Three types of lubricant (filled in hermetic compressor) samples named as pure POE oil, SUNISO 3GS oil (mineral oil) and SUNISO 3GS+ Al<sub>2</sub>O<sub>3</sub> nanoparticles were used in this study.. The condenser pressure was kept at 1.2 MPa and the evaporator pressure was 0.2 MPa. It was observed in this investigation that time required to bring the cooling load temperature from 28oC to 5oC was less in case of mineral oil + Al<sub>2</sub>O<sub>3</sub> as compared to other samples. Mineral oil based nanoparticles sample took about 16.7 % and 28.6 % less time than pure mineral oil and POE oil samples respectively. Freezing capacity also found improved, the time taken to reduce the temperature of the cooling load from 28oC to 1oC with POE oil was 110 minutes and it reduces by 27 % if mineral oil + Al<sub>2</sub>O<sub>3</sub> sample

used. Subcooling was also achieved in condenser with the use of nanolubricant. Power consumption of the compressor was also found to be decreased by 25 % with nanolubricant as compared to POE oil. Moreover the coefficient of performance (COP) of system was also found higher in case of nanolubricant, it was in order of 1.34, 1.6 and 1.78 for pure POE oil, pure mineral oil and mineral oil + Al<sub>2</sub>O<sub>3</sub> respectively.

**Hafez E.A. et al. (2011)** carried out an investigation using CuO nanoparticles in R134a in the vapour compression system. The evaporating coefficient of heat transfer was experimentally evaluated. Test rig consist hermetically sealed compressor of 1 HP, water cooled condenser, expansion device and evaporator (dipped in water). At the condenser inlet a specific amount of oil having the particular amount of CuO nanoparticles were added to refrigerant line. This mixture of refrigerant and nanoparticles (nanorefrigerant) flows through the condenser, expansion device and in evaporator it evaporates with the help of hot water around the evaporator. During the experiment heat flux to evaporator was varied from 10 to 40kW/m<sup>2</sup>. The investigations were carried out using CuO nanoparticles concentrations in order of 0, 0.1, 0.2, 0.3, 0.4, 0.5, 0.55, 0.6, 0.8 and 1 %. Nanoparticles of 15 to 70 nm were used for this study. It was found that the evaporating heat transfer coefficient increases linearly with increase in heat flux (applied to the evaporator) on the logarithmic scale up to 0.55 % CuO nanoparticles concentration and then it found to be decreasing for all heat flux values. Further it was observed that the heat transfer coefficient increases with size of nanoparticles upto 25 nm and beyond which it found to be decreasing with increase in particles size. This trend was followed for all heat flux values.

**Hao P. et al. (2010)** carried out an experimental study to evaluate heat transfer characteristics of refrigerant/oil with dispersed diamond nanoparticles during nucleate pool boiling. In this study R113 was taken as refrigerant, whereas VG68 was used as lubricating oil. Experiment was conducted at saturation pressure of 101.3 kPa. Heat flux had been varied from 10 to 80 kW/m<sup>2</sup>, whereas concentrations of nanoparticles in the oil was varied from 0 to 15 % by weight and nanoparticles + oil dispersion in refrigerant was varied from 0 to 5 % by weight. The results showed that during nucleate pool boiling the heat transfer coefficient of R113 + oil + diamond nanoparticles was found to be greater than R113 + oil mixture by maximum of 63.4 % under the above conditions. The improvement was found increasing with increase in concentration of

nanoparticles in the oil and decreases with the increase in nanoparticles + oil concentrations in refrigerant R113.

**Kedzierski M.A. et al. (2009)** carried out an investigation to study the boiling performance of R134a/ polyesters based nanofluid with CuO nanoparticles of 30 nm diameter. The behavior was studied by boiling the mixtures on a horizontal flat rough surface. 1 % volume fraction of CuO in polyesters lubricant was added and the same was used with R134a at three different mass fractions. Studies concluded that for 0.5 % mass fraction of nanolubricant with R134a heat transfer coefficient improves from 50 % to 275 % compared to heat transfer coefficient for pure R134a/polyolester (99.5/0.5). Whereas less improvement was found with 1 % mass fraction of nanolubricant in R134a, which was around 19 % more than pure R134a/ polyolester (99/1) mixture. Further nanolubricant with 2 % mass fraction resulted heat transfer improvement in order of 12 % as compared to R134a/polyesters (98/2) mixture. Therefore the investigation concluded that the improvement in performance with nanolubricant decreases with increase in nanolubricant concentration in R134a.

**Hao P. et al. (2009)** carried out an investigation to study the heat transfer coefficient of nanorefrigerant during flow boiling through a smooth tube. Following study was conducted with different nanoparticles concentration, heat fluxes, mass flow rates and inlet vapour qualities and the effect of nanoparticles on the heat transfer coefficient was analyzed. Investigation taken refrigerant R113a as base fluid and CuO of 40 nm diameter sizes was used as nanoparticles material. Mass fractions of nanoparticles in refrigerant were taken as 0.1 %, 0.2 % and 0.5 %. An ultrasonic vibration was used to stabilize the nanoparticles suspension in nanofluid. No surfactant was added to mixture as it may affect the heat transfer properties. The maximum enhancement in heat transfer coefficient was found to be 29.7 % during flow boiling.

**Jwo C.S et al. (2009)** had used mineral lubricant with Al<sub>2</sub>O<sub>3</sub> nanoparticles to improve the lubrication and heat-transfer performance. This study showed that R134a + 0.1 wt Al<sub>2</sub>O<sub>3</sub> nanoparticles were optimal for best performance and results in reduced power consumption by about 2.4 %. COP was increased by 4.4 %.

**Bi S. et al. (2007)** have experimented with R134a as refrigerant and a mixture of mineral oil and TiO<sub>2</sub> as the lubricant in a domestic refrigerator. It was found that the refrigeration system with

the above combination works normally and efficiently and also the energy consumption reduces by 21.2 % as compared with R134a/POE oil system.

**Kiliasslan A. et al. (2005)** investigate theoretically by computer simulation performance of refrigerant R718 (water) and compare with synthetic refrigerants R12, R22, R134a, R152a and some of current natural refrigerant R717 and R290. The simulation is develop for the calculation of performance of vapour compression refrigeration system like outlet temperature, COP and pressure ratios of compressor outlet to inlet. The investigation states that the loss of adiabatic efficiency is due to irrevesibilities during compression process. The results shows that by decrease in the pressure ratio the polytropic and adiabatic efficiency is improved, for the evaporator temperature above 20°C the refrigerant R718 gives highest COP at same parameters and as the evaporator temperature is increased the polytropic efficiency, adiabatic efficiency and COP are improved.

**Aprea C. et al. (2003)** investigate the performance of reciprocating compressor with R22 and R407c refrigerant in vapour compression refrigeration system. In this study the phase out problem of R22 is addressed and the irreversibilities of compressor cycle is devoted. The overall performance of energy consumption and transfer of R22 is better than the R407c by 8-14 %. The investigation result shows that the isentropic efficiency and volumetric efficiency of semi-hematic refrigerant compressor is batter with 6-14 % and 3-7 % respectively compare to R407c. This study gives the new approach to design the refrigeration system and find out the performance of compressor.

**Kurtulus O. et al. (2003)** experimentally investigates the operating characteristics and the performance of oil free CO<sub>2</sub> compressor. The test parameters are volumetric efficiency, isentropic efficiency, discharge temperature, power consumption and mass flow rate of compressor. A new approach has been adopted to improve the efficiency of compressor studied by using of hot gas bypass design. In this bypass system the hot gas of condenser is bypassed to the evaporator. The superheating in suction side is improved due to bypass design. The superheating in suction side effects in improvement in overall efficiency maximum 75.66 % and minimum 54.55 % and improvement in volumetric efficiency is maximum 94.53 % and 86.18 %.

**Dutta A.K. et al. (2003)** investigate the performance of different type of compressor with various type of pumping mechanism. The performance is investigated under different topical ambient temperature condition. The compressor uses to study are scroll type, reciprocating type and rotary type at low pressure and high pressure shell. The experimental results states that at high mass flow rate high pressure shell favorable compressor is scroll type. The point of view of adiabatic efficiency reciprocating compressor is better than scroll type and rotary type compressor because of power recovery that is due to re-expansion of gas in the clearance volume. The COP of system is improved at high ambient temperature.

**Grace I. et al. (2002)** experimentally investigate the performance comparison of reciprocating compressor with scroll compressor at different type of loads and refrigerant charge. The refrigerant used is R407a and the operating conditions are different condenser temperature and evaporating temperature. The experiment results show that at the point of view of cooling capacity and COP the scroll compressor gives better results than reciprocating compressor. The scroll compressor produces the lower discharge temperature compare to reciprocating compressor. The scroll compressor consumes more power than reciprocating compressor at the operating condition of overcharging but COP is same for both compressors.

**Cavallini A. et al. (1996)** theoretically analyzed a new approach to estimate the performance of reciprocating compressor. All the important factors and formulas were taken into account in this study. The study gives the formula for the volumetric efficiency and gives good results for both empirical and theoretical approach. This method is used to predict the performance of reciprocating compressor. The accuracy of this method is  $\pm 10\%$  as the results are computed between analytical and experimental values of cooling capacity of same compressor. It is very useful to design the refrigeration system for a design engineer.

**Sauls J. R. et al. (1982)** conducted study to find the performance of positive displacement compressor with fixed volume ratio. The analysis is done with unloaded fully loaded operating conditions. The analysis is done at on basis of power consumption and adiabatic efficiency parameters and compare with other compressor without fixed volume ratio. The analysis state that built in fixed volume ratio affects the operating parameters and the adiabatic efficiency is

improved by increase in pressure ratio. The study show that the losses become more when built in fixed volume ratio is used when it compare with actual performance.

**Pandeya P.N. et al. (1978)** formulated a new approach to find out the compressor performance analysis containing isentropic efficiency, polytropic efficiency, electrical efficiency, mechanical efficiency and give a new terminology to describe the refrigerant compressor as 'efficiency of performance'. The study gives formula for efficiency of performance, the factor affecting it and the effect of efficiency of performance on design performance. The results shows the losses in energy in terms of motor losses, friction losses, compression losses, valve losses, and oil pumping losses. The study states that the performance of the refrigerant compressor is improve by the increase in mass flow rate and deteriorate with increase in energy consumption.

# Chapter-3

## Gaps Study and Research Objectives

---

Literature review shows that research work is being reported on the nanofluid's thermal conductivity, its properties, effect of particle volume fraction, particle material, base fluid, particle size, particle Shape etc. The work has been also done on refrigeration and air conditioning using HFC refrigerant like R134a, R12, and R22 etc. with nanoparticles. Also a limited research work has been reported on the performance of refrigerant compressors by using of nanorefrigerant. Therefore, in this work the investigations are made on the performance of the compressors by using of nanorefrigerant.

### 3.1 Gaps Study

Following are the points which helped me to take my thesis work on performance of reciprocating compressor with nanorefrigerant in a vapour compression system:

- i. A limited work has been reported on effect of thermophysical properties of refrigerant on compressor performance
- ii. A limited work was available on the effect of variation in evaporator heat load and refrigerant mass flow rate on refrigeration system and reciprocating compressor performance
- iii. A very limited literature with experimental data for nanorefrigerant based system

### 3.2 Study Objectives

After an extensive literature survey it has been decided to investigate the performance of reciprocating compressor with  $\text{Al}_2\text{O}_3$  based nanorefrigerant in the vapor compression cycle. Following are the parameters for both compressors with and without nanorefrigerant which are set as thesis's objectives and undertaken for investigation. To determine:

- i. COP of refrigeration system
- ii. Power consumption by the reciprocating compressor
- iii. Refrigeration effect of the refrigerant

- iv. Adiabatic efficiency of reciprocating compressor
- v. Electromechanical efficiency and overall efficiency of reciprocating compressor
- vi. Temperature change across the compressor, temperature gain across the evaporator
- vii. Effect of volumetric concentration of nanoparticles on refrigeration system and reciprocating compressor performance
- viii. Study the performance under varying mass flow rates on refrigeration system and reciprocating compressor performance

## Chapter- 4

# Experimental Setup and Methodology

---

### 4.1 Experimental Setup

This section provides a detailed description of the components and their working for experimentation in this system. The charging and evacuation of nanoparticles also discussed there.



Figure 4.1: Experimental Setup, RAC Lab, MED, TU Patiala

Above figure is the actual vapor compression refrigeration system (domestic) where experimentation of pure hydrocarbon refrigerant along with nanoparticles is performed.

## 4.2 Components of Setup

Table 4.1: Components of Experimental Setup

S. NO.	COMPONENTS	QTY.	SPECIFICATION
1	Compressor	1	165 Litre
2	Expansion Device	1	Manual
3	Condenser	1	Finned Type
4	Evaporator	1	Coil Type
5	Filter	1	With Silica Gel
6	Pressure Gauge	4	R134a Low And High Pressure
7	Heating Element	1	230 W
8	Rotameter	1	2-40 LPH
9	Refrigerant	500gms	R134a
10	Voltmeter	1	0-300 volt
11	Amp Meter	1	0-15 Amp
12	Energy Meter	2	
13	Digital Temperature Controller	1	
14	Hand Shut Valve	4	For 1/4 inch pipe
15	Digital panel meter	1	
16	Flexible Charging Line	1	
17	Vacuum Pump	1	

### 4.2.1 Refrigeration Compressor

Compressor is an integral and important part of any refrigeration system. Its main work is to raise the pressure and temperature of the refrigerant across the pipe by giving some pumping power. There are different types of compressors like; reciprocating compressors, rotary screw

compressors, centrifugal compressors, scroll compressors and hermetically sealed compressor which are commonly used in refrigeration systems depending upon the requirements. In this setup hermetically sealed compressor of 165L capacity has been used. Normally in hermetic and mainly semi-hermetic compressors the compressor and motor driving the compressor are integral part of compressor, and run inside the refrigerant system.



Figure 4.2: Compressor of the Experimental Setup

Table 4.2: Compressor Specifications

<b>Compressor specification</b>	
Manufacturer	Godrej & Boyce Mfg. Co. Ltd.
Model	Power cool comp R134a G1-1+CAPCT
Dimensions	0.201×0.164×0.175 m <sup>3</sup>
Capacity	410 Btu hr
Motor Input	107Watts
EER	3.83 Btu W hr
Displacement	4.6 CC
Voltage Range	150-260 V
Oil Charge	300 CC
Net Weight	7.8 kg

## 4.2.2 Refrigerant Flow Device

An expansion valve is a component in vapour compression refrigeration system which controls the quantity of refrigerant flow into the evaporator. It maintains the required pressure & temperature in the evaporator. There are different types of expansion devices which are commonly used. They are as follows:-

- i. Capillary tube
- ii. Automatic expansion valve
- iii. Thermostatic expansion valve
- iv. Manual expansion valve

In this setup flow control device used is hand operated manual expansion valve to control the flow of refrigerant. The valve needle remains open during steady state operation. The size of the opening or the position of the needle is related to the pressure and temperature of the evaporator where smaller is the opening lower is the pressure and temperature after expansion device.



Figure 4.3: Hand Operated Expansion Valve

## 4.2.3 Condenser

A condenser is a device used to condense a fluid from its gaseous state to its liquid state. In vapor compression refrigeration system condenser is used to condense refrigerant from vapor phase into liquid phase. It rejects heat to the environment and its inlet is outlet of the compressor from which high temperature and pressure refrigerant enters. It rejects heat to the environment

through the surface which is either air cooled or water cooled. The heat rejection capacity of a condenser depends mainly on following factors:

- i. The temperature difference between the refrigerant and the cooling media
- ii. The flow rate of the cooling media through the condenser
- iii. The flow rate of the refrigerant through the condenser

Types of condensers are

- i. Finned-static condenser
- ii. Finned-forced convection condenser
- iii. Wire-static condenser
- iv. Plate-static condenser

In this system finned-static condenser has been used.



Figure 4.4: Finned static condenser

Table 4.3: Condenser Specifications

<b>Condenser Specifications</b>	
Type	Natural Draught
Diameter of Pipe	0.00635 m
Length of Pipe	13.7m
Area of Condenser	0.2732 m <sup>2</sup>
Material of Pipe	Copper

## 4.2.4 Evaporator

The liquid refrigerant enters the evaporator from the refrigerant flow control device is under low pressure and temperature. Evaporator makes contact with the water and the medium from which heat has to be removed. Here liquid refrigerant changes phase to vapor phase. In this set up emersion coil type evaporator is used. Evaporator is dipped in 10.5 litre of water. Water is stirred with help of the agitator to ensure uniform heat transfer. The heat exchange rate within an evaporator is influenced by these factors:

- i. The temperature difference between the refrigerant and the water being cooled
- ii. The flow rate of the water through the evaporator
- iii. The flow rate of the refrigerant through the evaporator

Table 4.4: Evaporator Specifications

Evaporator Specifications	
Type	Emersion Coil Type
Diameter of Pipe	0.00635 m
Length of Pipe	7.62m
Area of Condenser	0.152 m <sup>2</sup>
Material of Pipe	Copper



Figure 4.5: Emersion Coil Type Evaporator

### 4.2.5 Heating Element

A heating element is a component which converts electricity into heat through the process of resistivity or Joule heating. Refrigerant takes the heat from the water present in evaporator which is added by heating element to the water at constant rate in evaporator. It is used to add heating load or to maintain the required flux or temperature in the evaporator. In this setup metal heating element is used.

Table 4.5: Heater Specifications

Heating Element Specification	
Power	230W
Specification	230V,50Hz A/C



Figure 4.6: Heating Element

### 5.2.6 Filter

Impurities present in the vapor compression refrigeration system can damage number of components of the system like compressor and expansion device can damage due to impurities. To obstruct any impurity present in the system and to avoid any kind of choking filter has been used in experimental setup at condenser outlet. Mesh size of filter varies from 5-5000 micrometers. Nanoparticles can pass through this filter easily.



Figure 4.7: Filter

### 4.2.7 Pressure Gauge

It is used to measure pressure of the hydrocarbon Refrigerant at respective points. Four pressure gauges are used in which one gauge is at compressor inlet, and other at outlet, one gauge after expansion device and other after evaporator outlet. Bourdon tube type refrigeration pressure gauges are used to measure the pressure. The bourdon pressure gauge works on the principle that a flattened tube tends to straighten or regain its original form in cross-section when pressurized. In this set up two types of gauges are used high pressure gauge and low pressure gauge.

Table 4.6: Pressure gauge Specifications

Pressure Gauge Specifications	
Low pressure	(-50)-150 Psi
High pressure	0-300 Psi



Figure 4.8: Pressure Gauge

## 4.2.8 Refrigerant

In the experimental setup it has been decided to use R-134a refrigerant, due to reason of its wide commercial use and acceptability. R134a is commonly used refrigerant in domestic refrigerators and cars. Specifications of used refrigerant are listed below.



Figure 4.9: R134a Refrigerant Can

Table 4.7: Refrigerant Specifications

Refrigerant Specifications	
Name	Hydrocarbon Refrigerant
Weight	500gms
Purity	0.999
Gas Content	1.1.1.2-Tetraflouroethane
Charged mass	50 gms

### 4.2.9 Rotameter

A rotameter consists of glass tube, with a float actually a shaped weight which is pushed up by the drag force of the flow and pulled down by gravity. For the flow rate of refrigerant glass tube rotameter has been used. Its position is vertical and its range is 2- 40LPH. The liquid refrigerant coming from the condenser passes through the rotameter and in this way moving element gives reading. The rotameter is manufactured by Zest engineering Delhi.



Figure 4.10: Rotameter

### 4.2.10 Voltmeter

A voltmeter is a device used to calculate electrical potential difference between two points in an electric circuit. Analog voltmeters move a pointer across a scale in proportion to the voltage of the circuit whereas digital voltmeter shows the voltage digitally. It draws only a smallest amount of current to operate.

Table 4.8: Voltage Specifications

<b>Voltage Specifications</b>	
Manufacturer	ESS VEE Electricals
Range	0-300 V



Figure 4.11 Voltmeter

#### 4.2.11 Ammeter

An ammeter is a measuring device used to measure the electric current in an electrical circuit. Electric currents are measured in amperes (A). In this set up digital ammeter has been used.



Figure 4.12 Ammeter

Table 4.9: Ammeter Specifications

Ammeter Specifications	
Manufacturer	Pyrotron
Range	0-15 A
Type	Digital

#### 4.2.12 Energy-meter

An Energy meter is an instrument that measures the amount of electric energy consumed by an electrically powered machine. There are two energy meters used in the system in which one is used to measure the power consumed by the compressor and other to measure the power

consumed by the heater. The unit to measure energy is kilowatt hour (kWh). The energy input for both the devices is used to calculate the coefficient of performance of the system.



Figure 4.13 Energy meter

Table 4.10: Energy-meter Specifications

<b>Energy-meter Specifications</b>	
Manufacturer	Jaipur Metals and Electricals
Range	0-20 KWh
Type	AC, 1 Phase, 2 wire, 50Hz
Rev/KWh	600

### 4.2.13 Digital Temperature Controller

Temperature controller is a device used to measure variation in temperature of space and can be adjusted to achieve a desired temperature. Digital temperature controller is used to cut off the heater supply when the temperature exceeds a particular set value in the evaporator. It is connected to a Relay device which is connected to heating element in which it sends signal to the relay switch which cuts off the supply as well as on the supply of the heating element. There is a sensing element which always dipped in the water in evaporator. With the help of digital temperature controller constant heat flux in the evaporator can be maintained.



Figure 4.14: Digital Temperature Controller

Figure 4.15: Relay Switch

Table 4.11: Digital Temperature Controller Specifications

<b>Digital Temperature Controller Specifications</b>	
Manufacturer	ACR Inst & Valve Pvt. Ltd
Range	(-40 ) °C – 50 °C
Type	Digital

#### 4.2.14 Hand Shut off Valve

A valve is a device that regulates, directs or controls the flow of a fluid by opening, closing or partially obstructing various passageways. Hand shut off valves are used to control the flow in the line. It is also used to divert the flow towards rotameter. Four valves of this type are used in which one valve is fitted at charging line inlet two valves are used at each end of rotameter. If there is need to bypass the flow then parallel valve to the rotameter is opened.



Figure 4.16: Hand Shut off Valve

#### 4.2.15 Temperature Gauge (Digital Panel Meter)

Temperature sensors are used to measure temperature at different points in the vapour compression refrigeration system. The temperature sensors used here is PT100 thermocouples. The temperature sensors are placed at 4 different points, namely, the inlet and outlet of compressor and the inlet and outlet of the expansion valve. The readings from all the temperature sensors are displayed on a digital panel meter. The temperature at the required point can be noted by operating the selector switch present on the digital panel meter.



Figure 4.17: Digital panel meter

#### 4.2.16 Flexible Charging Line

Flexible line is used to charge the refrigerant into the system through compressor charging line. Line is connected to the gas cylinder and then connected to the valve from where refrigerant goes in the vapor compression system.



Figure 4.18: Flexible Charging line

### 4.2.17 Vacuum Compressor

Vacuum compressor is a compressor similar to the compressor used in the vapor compression refrigeration system. It can be used to check for any leakage and is also used to do charging of the system with the air. Also before charging refrigerant the vacuum is produced in the system to remove moisture or any air.



Figure 4.19: Vacuum Compressor

## 4.3 Test Procedure and Methodology

To study the performance of reciprocating compressor with pure refrigerant (R134a) and compared with the nanorefrigerant in which different concentrations of  $\text{Al}_2\text{O}_3$  nanoparticle and with different evaporating temperatures in vapor compression refrigeration system by following test procedure has been adopted.

**Refrigerant** – R134a

**Nanoparticle material** – Aluminum Oxide ( $\text{Al}_2\text{O}_3$ )

**Nanoparticle size** – 20 nm

**4.3.1 Parameters to be Varied** – To investigate the performance of reciprocating compressor following parameters have been varied:-

(i) **Mass fraction of nanoparticles** - The mass fraction of nanoparticles mixed in base refrigerant results a significant effect on compressor performance. So, three different mass fractions have been taken for this study as 0.4 % and 0.8 %/gm of refrigerant.

(ii) **Heat flux** - The performance of the system is greatly influenced by the state or quality of vapours entering the compressor. It directly affects the compressor work e.g. superheated vapours has more enthalpy difference so needs more compressor work. Thus to study this phenomenon the evaporator of the refrigeration system has been placed in water, therefore by heating water (by means of heater) the measured heat flux has been given to evaporator coil and the same will be varied by adjusting temperature of thermal load (water). Temperatures taken are 20-21°C, 25-26°C, 30-31°C and 35-36°C.

(iii) **Volume flow rate** - The refrigerant volume flow rate through the evaporator also affect the energy consumption e.g. increases in volume flow rate, mass flow rate will increases by means of this compressor work require is more . Therefore the volume flow rate has been regulated by using hand operated expansion valve. The volume flow rate has been measured with help of the Rotameter. Flow rates taken (in Litre/hr) – 6 LPH, 8LPH and 10 LPH.

**4.3.2 Performance Parameters to be Studied** – Following parameters to be examined to evaluate their effect on the performance of refrigeration system:-

- i. Coefficient of Performance (COP)
- ii. Temp. at all points, such as across condenser, evaporator, compressor inlet and outlet
- iii. Power consumption by the compressor
- iv. Refrigeration Effect (Power consumption by the heater)
- v. Adiabatic Efficiency of compressor

- vi. Electromechanical Efficiency of compressor
- vii. Overall Efficiency of compressor

**4.3.3 Methodology** – Following points explain the step by step procedure to work on the refrigeration system:-

- i. Firstly at 10LPH and 20-21°C constant heat flux temperature, vacuum has been created with the help of external compressor to withdraw air and moisture from the refrigeration system
- ii. After system evacuation pure refrigerant 50 grams of R134a has been charged into the system and measurement of above performance parameters are measured by varying the different parameters (mentioned above)
- iii. After collecting data at heat flux 25-26°C, 30-31°C and 35-36°C and at volume flow rate 8LPH and 6LPH for pure R134a, the refrigerant is discharged from the system and again system evacuation is done
- iv. Now measured mass fraction of 0.2gm (0.4 %) of Al<sub>2</sub>O<sub>3</sub> nanoparticles along with 50 grams of refrigerant has been charged into the system. Now the same procedure is repeated to collect the data with nanorefrigerant (R134a + Al<sub>2</sub>O<sub>3</sub>)
- v. The mass fraction of Al<sub>2</sub>O<sub>3</sub> nanoparticles in nanorefrigerant has been further increased to 0.4gm (0.8 %) and same procedure has been followed again
- vi. The mass fraction of Al<sub>2</sub>O<sub>3</sub> nanoparticles in nanorefrigerant has been further increased to 0.4gm (0.8 %) and same procedure has been followed again

#### **4.4 Properties of Base Refrigerant R134a**

R134a (1,1,1,2-Tetrafluoroethane) is a halo alkane refrigerant which is having similar thermophysical properties to R12, but the potential of ozone layer depletion is less than R12. Its numerical designation is R134a or Isobutene and chemical formula is CH<sub>2</sub>FCF<sub>3</sub>. R134a is primarily used in domestic refrigerators and automobile air conditioning. It usually stored in light blue colored cylinders.

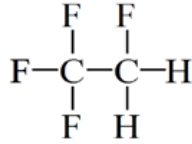


Figure 4.20: Molecular structure of R134a

Table 4.12 - Thermophysical properties of R134a Bi S. at el. [2009]

Property	Description
Molecular weight	102.03 g/mole
Melting point (1.013 bar)	101 °C
Liquid phase	
Liquid density (1.013 bar and 25 °C (77 °F))	1206 kg/m <sup>3</sup>
Boiling point (1.013 bar)	-26.55 °C
Latent heat of vaporization (1.013 bar at boiling point)	215.9 kJ/kg
Vapor pressure (at 20 °C or 68 °F)	5.7 bar
Vapor pressure (at 5 °C or 41 °F)	3.5 bar
Vapor pressure (at 15 °C or 59 °F)	4.9 bar
Vapor pressure (at 50 °C or 122 °F)	13.2 bar
Critical point	
Critical temperature	100.95 °C
Critical pressure	40.6 bar
Critical density	512 kg/m <sup>3</sup>
Triple point temperature	103.3 °C
Gaseous phase	
Gas density (1.013 bar and 15 °C (59 °F))	4.25 kg/m <sup>3</sup>
Compressibility Factor (Z) (1.013 bar and 15 °C (59 °F))	1
Specific gravity	3.25
Specific volume (1.013 bar and 15 °C (59 °F))	0.235 m <sup>3</sup> /kg
Heat capacity at constant pressure (C <sub>p</sub> ) (1.013 bar and 25 °C (77 °F))	0.08754 kJ/(mol.K)
Solubility in water (1.013 bar and 25 °C (77 °F))	0.21 vol/vol

## 4.5 Properties of Alumina (Al<sub>2</sub>O<sub>3</sub>) Nanoparticles

Aluminium is considered as very good conductor of heat with excellent heat transfer properties. Nowadays Aluminum Oxide (Al<sub>2</sub>O<sub>3</sub>) nanopowder is widely used in research work that is going on heat transfer characteristics enhancement. In periodic table Aluminum is found in block P as period 3rd element, while oxygen is a block P, period 2 element. Its properties includes:-

Table 4.13: Chemical properties of Al<sub>2</sub>O<sub>3</sub> Kumar R.R. at el. [2013]

<b>Chemical Data</b>	
Chemical symbol	Al <sub>2</sub> O <sub>3</sub>
Group	Aluminium 13
	Oxygen 16
Electronic configuration	Aluminium [Ne] 3s <sup>2</sup> 3p <sup>1</sup>
	Oxygen [He] 2s <sup>2</sup> 2p <sup>4</sup>

Table 4.14: Thermophysical properties of Al<sub>2</sub>O<sub>3</sub> Kumar R.R. at el. [2013]

<b>Property</b>	<b>Description</b>
Melting Point	2072°C
Boiling Point	2977°C
Colour	Ivory / White
Density	0.26 g/cm <sup>3</sup>
Specific heat	880 J/KgK
Thermal conductivity	30 W/mK
Molecular mass	101.96 g/mol
Specific Surface Area	0.5- 50 m <sup>2</sup> /g
Appearance	White powder
Ph	7-9

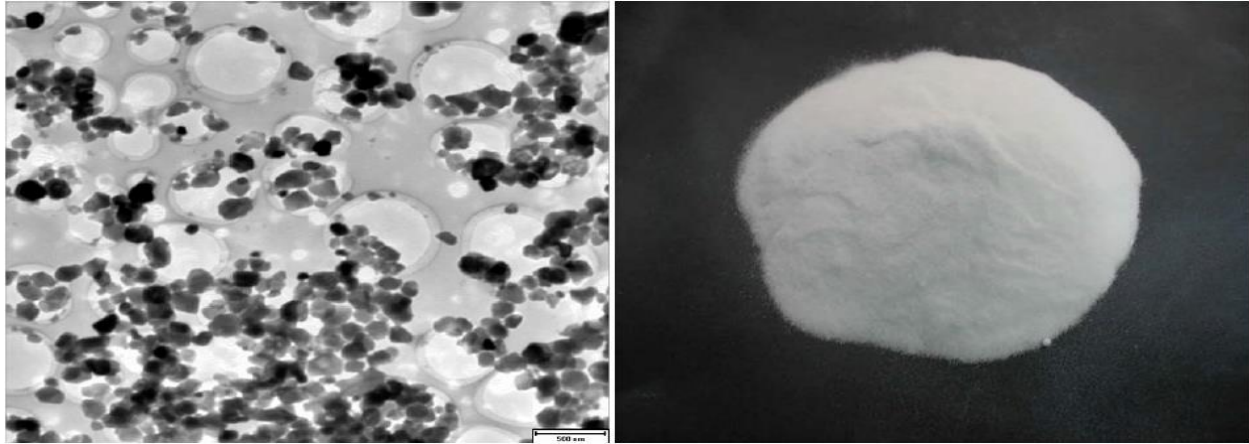


Figure 4.21: Crystal structure and appearance of nanopowder [Hwnag Y. at. el. (2008)]

In addition to these properties, it has also feature like insoluble in water, stable under normal pressure and temperature and it is odorless.

#### 4.5.1 XRD and TEM of $\text{Al}_2\text{O}_3$ nanoparticles

X-ray diffraction (XRD) is a technique used to identify the atomic and molecular structure of a crystal. This method is also known as X-ray crystallography. In this technique incident X-rays beam has been diffracted into many directions by crystalline atoms. After determining the intensities and angles of these beams a 3D picture of density of the crystal has been determined by crystallographer. Transmission electron microscopy (TEM) is a technique to microcopy. In this method beam of electrons is transmitted through the specimen, it interact with specimen as it passes through. Then the image is generated from this interaction of electron. The high resolution image can be generated with help of TEM as compared to SEM or other techniques. The fine details can be achieved by this even as small as single column of atoms. Figure 3.24 shows the XRD and TEM results for used  $\text{Al}_2\text{O}_3$  nanoparticles. As specified the resolution of TEM is 100nm.

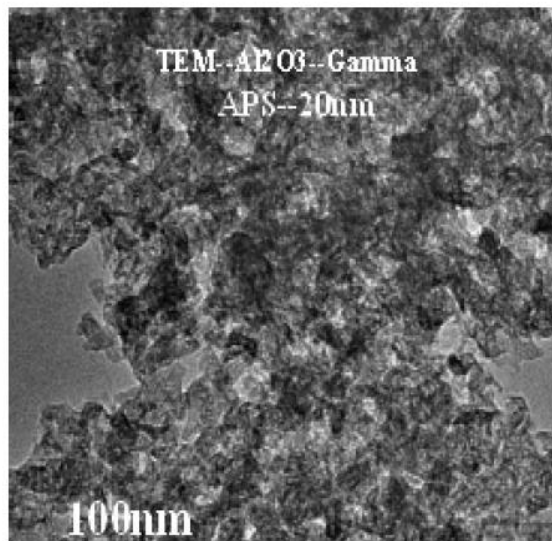
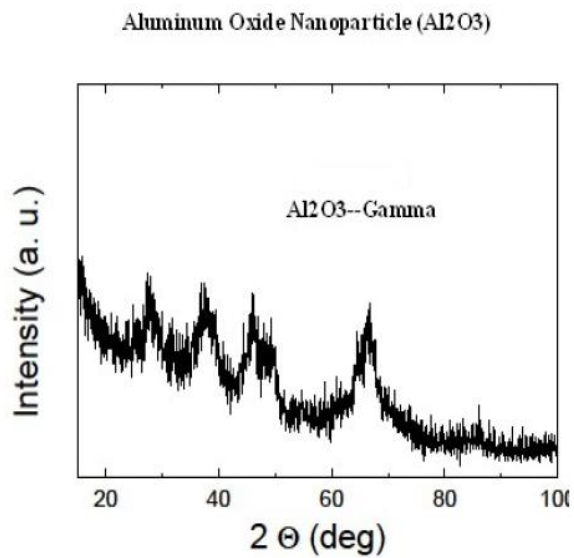


Figure 4.22: XRD and TEM of Al<sub>2</sub>O<sub>3</sub> (20nm) nanoparticles

# Chapter 5

## Results and Discussion

---

### 5.1 Coefficient of Performance (C.O.P.)

C.O.P. is defined as the ratio of refrigeration effect and work supply to the system. In this case, actual refrigeration effect is equal to of power required by heater submerged in water it means heat absorb by the evaporator coil is equal to heat released by heater submerged in water, therefore C.O.P. is the ratio of power required by heater submerged in water and power consumed by the compressor. The actual power required by heater submerged in water and power consumed by the compressor both are measured with the help of Energy meter.

$$\text{C. O. P} = \frac{\text{Refrigeration Effect}}{\text{Power input}} \quad (1)$$

#### 5.1.1 C.O.P. Comparison According to Constant Volume Flow Rate

Firstly the experiment is performed with 10 LPH volume flow rate of refrigerant maintaining constant evaporator load temperature around 20-21°C. As Figure 5.1 shows, the C.O.P. with pure R134a is found to be 0.652 whereas with R134a + 0.4 % Al<sub>2</sub>O<sub>3</sub> and R134a + 0.8 % Al<sub>2</sub>O<sub>3</sub>, COP is 0.668 and 0.687 respectively. Therefore it is found that, by using R134a + 0.4 % Al<sub>2</sub>O<sub>3</sub> nanorefrigerant sample COP is improved by 2.45 % and with R134a + 0.8 % Al<sub>2</sub>O<sub>3</sub> COP is improved by 5.37 % when compared to COP of pure refrigerant R134a.

Similarly readings are taken at heat flux 25-26°C, 30-35°C, and 35-36 °C at same flow rate. The C.O.P at 25-26°C heat flux with pure R134a is calculated to be 0.672 whereas with R134a + 0.4 % Al<sub>2</sub>O<sub>3</sub> and R134a + 0.8 % Al<sub>2</sub>O<sub>3</sub>, COP is 0.681 and 0.703 respectively. Therefore it is found that, by using R134a + 0.4 % Al<sub>2</sub>O<sub>3</sub> nanorefrigerant sample COP is improved by 1.34 % and with R134a + 0.8 % Al<sub>2</sub>O<sub>3</sub> COP is improved by 5.61 % when compared to COP of pure refrigerant R134a.

The C.O.P at 30-31°C heat flux with pure R134a is calculated to be 0.746 whereas with R134a + 0.4 % Al<sub>2</sub>O<sub>3</sub> and R134a + 0.8 % Al<sub>2</sub>O<sub>3</sub>, COP is 0.762 and 0.785 respectively. Therefore it is found that, by using R134a + 0.4 % Al<sub>2</sub>O<sub>3</sub> nanorefrigerant sample COP is improved by 2.14

% and with R134a + 0.8 % Al<sub>2</sub>O<sub>3</sub> COP is improved by 5.22 % when compared to COP of pure refrigerant R134a.

The C.O.P at 35-36°C heat flux with pure R134a is calculated to be 0.865 whereas with R134a + 0.4 % Al<sub>2</sub>O<sub>3</sub> and R134a + 0.8 % Al<sub>2</sub>O<sub>3</sub>, COP is 0.876 and 0.912 respectively. Therefore it is found that, by using R134a + 0.4 % Al<sub>2</sub>O<sub>3</sub> nanorefrigerant sample COP is improved by 1.27 % and with R134a + 0.8 % Al<sub>2</sub>O<sub>3</sub> COP is improved by 5.43 % when compared to COP of pure refrigerant R134a.

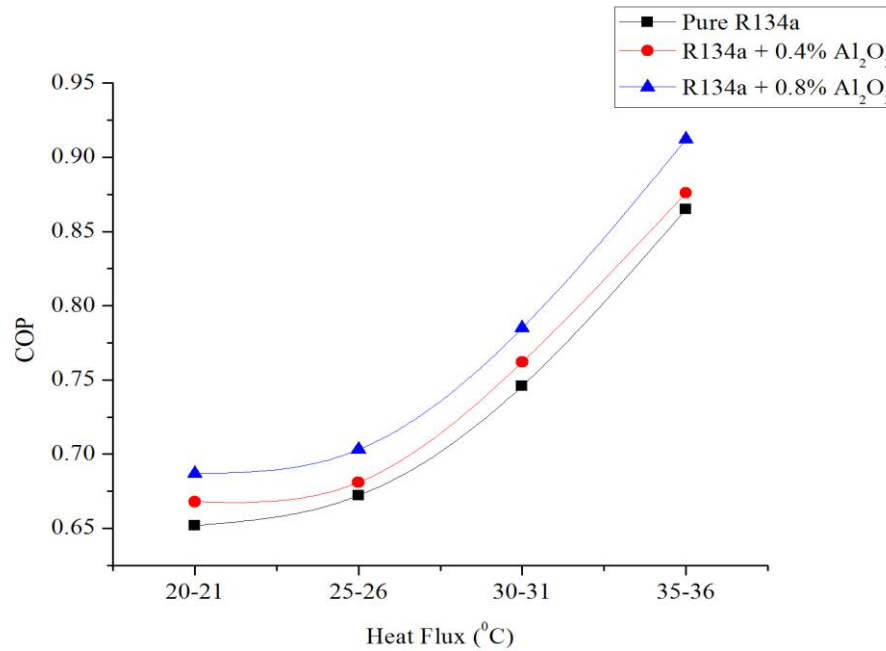


Figure 5.1: C.O.P. comparison for at 10 LPH volume flow rate and heat flux at 20-21°C, 25-26°C, 30-31°C and 35-36°C

After 10 LPH volume flow rate similar experiment is performed with 8 LPH volume flow rate of refrigerant maintaining constant evaporator load temperature around 20-21°C. As Figure 5.2 shows, the C.O.P. with pure R134a is found to be 0.731 whereas with R134a + 0.4 % Al<sub>2</sub>O<sub>3</sub> and R134a + 0.8 % Al<sub>2</sub>O<sub>3</sub>, COP is 0.745 and 0.769 respectively. Therefore it is found that, by using R134a + 0.4 % Al<sub>2</sub>O<sub>3</sub> nanorefrigerant sample COP is improved by 1.92 % and with R134a + 0.8 % Al<sub>2</sub>O<sub>3</sub> COP is improved by 5.20 % when compared to COP of pure refrigerant R134a.

Similarly readings are taken at heat flux 25-26°C, 30-35°C, and 35-36 °C at same flow rate. The C.O.P at 25-26°C heat flux with pure R134a is calculated to be 0.753 whereas with R134a +.4 % Al<sub>2</sub>O<sub>3</sub> and R134a + 0.8 % Al<sub>2</sub>O<sub>3</sub>, COP is 0.767 and 0.782 respectively. Therefore it

is found that, by using R134a + 0.4 % Al<sub>2</sub>O<sub>3</sub> nanorefrigerant sample COP is improved by 1.86 % and with R134a + 0.8 % Al<sub>2</sub>O<sub>3</sub> COP is improved by 3.85 % when compared to COP of pure refrigerant R134a.

The C.O.P at 30-31°C heat flux with pure R134a is calculated to be 0.802 whereas with R134a + 0.4 % Al<sub>2</sub>O<sub>3</sub> and R134a + 0.8 % Al<sub>2</sub>O<sub>3</sub>, COP is 0.815 and 0.845 respectively. Therefore it is found that, by using R134a + 0.4 % Al<sub>2</sub>O<sub>3</sub> nanorefrigerant sample COP is improved by 1.63 % and with R134a + 0.8 % Al<sub>2</sub>O<sub>3</sub> COP is improved by 5.36 % when compared to COP of pure refrigerant R134a.

The C.O.P at 35-36°C heat flux with pure R134a is calculated to be 0.901 whereas with R134a + 0.4 % Al<sub>2</sub>O<sub>3</sub> and R134a + 0.8 % Al<sub>2</sub>O<sub>3</sub>, COP is 0.918 and 0.962 respectively. Therefore it is found that, by using R134a + 0.4 % Al<sub>2</sub>O<sub>3</sub> nanorefrigerant sample COP is improved by 1.88 % and with R134a + 0.8 % Al<sub>2</sub>O<sub>3</sub> COP is improved by 6.77 % when compared to COP of pure refrigerant R134a.

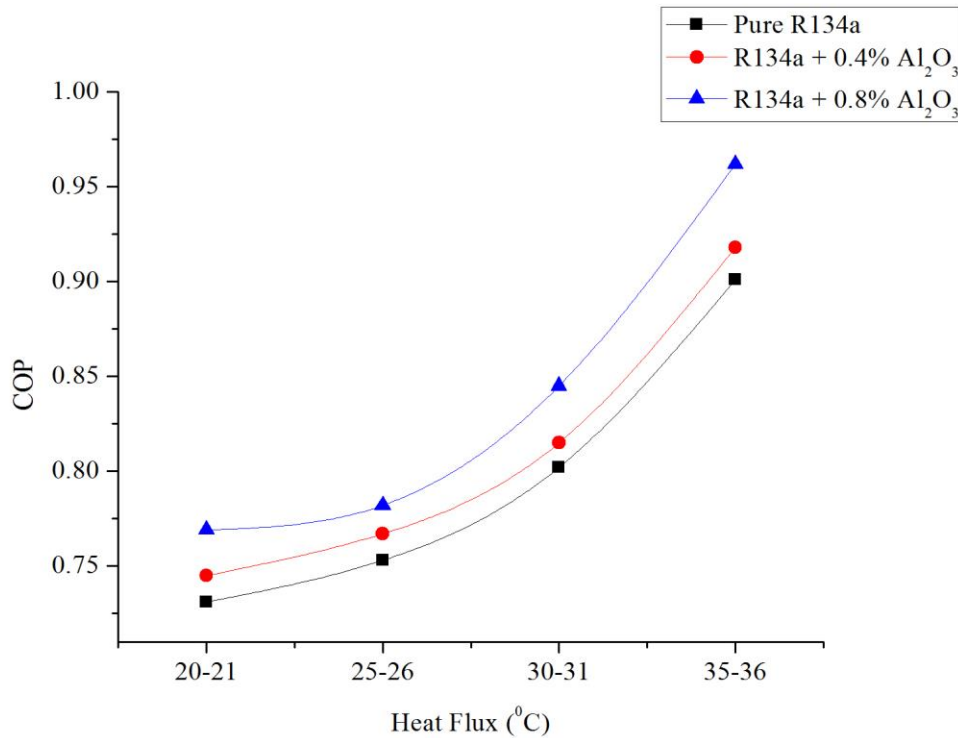


Figure 5.2: C.O.P. comparison for at 8 LPH volume flow rate and heat flux at 20-21°C, 25-26 °C, 30-31°C and 35-36°C

After 8 LPH volume flow rate similar experiment is performed with 6 LPH volume flow rate of refrigerant maintaining constant evaporator load temperature around 20-21°C. As Figure 5.3 shows, the C.O.P. with pure R134a is found to be 0.806 whereas with R134a + 0.4 % Al<sub>2</sub>O<sub>3</sub> and R134a + 0.8 % Al<sub>2</sub>O<sub>3</sub>, COP is 0.819 and 0.838 respectively. Therefore it is found that, by using R134a + 0.4 % Al<sub>2</sub>O<sub>3</sub> nanorefrigerant sample COP is improved by 1.61 % and with R134a + 0.8 % Al<sub>2</sub>O<sub>3</sub> COP is improved by 3.97 % when compared to COP of pure refrigerant R134a.

Similarly readings are taken at heat flux 25-26°C, 30-35°C, and 35-36 °C at same flow rate. The C.O.P at 25-26°C heat flux with pure R134a is calculated to be 0.824 whereas with R134a + 0.4 % Al<sub>2</sub>O<sub>3</sub> and R134a + 0.8 % Al<sub>2</sub>O<sub>3</sub>, COP is 0.841 and 0.873 respectively. Therefore it is found that, by using R134a + 0.4 % Al<sub>2</sub>O<sub>3</sub> nanorefrigerant sample COP is improved by 2.06 % and with R134a + 0.8 % Al<sub>2</sub>O<sub>3</sub> is improved by 5.94 % when compared to COP of pure refrigerant R134a.

The C.O.P at 30-31°C heat flux with pure R134a is calculated to be 0.862 whereas with R134a + 0.4 % Al<sub>2</sub>O<sub>3</sub> and R134a + 0.8 % Al<sub>2</sub>O<sub>3</sub>, COP is 0.879 and 0.896 respectively. Therefore it is found that, by using R134a + 0.4 % Al<sub>2</sub>O<sub>3</sub> nanorefrigerant sample COP is improved by 1.97 % and with R134a + 0.8 % Al<sub>2</sub>O<sub>3</sub> COP is improved by 3.94 % when compared to COP of pure refrigerant R134a.

The C.O.P at 35-36°C heat flux with pure R134a is calculated to be 0.943 whereas with R134a + 0.4 % Al<sub>2</sub>O<sub>3</sub> and R134a + 0.8 % Al<sub>2</sub>O<sub>3</sub>, COP is 0.959 and 0.985 respectively. Therefore it is found that, by using R134a + 0.4 % Al<sub>2</sub>O<sub>3</sub> nanorefrigerant sample COP is improved by 1.67 % and with R134a + 0.8 % Al<sub>2</sub>O<sub>3</sub> COP is improved by 5.45 % when compared to COP of pure refrigerant R134a.

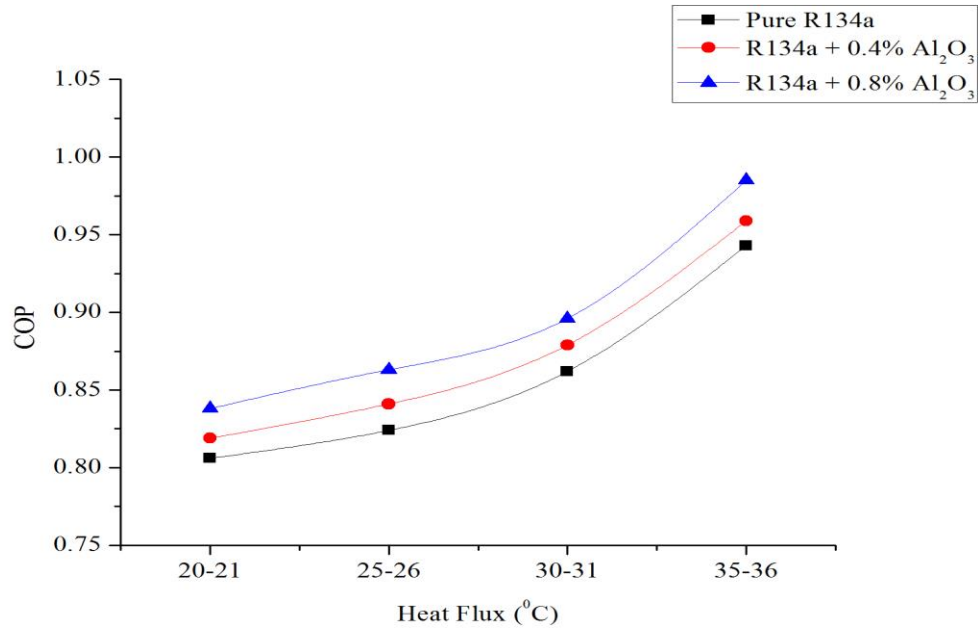


Figure 5.3: C.O.P. comparison for at 6 LPH volume flow rate and heat flux at 20-21<sup>0</sup>C, 25-26 <sup>0</sup>C, 30-31<sup>0</sup>C and 35-36<sup>0</sup>C

As Figure 5.1, Figure 5.2, Figure 5.3 shows that by using nanorefrigerant (R134a + 0.4 % Al<sub>2</sub>O<sub>3</sub> and R134a + 0.8 % Al<sub>2</sub>O<sub>3</sub>) the COP is improved in every case of heat flux (20-21, 25-26, 30-31, 35-36). Experimental results show that by using nanorefrigerant the power consumption is increasing due to increment of pressure ratio between compressor discharge and suction. The isobaric specific heat capacity and density of nanorefrigerant are also increasing this may cause the increment in power consumption. In other hand experimental results show that by using nanorefrigerant refrigeration effect is increasing this is also effect of increment of pressure ratio between compressor discharge and suction. The isobaric specific heat capacity and density of nanorefrigerant are also increasing this may cause the increment in refrigeration effect. But the increment in refrigeration effect is considerably more than the increment in refrigeration effect so, the COP is increasing.

As the heat flux is increases, the evaporator temperature and the evaporator pressure increases but the pressure ratio is decreasing due to this the power consumption is decrease. However, the increase in the evaporator pressure the refrigeration effect is increasing. Above two factors may affect the increment in the COP with increase constant heat flux.

### 5.1.2 C.O.P. Comparison According to Constant Heat Flux

To comparison according to constant heat flux first calculation is done on 20-21<sup>0</sup>C at 6LPH, 8LPH and 10LPH volume flow rate. Firstly Figure 5.4 show that with pure R134a at 6LPH C.O.P. is found to be 0.806 whereas at 8 LPH and 10LPH is 0.731 and 0.652 respectively. Therefore it is calculated that, COP decreases by 9.31 % at 8LPH and at 10LPH COP decreases 19.11 % when compared to COP at 6 LPH.

Similarly calculation is done with R134a + 0.4 % Al<sub>2</sub>O<sub>3</sub> and R134a + 0.8 % Al<sub>2</sub>O<sub>3</sub>at constant heat flux 20-21<sup>0</sup>C. The results shows that with R134a + 0.4 % Al<sub>2</sub>O<sub>3</sub> at 6LPH C.O.P. is found to be 0.819 whereas at 8 LPH and 10LPH is 0.745 and 0.668 respectively. Therefore it is calculated that, COP decreases 9.04 % at 8LPH and at 10LPH COP decreases by 18.44 % when compared to COP at 6 LPH.

Now with R134a + 0.8 % Al<sub>2</sub>O<sub>3</sub> at 6LPH C.O.P. is found to be 0.838 whereas at 8 LPH and 10LPH is 0.769 and 0.687 respectively. Therefore it is calculated that, COP decreases by 8.23 % at 8LPH and at 10LPH COP decreases by 18.02 % when compared to COP at 6 LPH.

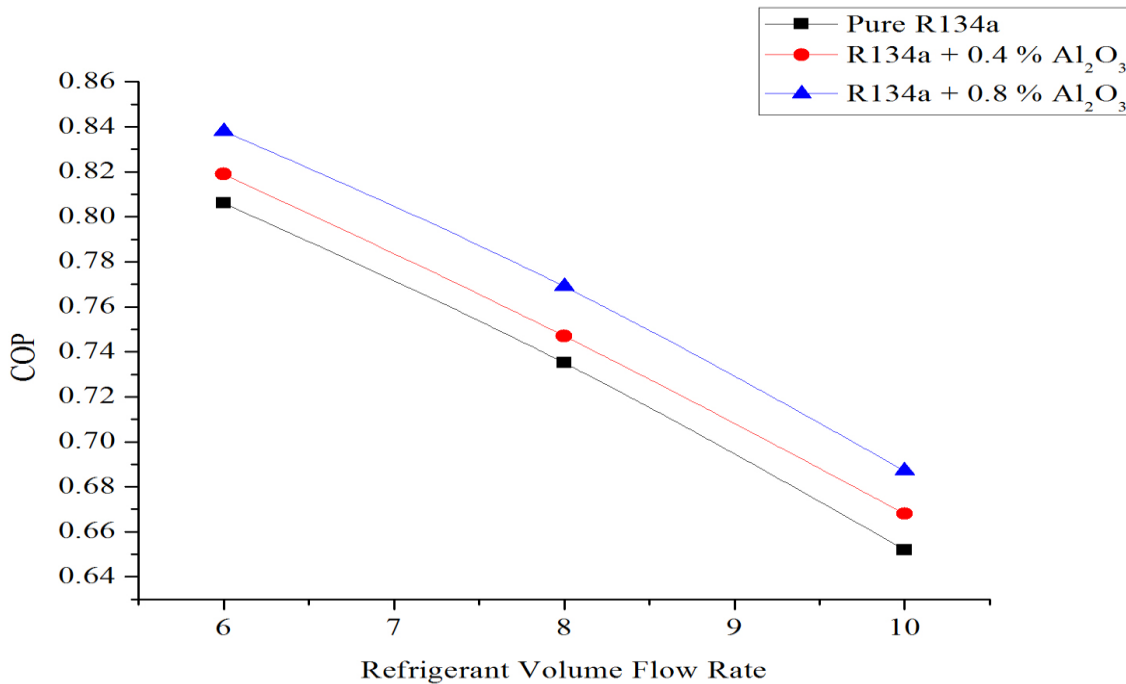


Figure 5.4: C.O.P. comparison for heat flux at 20-21<sup>0</sup>C and volume flow rate 6LPH, 8LPH and 10 LPH

Now comparison according to constant heat flux first calculation is done on 25-26<sup>0</sup>C at 6LPH, 8LPH and 10LPH volume flow rate. Firstly Figure 5.5 show that with pure R134a at 6LPH C.O.P. is found to be 0.824 whereas at 8 LPH and 10LPH is 0.753 and 0.672 respectively. Therefore it is calculated that, COP decreases by 8.62 % at 8LPH and at 10LPH COP decreases by 18.45 % when compared to COP at 6 LPH.

Similarly calculation is done with R134a + 0.4 % Al<sub>2</sub>O<sub>3</sub> and R134a + 0.8 % Al<sub>2</sub>O<sub>3</sub> at constant heat flux 25-26<sup>0</sup>C. The results shows that with R134a + 0.8 % Al<sub>2</sub>O<sub>3</sub> at 6LPH C.O.P. is found to be 0.841 whereas at 8 LPH and 10LPH is 0.767 and 0.681 respectively. Therefore it is found that, COP decreases by 8.80 % at 8LPH and at 10LPH COP decreases by 19.02 % when compared to COP at 6 LPH.

Now with R134a + 0.8 % Al<sub>2</sub>O<sub>3</sub> at 6LPH C.O.P. is found to be 0.873 whereas at 8 LPH and 10LPH is 0.782 and 0.703 respectively. Therefore it is calculated that, COP decreases by 10.42 % at 8LPH and at 10LPH COP decreases by 19.47 % when compared to COP at 6 LPH.

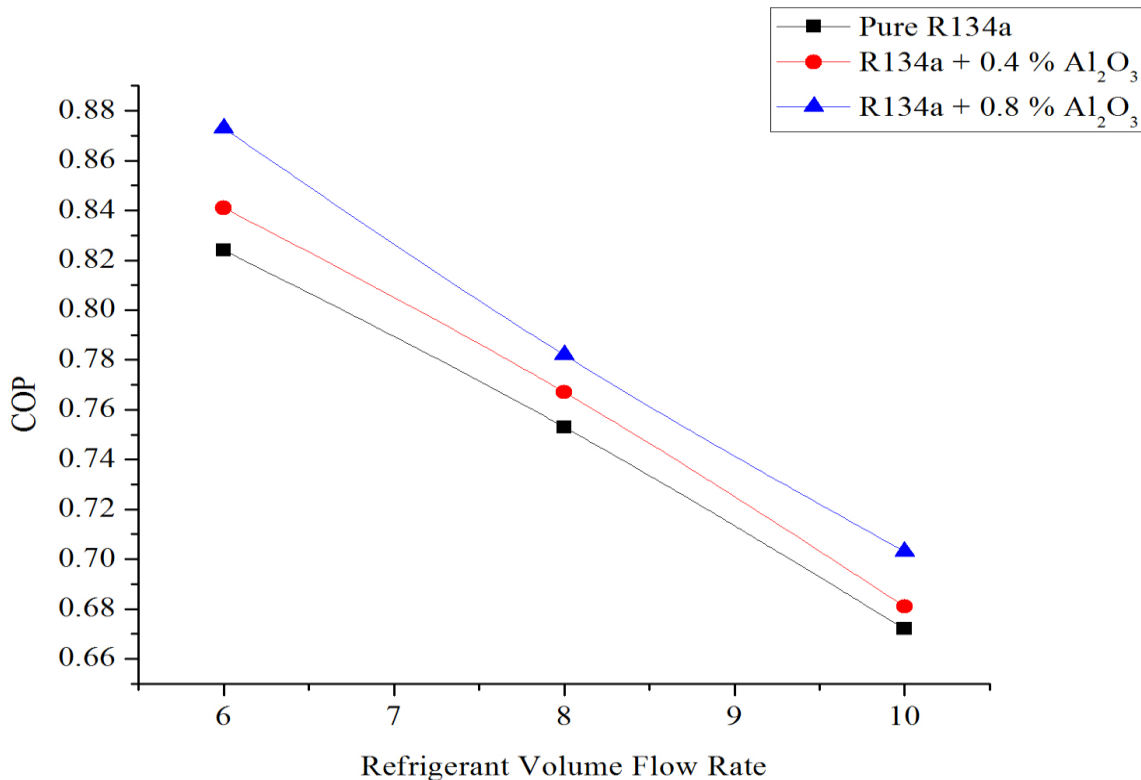


Figure 5.5: C.O.P. comparison for heat flux at 25-26<sup>0</sup>C and volume flow rate 6LPH, 8LPH and 10 LPH

Now comparison according to constant heat flux first calculation is done on 30-31<sup>0</sup>C at 6LPH, 8LPH and 10LPH volume flow rate. Firstly Figure 5.6 show that with pure R134a at 6LPH C.O.P. is found to be 0.862 whereas at 8 LPH and 10LPH is 0.802 and 0.746 respectively. Therefore it is calculated that, COP decreases by 6.96 % at 8LPH and at 10LPH COP decreases by 13.46 % when compared to COP at 6 LPH.

Similarly calculation is done with R134a + 0.4 % Al<sub>2</sub>O<sub>3</sub> and R134a + 0.8 % Al<sub>2</sub>O<sub>3</sub> at constant heat flux 30-31<sup>0</sup>C. The results shows that with R134a + 0.4 % Al<sub>2</sub>O<sub>3</sub> at 6LPH C.O.P. is found to be 0.879 whereas at 8 LPH and 10LPH is 0.815 and 0.762 respectively. Therefore it is found that, COP decreases by 7.28 % at 8LPH and at 10LPH COP decreases by 13.31 % when compared to COP at 6 LPH.

Now with R134a + 0.8 % Al<sub>2</sub>O<sub>3</sub> at 6LPH C.O.P. is found to be 0.896 whereas at 8 LPH and 10LPH is 0.845 and 0.787 respectively. Therefore it is calculated that, COP decreases by 5.69 % at 8LPH and at 10LPH COP decreases by 12.39 % when compared to COP at 6 LPH.

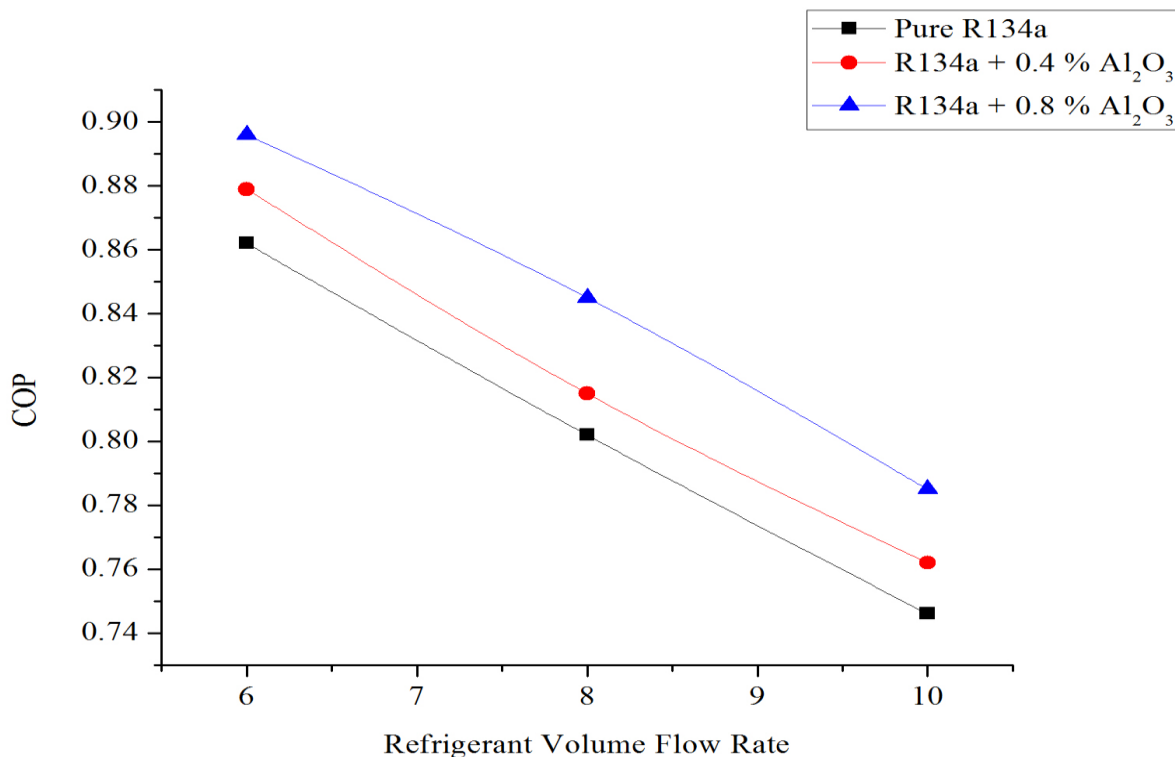


Figure 5.6: C.O.P. comparison for heat flux at 30-31<sup>0</sup>C and volume flow rate 6LPH, 8LPH and 10 LPH

Now comparison according to constant heat flux first calculation is done on 35-36<sup>0</sup>C at 6LPH, 8LPH and 10LPH volume flow rate. Firstly Figure 5.7 show that with pure R134a at 6LPH C.O.P. is found to be 0.943 whereas at 8 LPH and 10LPH is 0.901 and 0.865 respectively. Therefore it is calculated that, COP decreases by 5.45 % at 8LPH and at 10LPH COP decreases by 8.27 % when compared to COP at 6 LPH.

Similarly calculation is done with R134a + 0.4 % Al<sub>2</sub>O<sub>3</sub> and R134a + 0.8 % Al<sub>2</sub>O<sub>3</sub> at constant heat flux 35-36<sup>0</sup>C. The results shows that with R134a + 0.4 % Al<sub>2</sub>O<sub>3</sub> at 6LPH C.O.P. is found to be 0.959 whereas at 8 LPH and 10LPH is 0.918 and 0.876 respectively. Therefore it is found that, COP decreases by 5.28 % at 8LPH and at 10LPH COP decreases by 8.65 % when compared to COP at 6 LPH.

Now with R134a + 0.8 % Al<sub>2</sub>O<sub>3</sub> at 6LPH C.O.P. is found to be 0.985 whereas at 8 LPH and 10LPH is 0.962 and 0.912 respectively. Therefore it is calculated that, COP decreases by 2.34 % at 8LPH and at 10LPH COP decreases by 7.41 % when compared to COP at 6 LPH.

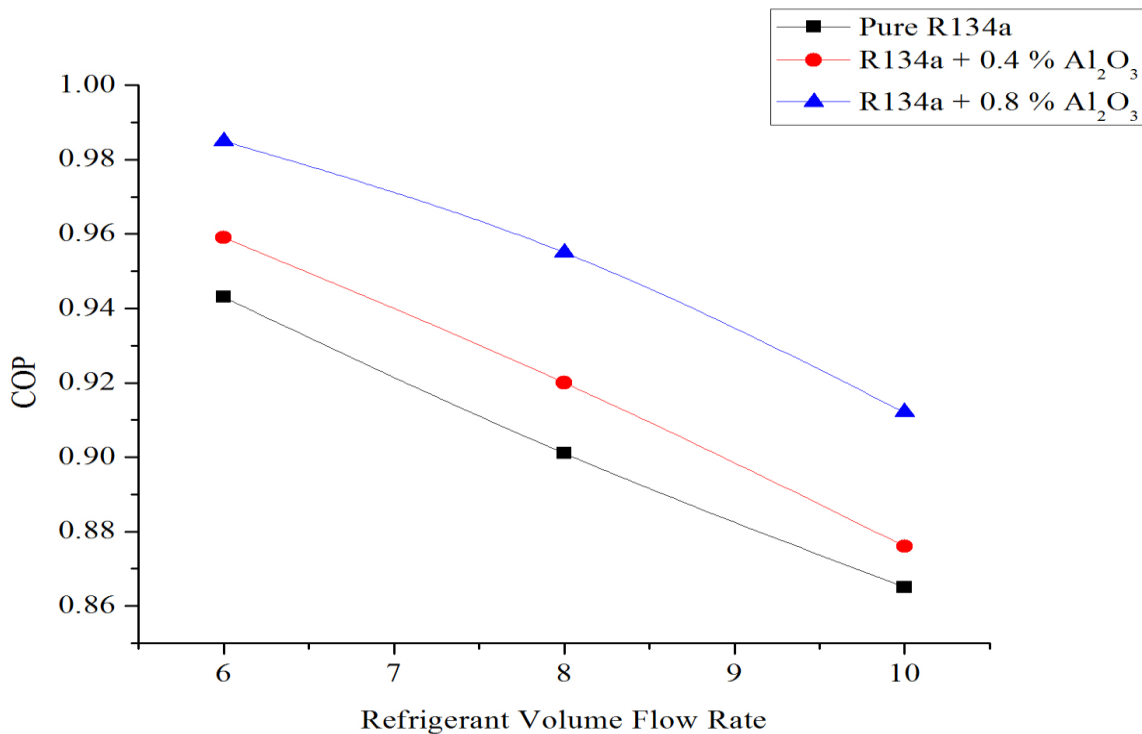


Figure 5.7: C.O.P. comparison for heat flux at 35-36<sup>0</sup>C and volume flow rate 6LPH, 8LPH and 10LPH

As Figure 5.4, Figure 5.5, Figure 5.6 and Figure 5.7 shows that by using nanorefrigerant (R134a + 0.4 % Al<sub>2</sub>O<sub>3</sub> and R134a + 0.8 % Al<sub>2</sub>O<sub>3</sub>) the COP is improved but as volume flow rate increase the COP is decreasing. By increased volume flow rate both power consumption and refrigeration effect is increase this may be due to increment in temperature difference in evaporator section and pressure ratio in compressor outlet to inlet respectively. The increment in power consumption is more significant than increment in refrigeration effect so this may affect decrement in COP with increment in volume flow rate 6LPH to 10LPH.

## 5.2 Adiabatic Efficiency

The adiabatic efficiency expresses the compression process how much resembles an adiabatic compression process. The value of efficiency can be said that, the compression process is an ideal adiabatic process. Adiabatic efficiency is similar to isentropic efficiency but isentropic process has not any kind of losses like mechanical friction etc. Adiabatic efficiency is defined as ratio of the change in specific enthalpy in the adiabatic compression process the change in specific enthalpy in an ideal compression process. Adiabatic efficiency for a compression process can be calculated with the equation

$$\text{Adiabatic Efficiency } (\eta_{adia}) = \frac{c_{p(ideal)} (T_{dis(ideal)} - T_{suc(actual)})}{c_{p(actual)} (T_{dis(actual)} - T_{suc(actual)})} \quad (2)$$

Where  $T_{dis(ideal)}$  find out by using adiabatic operations such as

$$\frac{T_{dis(ideal)}}{T_{suc(actual)}} = \left( \frac{P_{dis(actual)}}{P_{suc(actual)}} \right)^{\frac{R}{c_{p(ideal)}}} \quad (3)$$

$T_{dis(actual)}$ ,  $T_{suc(actual)}$ , measured by digital temperature meter and  $P_{dis(actual)}$ ,  $P_{suc(actual)}$  measured by pressure gauges. For two phase flow  $C_p(actual)$  and  $C_p(ideal)$  for R134a+Al<sub>2</sub>O<sub>3</sub> nanorefrigerant calculated by with the equation

$$c_{p(ideal)(nano+ref)} = (1 - \varphi_{R134a}) c_{p(ideal)(R134a)} + \varphi_{Al_2O_3} c_{p(Al_2O_3)} \quad (4)$$

$$c_{p(actual)(nano+ref)} = (1 - \varphi_{R134a}) c_{p(actual)(R134a)} + \varphi_{Al_2O_3} c_{p(Al_2O_3)} \quad (5)$$

### 5.2.1 Adiabatic Efficiency Comparison According to Constant Volume Flow Rate

Firstly the experiment is performed with 10 LPH volume flow rate of refrigerant maintaining constant evaporator load temperature around 20-21°C. As Figure 5.8 shows, the adiabatic efficiency with pure R134a is found to be 66.28 % whereas with R134a + 0.4 % Al<sub>2</sub>O<sub>3</sub> and R134a + 0.8 % Al<sub>2</sub>O<sub>3</sub>, adiabatic efficiency is 67.33 % and 67.68 % respectively. Therefore it is found that, by using R134a + 0.4 % Al<sub>2</sub>O<sub>3</sub> nanorefrigerant sample adiabatic efficiency is improved by 1.59 % and with R134a + 0.8 % Al<sub>2</sub>O<sub>3</sub> adiabatic efficiency is improved by 2.12 % when compared to adiabatic efficiency of pure refrigerant R134a.

Similarly readings are taken at heat flux 25-26°C, 30-35°C, and 35-36 °C at same flow rate. The C.O.P at 25-26°C heat flux with pure R134a is calculated to be 67.08 % whereas with R134a + 0.4 % Al<sub>2</sub>O<sub>3</sub> and R134a + 0.8 % Al<sub>2</sub>O<sub>3</sub>, adiabatic efficiency is 68.63 % and 69.07 % respectively. Therefore it is found that, by using R134a + 0.4 % Al<sub>2</sub>O<sub>3</sub> nanorefrigerant sample adiabatic efficiency is improved by 2.29 % and with R134a + 0.8 % Al<sub>2</sub>O<sub>3</sub> adiabatic efficiency is improved by 2.58 % when compared to adiabatic efficiency of pure refrigerant R134a.

The adiabatic efficiency at 30-31°C heat flux with pure R134a is calculated to be 69.04 % whereas with R134a + 0.4 % Al<sub>2</sub>O<sub>3</sub> and R134a + 0.8 % Al<sub>2</sub>O<sub>3</sub>, adiabatic efficiency is 71.14 % and 71.66 % respectively. Therefore it is found that, by using R134a + 0.4 % Al<sub>2</sub>O<sub>3</sub> nanorefrigerant sample adiabatic efficiency is improved by 2.89 % and with R134a + 0.8 % Al<sub>2</sub>O<sub>3</sub> adiabatic efficiency is improved by 3.79 % when compared to adiabatic efficiency of pure refrigerant R134a.

The C.O.P at 35-36°C heat flux with pure R134a is calculated to be 70.41 % whereas with R134a + 0.4 % Al<sub>2</sub>O<sub>3</sub> and R134a + 0.8 % Al<sub>2</sub>O<sub>3</sub>, adiabatic efficiency is 72.73 % and 73.20 % respectively. Therefore it is found that, by using R134a + 0.4 % Al<sub>2</sub>O<sub>3</sub> nanorefrigerant sample adiabatic efficiency is improved by 3.29 % and with R134a + 0.8 % Al<sub>2</sub>O<sub>3</sub> adiabatic efficiency is improved by 3.98 % when compared to adiabatic efficiency of pure refrigerant R134a.

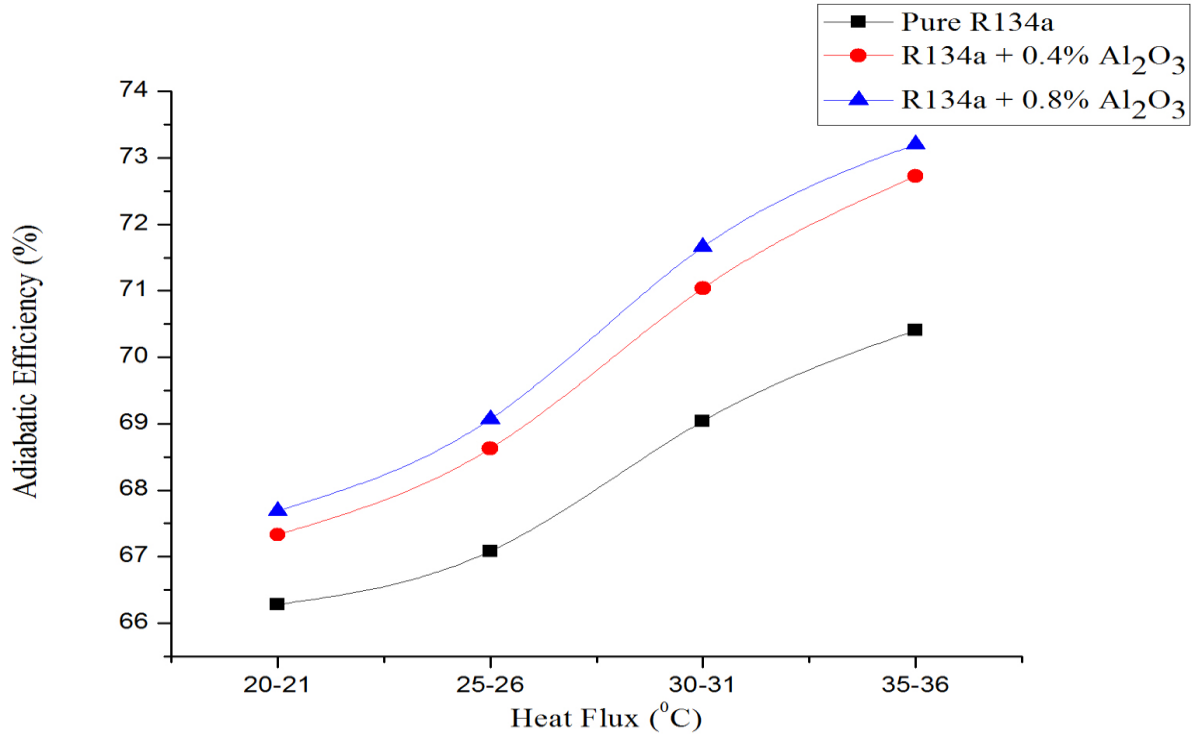


Figure 5.8: Adiabatic Efficiency comparison for at 10 LPH volume flow rate and heat flux at 20-21°C, 25-26°C, 30-31°C and 35-36°C

After 10 LPH volume flow rate similar experiment is performed with 8 LPH volume flow rate of refrigerant maintaining constant evaporator load temperature around 20-21°C. As Figure 5.9 shows, the adiabatic efficiency with pure R134a is found to be 65.95 % whereas with R134a + 0.4 % Al<sub>2</sub>O<sub>3</sub> and R134a + 0.8 % Al<sub>2</sub>O<sub>3</sub>, adiabatic efficiency is 67.04 % and 67.92 % respectively. Therefore it is found that, by using R134a + 0.4 % Al<sub>2</sub>O<sub>3</sub> nanorefrigerant sample adiabatic efficiency is improved by 1.65 % and with R134a + 0.8 % Al<sub>2</sub>O<sub>3</sub> adiabatic efficiency is improved by 2.98 % when compared to adiabatic efficiency of pure refrigerant R134a.

Similarly readings are taken at heat flux 25-26°C, 30-35°C, and 35-36 °C at same flow rate. The adiabatic efficiency at 25-26°C heat flux with pure R134a is calculated to be 66.72 % whereas with R134a + 0.4 % Al<sub>2</sub>O<sub>3</sub> and R134a + 0.8 % Al<sub>2</sub>O<sub>3</sub>, adiabatic efficiency is 68.28 % and 68.49 % respectively. Therefore it is found that, by using R134a + 0.4 % Al<sub>2</sub>O<sub>3</sub> nanorefrigerant sample adiabatic efficiency is improved by 2.35 % and with R134a + 0.8 % Al<sub>2</sub>O<sub>3</sub> adiabatic efficiency is improved by 2.57 % when compared to adiabatic efficiency of pure refrigerant R134a.

The adiabatic efficiency at 30-31°C heat flux with pure R134a is calculated to be 67.82 % whereas with R134a + 0.4 % Al<sub>2</sub>O<sub>3</sub> and R134a + 0.8 % Al<sub>2</sub>O<sub>3</sub>, adiabatic efficiency is 69.76 % and 70.36 % respectively. Therefore it is found that, by using R134a + 0.4 % Al<sub>2</sub>O<sub>3</sub> nanorefrigerant sample adiabatic efficiency is improved by 5.56 % and with R134a + 0.4 % Al<sub>2</sub>O<sub>3</sub> adiabatic efficiency is improved by 5.46 % when compared to adiabatic efficiency of pure refrigerant R134a.

The adiabatic efficiency at 35-36°C heat flux with pure R134a is calculated to be 69.89 % whereas with R134a + 0.4 % Al<sub>2</sub>O<sub>3</sub> and R134a + 0.8 % Al<sub>2</sub>O<sub>3</sub>, adiabatic efficiency is 71.99 % and 72.58 respectively. Therefore it is found that, by using R134a + 0.4 % Al<sub>2</sub>O<sub>3</sub> nanorefrigerant sample adiabatic efficiency is improved by 3.02 % and with R134a + 0.4 % Al<sub>2</sub>O<sub>3</sub> adiabatic efficiency is improved by 3.86 % when compared to adiabatic efficiency of pure refrigerant R134a.

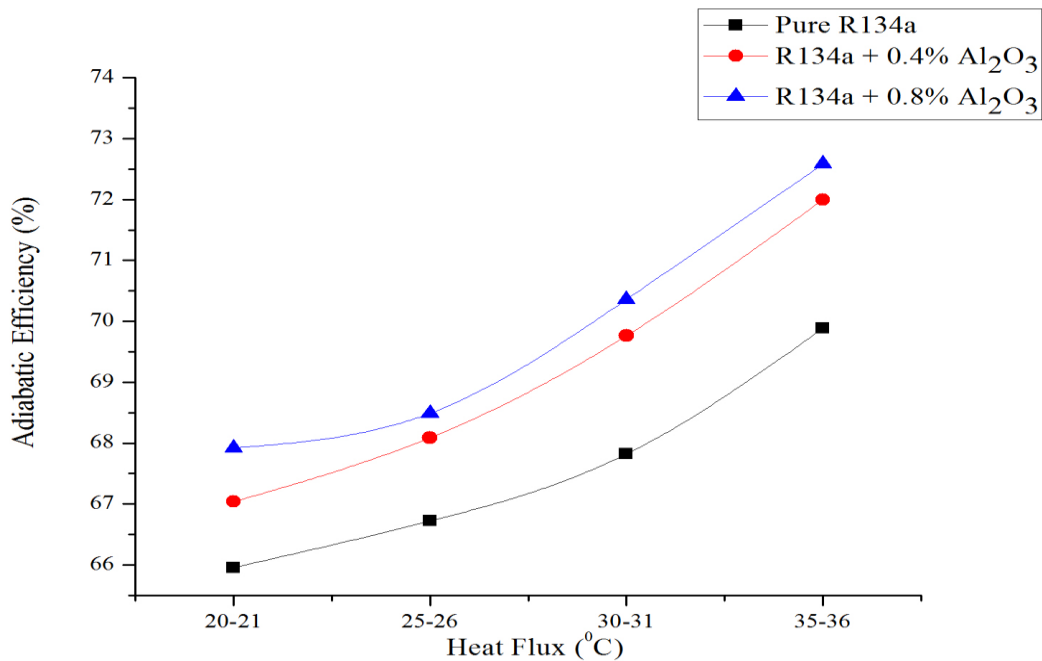


Figure 5.9: Adiabatic Efficiency comparison for at 8 LPH volume flow rate and heat flux at 20-21°C, 25-26 °C, 30-31°C and 35-36°C

After 8 LPH volume flow rate similar experiment is performed with 6 LPH volume flow rate of refrigerant maintaining constant evaporator load temperature around 20-21°C. As Figure 5.10 shows, the adiabatic efficiency with pure R134a is found to be 65.39 % whereas with R134a + 0.4 % Al<sub>2</sub>O<sub>3</sub> and R134a + 0.8 % Al<sub>2</sub>O<sub>3</sub>, adiabatic efficiency is 66.23 % and 66.45 % respectively. Therefore it is found that, by using R134a + 0.4 % Al<sub>2</sub>O<sub>3</sub> nanorefrigerant sample adiabatic efficiency is improved by 1.29 % and with R134a + 0.8 % Al<sub>2</sub>O<sub>3</sub> adiabatic efficiency is improved by 1.62 % when compared to adiabatic efficiency of pure refrigerant R134a.

Similarly readings are taken at heat flux 25-26°C, 30-35°C, and 35-36 °C at same flow rate. The adiabatic efficiency at 25-26°C heat flux with pure R134a is calculated to be 66.37 % whereas with R134a + 0.4 % Al<sub>2</sub>O<sub>3</sub> and R134a + 0.8 % Al<sub>2</sub>O<sub>3</sub>, adiabatic efficiency is 67.56 % and 67.77 respectively. Therefore it is found that, by using R134a + 0.4 % Al<sub>2</sub>O<sub>3</sub> nanorefrigerant sample adiabatic efficiency is improved by 1.78 % and with R134a + 0.8 % Al<sub>2</sub>O<sub>3</sub> adiabatic efficiency is improved by 2.08 % when compared to adiabatic efficiency of pure refrigerant R134a.

The adiabatic efficiency at 30-31°C heat flux with pure R134a is calculated to be 67.58 % whereas with R134a + 0.4 % Al<sub>2</sub>O<sub>3</sub> and R134a + 0.8 % Al<sub>2</sub>O<sub>3</sub>, adiabatic efficiency is 69.43 % and 69.55 % respectively. Therefore it is found that, by using R134a + 0.4 % Al<sub>2</sub>O<sub>3</sub> nanorefrigerant sample adiabatic efficiency is improved by 2.74 % and with R134a + 0.8 % Al<sub>2</sub>O<sub>3</sub> adiabatic efficiency is improved by 2.92 % when compared to adiabatic efficiency of pure refrigerant R134a.

The C.O.P at 35-36°C heat flux with pure R134a is calculated to be 69.46 % whereas with R134a + 0.4 % Al<sub>2</sub>O<sub>3</sub> and R134a + 0.8 % Al<sub>2</sub>O<sub>3</sub>, adiabatic efficiency is 71.60 % and 72.05 % respectively. Therefore it is found that, by using R134a + 0.4 % Al<sub>2</sub>O<sub>3</sub> nanorefrigerant sample adiabatic efficiency is improved by 3.08 % and with R134a + 0.8 % Al<sub>2</sub>O<sub>3</sub> adiabatic efficiency is improved by 3.73 % when compared to adiabatic efficiency of pure refrigerant R134a.

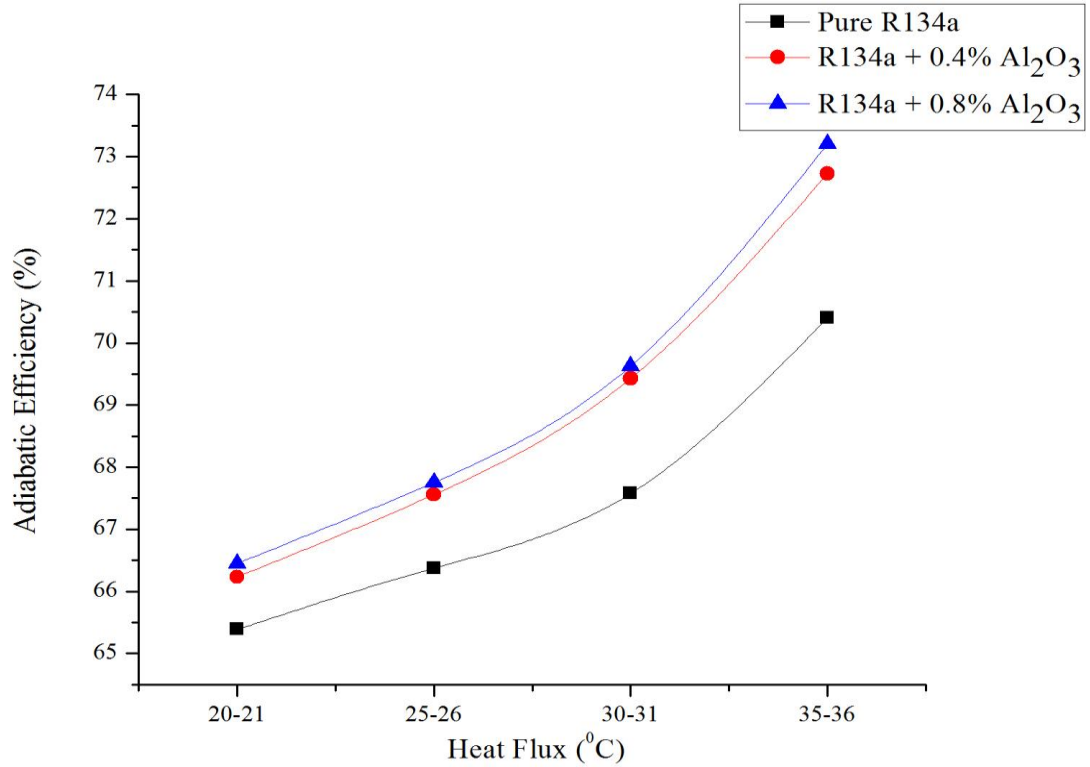


Figure 5.10: Adiabatic Efficiency comparison for at 6 LPH volume flow rate and heat flux at 20-21<sup>o</sup>C, 25-26<sup>o</sup>C, 30-31<sup>o</sup>C and 35-36<sup>o</sup>C

As Figure 5.8, Figure 5.9 and Figure 5.10 shows by using nanorefrigerant (R134a + 0.4 % Al<sub>2</sub>O<sub>3</sub> and R134a + 0.8 % Al<sub>2</sub>O<sub>3</sub>) the adiabatic efficiency is improved in every case of heat flux (20-21, 25-26, 30-31, 35-36), this could be due to by using nanorefrigerant both suction pressure and discharge pressure is decrease. By decrement in suction pressure and discharge pressure the increment in specific entropy generation become less compare with adiabatic process this may be affect as the increment in the adiabatic efficiency.

The other thing that might affect the increment in the adiabatic efficiency is isobaric specific heat capacity. As the isobaric specific heat capacity increases using of nanorefrigerant the adiabatic efficiency is improved.

As the heat flux is increases, the evaporator temperature and the evaporator pressure increase because of lift in the constant temperature. However, the increase in the ratio of the condenser pressure to the evaporator pressure will decrease this affect the increment in the adiabatic efficiency.

## 5.2.2 Adiabatic Efficiency Comparison According to Constant Heat Flux

To comparison according to constant heat flux first calculation is done on 20-21<sup>0</sup>C at 6LPH, 8LPH and 10LPH volume flow rate. Firstly Figure 5.11 show that with pure R134a at 6LPH adiabatic efficiency is found to be 65.39 % whereas at 8 LPH and 10LPH is 65.95 % and 66.28 % respectively. Therefore it is calculated that, adiabatic efficiency is improved by 0.87 % at 8LPH and at 10LPH adiabatic efficiency is improved by 1.37 % when compared to adiabatic efficiency at 6 LPH.

Similarly calculation is done with R134a + 0.4 % Al<sub>2</sub>O<sub>3</sub> and R134a + 0.8 % Al<sub>2</sub>O<sub>3</sub> at constant heat flux 20-21<sup>0</sup>C. The results shows that with R134a + 0.4 % Al<sub>2</sub>O<sub>3</sub> at 6LPH adiabatic efficiency is found to be 66.23 % whereas at 8 LPH and 10LPH is 67.04 % and 67.33 % respectively. Therefore it is calculated that, adiabatic efficiency is improved by 1.22 % at 8LPH and at 10LPH adiabatic efficiency is improved by 1.66 % when compared to adiabatic efficiency at 6 LPH.

Now with R134a + 0.8 % Al<sub>2</sub>O<sub>3</sub> at 6LPH adiabatic efficiency is found to be 66.45 % whereas at 8 LPH and 10LPH is 67.92 % and 68.00 % respectively. Therefore it is calculated that, adiabatic efficiency is improved by 2.21 % at 8LPH and at 10LPH adiabatic efficiency is improved by 2.33 % when compared to adiabatic efficiency at 6 LPH.

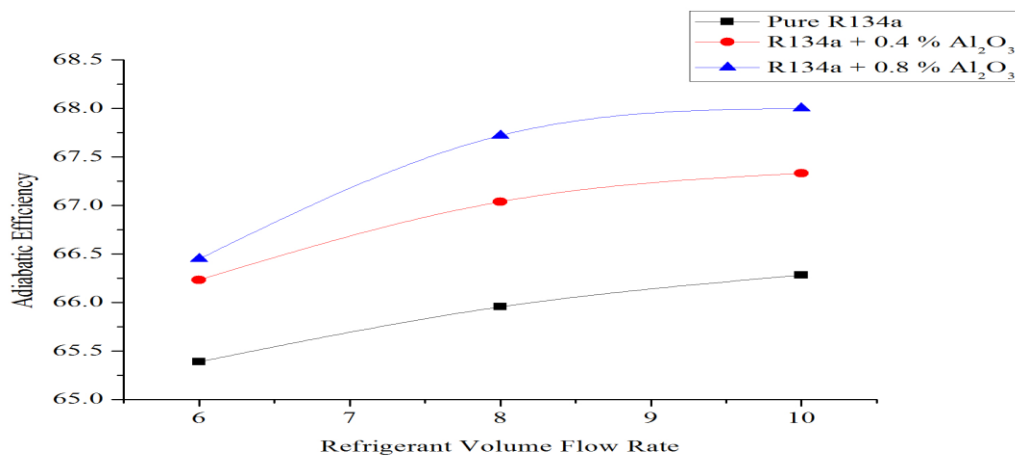


Figure 5.11: Adiabatic Efficiency comparison for heat flux at 20-21<sup>0</sup>C and volume flow rate 6LPH, 8LPH and 10 LPH

Now comparison according to constant heat flux first calculation is done on 25-26<sup>0</sup>C at 6LPH, 8LPH and 10LPH volume flow rate. Firstly Figure 5.12 show that with pure R134a at 6LPH adiabatic efficiency is found to be 66.37 % whereas at 8 LPH and 10LPH is 66.72 % and 67.08 % respectively. Therefore it is calculated that, adiabatic efficiency is improved by 0.52 % at 8LPH and at 10LPH adiabatic efficiency is improved by 1.07 % when compared to adiabatic efficiency at 6 LPH.

Similarly calculation is done with R134a + 0.4 % Al<sub>2</sub>O<sub>3</sub> and R134a + 0.8 % Al<sub>2</sub>O<sub>3</sub> at constant heat flux 25-26<sup>0</sup>C. The results shows that with R134a + 0.4 % Al<sub>2</sub>O<sub>3</sub> at 6LPH adiabatic efficiency is found to be 67.56 % whereas at 8 LPH and 10LPH is 68.29 % and 68.63 % respectively. Therefore it is found that, adiabatic efficiency is improved by 1.08 % at 8LPH and at 10LPH adiabatic efficiency is improved by 1.58 % when compared to adiabatic efficiency at 6 LPH.

Now with R134a + 0.8 % Al<sub>2</sub>O<sub>3</sub> at 6LPH adiabatic efficiency is found to be 67.76 % whereas at 8 LPH and 10LPH is 68.09 % and 68.63 % respectively. Therefore it is calculated that, adiabatic efficiency is improved by 0.49 % at 8LPH and at 10LPH adiabatic efficiency is improved by 1.28 % when compared to adiabatic efficiency at 6 LPH.

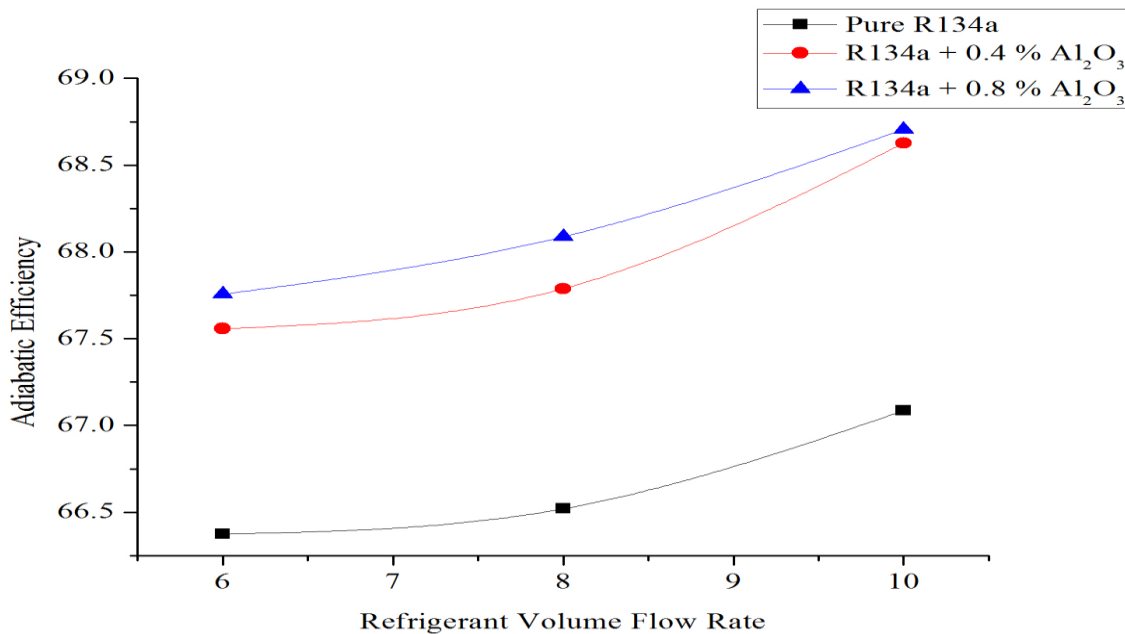


Figure 5.12: Adiabatic Efficiency comparison for heat flux at 25-26<sup>0</sup>C and volume flow rate 6LPH, 8LPH and 10 LPH

Now comparison according to constant heat flux first calculation is done on 30-31<sup>0</sup>C at 6LPH, 8LPH and 10LPH volume flow rate. Firstly Figure 5.13 show that with pure R134a at 6LPH adiabatic efficiency is found to be 67.58 % whereas at 8 LPH and 10LPH is 67.82 % and 69.04 % respectively. Therefore it is calculated that, adiabatic efficiency is improved by 0.36 % at 8LPH and at 10LPH adiabatic efficiency is improved by 2.17 % when compared to adiabatic efficiency at 6 LPH.

Similarly calculation is done with R134a + 0.4 % Al<sub>2</sub>O<sub>3</sub> and R134a + 0.8 % Al<sub>2</sub>O<sub>3</sub> at constant heat flux 30-31<sup>0</sup>C. The results shows that with R134a + 0.4 % Al<sub>2</sub>O<sub>3</sub> at 6LPH adiabatic efficiency is found to be 69.43 % whereas at 8 LPH and 10LPH is 69.76 % and 71.04 % respectively. Therefore it is found that, adiabatic efficiency is improved by 0.48 % at 8LPH and at 10LPH adiabatic efficiency is improved by 2.32 % when compared to adiabatic efficiency at 6 LPH.

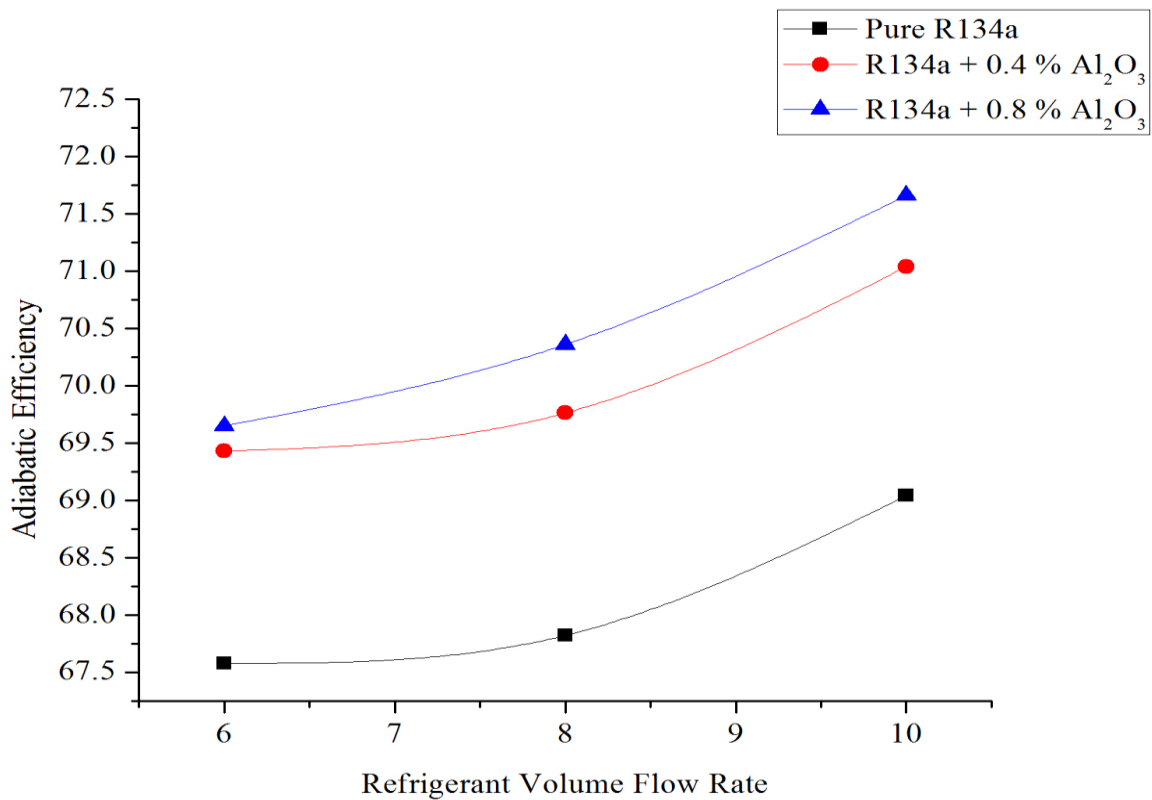


Figure 5.13: Adiabatic Efficiency comparison for heat flux at 30-31<sup>0</sup>C and volume flow rate 6LPH, 8LPH and 10 LPH

Now with R134a + 0.8 % Al<sub>2</sub>O<sub>3</sub> at 6LPH adiabatic efficiency is found to be 69.55 % whereas at 8 LPH and 10LPH is 70.36 % and 71.66 % respectively. Therefore it is calculated that, adiabatic efficiency is improved by 1.16 % at 8LPH and at 10LPH adiabatic efficiency is improved by 3.03 % when compared to adiabatic efficiency at 6 LPH.

Now comparison according to constant heat flux first calculation is done on 35-36<sup>0</sup>C at 6LPH, 8LPH and 10LPH volume flow rate. Firstly Figure 5.14 show that with pure R134a at 6LPH adiabatic efficiency is found to be 69.46 % whereas at 8 LPH and 10LPH is 69.89 % and 70.41 % respectively. Therefore it is calculated that, adiabatic efficiency is improved by 0.61 % at 8LPH and at 10LPH adiabatic efficiency is improved by 1.36 % when compared to adiabatic efficiency at 6 LPH.

Similarly calculation is done with R134a + 0.4 % Al<sub>2</sub>O<sub>3</sub> and R134a + 0.4 % Al<sub>2</sub>O<sub>3</sub> at constant heat flux 35-36<sup>0</sup>C. The results shows that with R134a + 0.4 % Al<sub>2</sub>O<sub>3</sub> at 6LPH adiabatic efficiency is found to be 71.60 % whereas at 8 LPH and 10LPH is 72.00 % and 72.73 % respectively. Therefore it is found that, adiabatic efficiency is improved by 0.55 % at 8LPH and at 10LPH adiabatic efficiency is improved by 1.57 % when compared to adiabatic efficiency at 6 LPH.

Now with R134a + 0.4 % Al<sub>2</sub>O<sub>3</sub> at 6LPH adiabatic efficiency is found to be 72.05 % whereas at 8 LPH and 10LPH is 72.58 % and 73.20 % respectively. Therefore it is calculated that, adiabatic efficiency is improved by 0.73 % at 8LPH and at 10LPH adiabatic efficiency is improved by 1.60 % when compared to adiabatic efficiency at 6 LPH.

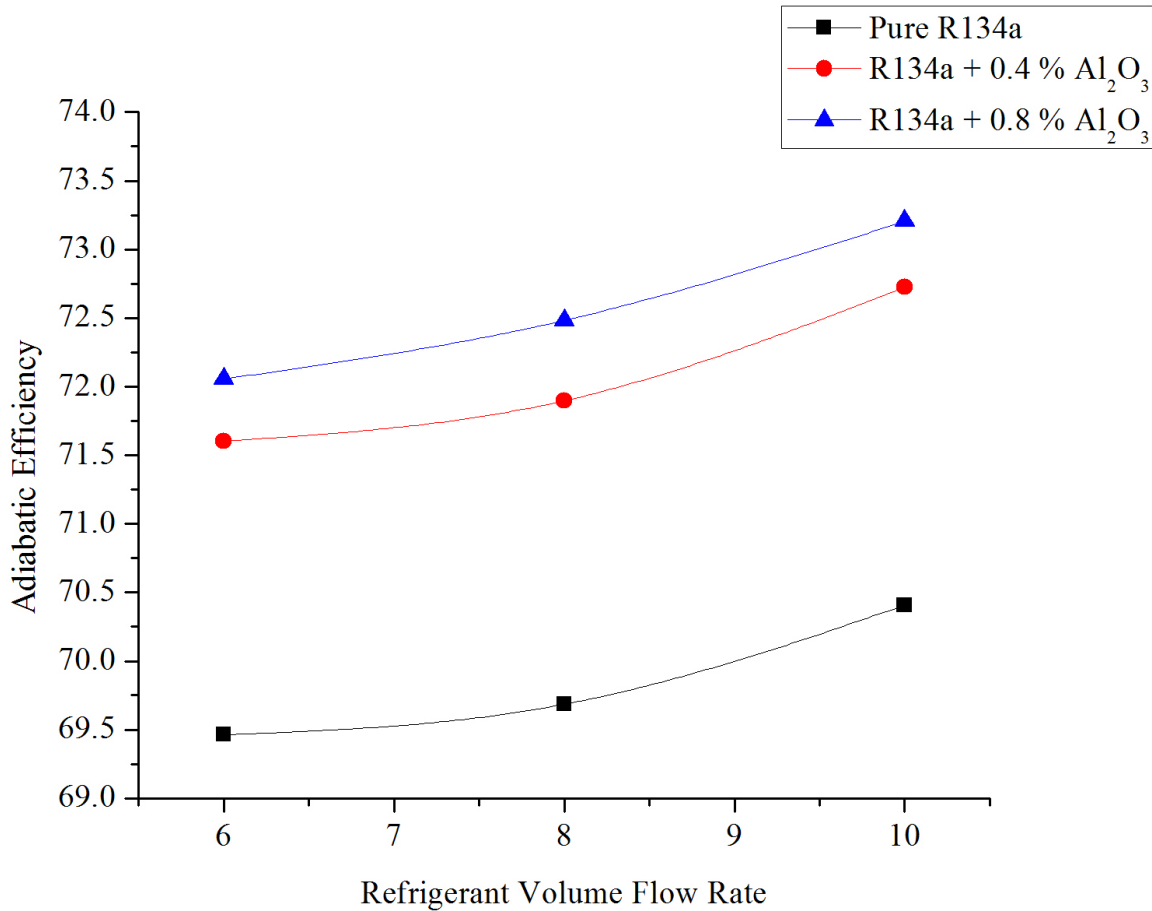


Figure 5.14: Adiabatic Efficiency comparison for heat flux at 35-36<sup>0</sup>C and volume flow rate 6LPH, 8LPH and 10 LPH

As Figure 5.11, Figure 5.12, Figure 5.13 and Figure 5.14 show that by using nanorefrigerant (R134a + 0.4 % Al<sub>2</sub>O<sub>3</sub> and R134a + 0.8 % Al<sub>2</sub>O<sub>3</sub>) the adiabatic efficiency is improved and as volume flow rate increases the adiabatic efficiency is found to be improved. By increase in volume flow rate both suction temperature and discharge temperature increases as well as both suction pressure and discharge pressure increases but increment in suction pressure is less than the increment in discharge pressure this causes the increase in specific entropy generation compare with adiabatic process at lower volume flow rate so, this may affect improvement in adiabatic efficiency with increment in volume flow rate 6LPH to 10LPH. Hence the vapor compression refrigerant system works better at higher volume flow rate.

### 5.3 Electromechanical Efficiency

The electromechanical efficiency defines as the energy gain by the refrigerant how much resembles the electrical power input to compressor. The electromechanical efficiency is combination product of mechanical efficiency and electrical efficiency, where mechanical efficiency defines as the energy gain by the refrigerant how much equate the shaft power of compressor and the electrical efficiency is defines as the shaft power of compressor how much equates the electrical power required to compression. The electromechanical efficiency calculates as the ratio energy gain (in KW) by the refrigerant/nanorefrigerant to electrical power input to compressor which can be measured by energy meter. The electromechanical efficiency for a compression process can be calculated with the equation

$$\text{Electromechanical Efficiency } (\eta_{\text{eleme}}) = \frac{\dot{m}_2 h_2 - \dot{m}_1 h_1}{W_{\text{ele}}} \quad (6)$$

Where  $W_{\text{ele}}$  is refer to electrical power consumption by compressor in KW and  $\dot{m}$  is mass flow rare it can be calculated with the equation

$$\dot{m} = \dot{v} \rho \quad (7)$$

For two phase flow  $\rho$  for R134a+Al<sub>2</sub>O<sub>3</sub> nanorefrigerant calculated by with the equation

$$\rho_{(\text{nano+ref})} = (1 - \phi_{\text{R134a}}) \rho_{(\text{R134a})} + \phi_{\text{Al}_2\text{O}_3} \rho_{(\text{Al}_2\text{O}_3)} \quad (8)$$

#### 5.3.1 Electromechanical Efficiency Comparison According to Constant Volume Flow Rate

Firstly the experiment is performed with 10 LPH volume flow rate of refrigerant maintaining constant evaporator load temperature around 20-21°C. As Figure 5.15 shows, the electromechanical efficiency with pure R134a is found to be 75.97 % whereas with R134a+ 0.4 % Al<sub>2</sub>O<sub>3</sub> and R134a + 0.8 % Al<sub>2</sub>O<sub>3</sub>, electromechanical efficiency is 75.75 % and 75.48 % respectively. Therefore it is found that, by using R134a + 0.4 % Al<sub>2</sub>O<sub>3</sub> nanorefrigerant sample electromechanical efficiency is improved by 0.65 % and with R134a + 0.8 % Al<sub>2</sub>O<sub>3</sub> electromechanical efficiency is improved by 0.69 % when compared to electromechanical efficiency of pure refrigerant R134a.

Similarly readings are taken at heat flux 25-26°C, 30-35°C, and 35-36 °C at same flow rate. The C.O.P at 25-26°C heat flux with pure R134a is calculated to be 75.22 % whereas with R134a + 0.4 % Al<sub>2</sub>O<sub>3</sub> and R134a + 0.8 % Al<sub>2</sub>O<sub>3</sub>, electromechanical efficiency is 75.72 % and 75.78 % respectively. Therefore it is found that, by using R134a + 0.4 % Al<sub>2</sub>O<sub>3</sub> nanorefrigerant sample electromechanical efficiency is improved by 0.67 % and with R134a + 0.8 % Al<sub>2</sub>O<sub>3</sub> electromechanical efficiency is improved by 0.74 % when compared to electromechanical efficiency of pure refrigerant R134a.

The C.O.P at 30-31°C heat flux with pure R134a is calculated to be 75.96 % whereas with R134a + 0.4 % Al<sub>2</sub>O<sub>3</sub> and R134a + 0.8 % Al<sub>2</sub>O<sub>3</sub>, electromechanical efficiency is 76.50 % and 76.54 % respectively. Therefore it is found that, by using R134a + 0.4 % Al<sub>2</sub>O<sub>3</sub> nanorefrigerant sample electromechanical efficiency is improved by 0.72 % and with R134a + 0.8 % Al<sub>2</sub>O<sub>3</sub> electromechanical efficiency is improved by 0.77 % when compared to electromechanical efficiency of pure refrigerant R134a.

The C.O.P at 35-36°C heat flux with pure R134a is calculated to be 76.15 % whereas with R134a + 0.4 % Al<sub>2</sub>O<sub>3</sub> and R134a + 0.8 % Al<sub>2</sub>O<sub>3</sub>, electromechanical efficiency is 76.72 % and 76.77 % respectively. Therefore it is found that, by using R134a + 0.4 % Al<sub>2</sub>O<sub>3</sub> nanorefrigerant sample electromechanical efficiency is improved by 0.74 % and with R134a + 0.8 % Al<sub>2</sub>O<sub>3</sub> electromechanical efficiency is improved by 0.81 % when compared to electromechanical efficiency of pure refrigerant R134a.

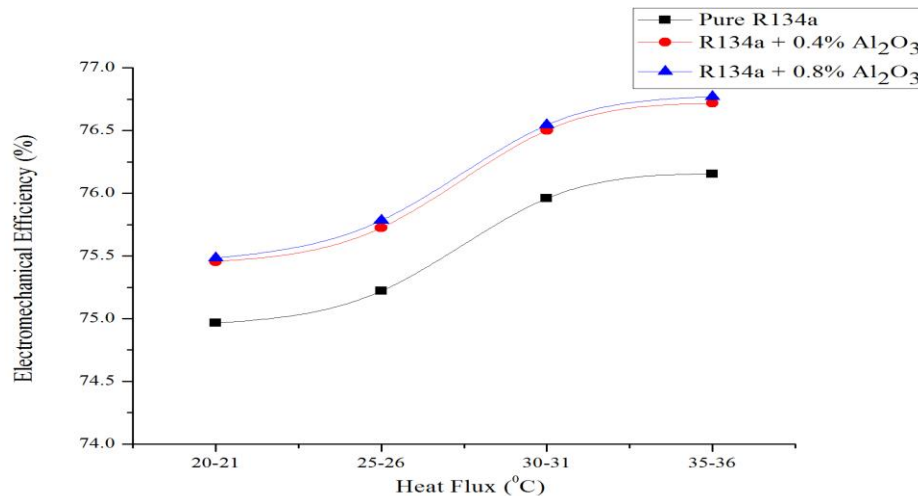


Figure 5.15: Electromechanical Efficiency comparison for at 10 LPH volume flow rate and heat flux at 20-21°C, 25-26°C, 30-31°C and 35-36°C

After 10 LPH volume flow rate similar experiment is performed with 8 LPH volume flow rate of refrigerant maintaining constant evaporator load temperature around 20-21°C. As Figure 5.16 shows, the electromechanical efficiency with pure R134a is found to be 73.85 % whereas with R134a + 0.4 % Al<sub>2</sub>O<sub>3</sub> and R134a + 0.8 % Al<sub>2</sub>O<sub>3</sub>, electromechanical efficiency is 75.28 % and 75.30 % respectively. Therefore it is found that, by using R134a + 0.4 % Al<sub>2</sub>O<sub>3</sub> nanorefrigerant sample electromechanical efficiency is improved by 0.58 % and with R134a + 0.8 % Al<sub>2</sub>O<sub>3</sub> electromechanical efficiency is improved by 0.61 % when compared to electromechanical efficiency of pure refrigerant R134a.

Similarly readings are taken at heat flux 25-26°C, 30-35°C, and 35-36 °C at same flow rate. The electromechanical efficiency at 25-26°C heat flux with pure R134a is calculated to be 75.30 % whereas with R134a + 0.4 % Al<sub>2</sub>O<sub>3</sub> and R134a + 0.8 % Al<sub>2</sub>O<sub>3</sub>, electromechanical efficiency is 75.47 % and 75.94 % respectively. Therefore it is found that, by using R134a + 0.4 % Al<sub>2</sub>O<sub>3</sub> nanorefrigerant sample electromechanical efficiency is improved by 0.64 % and with R134a + 0.8 % Al<sub>2</sub>O<sub>3</sub> electromechanical efficiency is improved by 0.70 % when compared to electromechanical efficiency of pure refrigerant R134a.

The electromechanical efficiency at 30-31°C heat flux with pure R134a is calculated to be 75.99 % whereas with R134a + 0.4 % Al<sub>2</sub>O<sub>3</sub> and R134a + 0.8 % Al<sub>2</sub>O<sub>3</sub>, electromechanical efficiency is 75.52 % and 75.56 % respectively. Therefore it is found that, by using R134a + 0.4 % Al<sub>2</sub>O<sub>3</sub> nanorefrigerant sample electromechanical efficiency is improved by 0.71 % and with R134a + 0.4 % Al<sub>2</sub>O<sub>3</sub> electromechanical efficiency is improved by 0.76 % when compared to electromechanical efficiency of pure refrigerant R134a.

The electromechanical efficiency at 35-36°C heat flux with pure R134a is calculated to be 75.10 % whereas with R134a + 0.4 % Al<sub>2</sub>O<sub>3</sub> and R134a + 0.8 % Al<sub>2</sub>O<sub>3</sub>, electromechanical efficiency is 75.66 % and 75.75 % respectively. Therefore it is found that, by using R134a + 0.4 % Al<sub>2</sub>O<sub>3</sub> nanorefrigerant sample electromechanical efficiency is improved by 0.75 % and with R134a + 0.4 % Al<sub>2</sub>O<sub>3</sub> electromechanical efficiency is improved by 0.86 % when compared to electromechanical efficiency of pure refrigerant R134a.

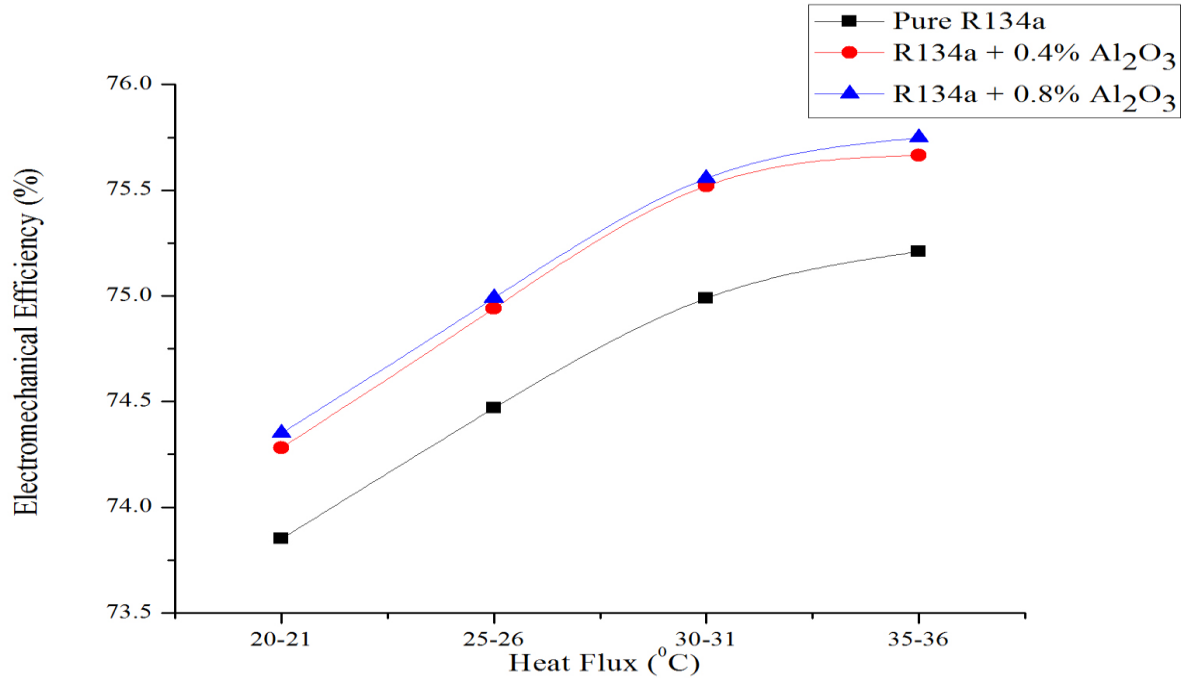


Figure 5.16: Electromechanical Efficiency comparison for at 8 LPH volume flow rate and heat flux at 20-21<sup>o</sup>C, 25-26<sup>o</sup>C, 30-31<sup>o</sup>C and 35-36<sup>o</sup>C

After 8 LPH volume flow rate similar experiment is performed with 6 LPH volume flow rate of refrigerant maintaining constant evaporator load temperature around 20-21<sup>o</sup>C. As Figure 5.17 shows, the electromechanical efficiency with pure R134a is found to be 73.02 % whereas with R134a + 0.4 % Al<sub>2</sub>O<sub>3</sub> and R134a + 0.8 % Al<sub>2</sub>O<sub>3</sub>, electromechanical efficiency is 73.43 % and 73.46 % respectively. Therefore it is found that, by using R134a + 0.4 % Al<sub>2</sub>O<sub>3</sub> nanorefrigerant sample electromechanical efficiency is improved by 0.56 % and with R134a + 0.8 % Al<sub>2</sub>O<sub>3</sub> electromechanical efficiency is improved by 0.60 % when compared to electromechanical efficiency of pure refrigerant R134a.

Similarly readings are taken at heat flux 25-26<sup>o</sup>C, 30-35<sup>o</sup>C, and 35-36<sup>o</sup>C at same flow rate. The electromechanical efficiency at 25-26<sup>o</sup>C heat flux with pure R134a is calculated to be 75.09 % whereas with R134a + 0.4 % Al<sub>2</sub>O<sub>3</sub> and R134a + 0.8 % Al<sub>2</sub>O<sub>3</sub>, electromechanical efficiency is 75.55 % and 75.60 % respectively. Therefore it is found that, by using R134a + 0.4 % Al<sub>2</sub>O<sub>3</sub> nanorefrigerant sample electromechanical efficiency is improved by 0.62 % and with

R134a + 0.8 % Al<sub>2</sub>O<sub>3</sub> electromechanical efficiency is improved by 0.68 % when compared to electromechanical efficiency of pure refrigerant R134a.

The electromechanical efficiency at 30-31°C heat flux with pure R134a is calculated to be 75.52 % whereas with R134a + 0.4 % Al<sub>2</sub>O<sub>3</sub> and R134a + 0.8 % Al<sub>2</sub>O<sub>3</sub>, electromechanical efficiency is 75.04 % and 75.07 % respectively. Therefore it is found that, by using R134a + 0.4 % Al<sub>2</sub>O<sub>3</sub> nanorefrigerant sample electromechanical efficiency is improved by 0.71 % and with R134a + 0.8 % Al<sub>2</sub>O<sub>3</sub> electromechanical efficiency is improved by 0.75 % when compared to electromechanical efficiency of pure refrigerant R134a.

The C.O.P at 35-36°C heat flux with pure R134a is calculated to be 75.96 % whereas with R134a + 0.4 % Al<sub>2</sub>O<sub>3</sub> and R134a + 0.8 % Al<sub>2</sub>O<sub>3</sub>, electromechanical efficiency is 75.50 % and 75.57 % respectively. Therefore it is found that, by using R134a + 0.4 % Al<sub>2</sub>O<sub>3</sub> nanorefrigerant sample electromechanical efficiency is improved by 0.73 % and with R134a + 0.8 % Al<sub>2</sub>O<sub>3</sub> electromechanical efficiency is improved by 0.82 % when compared to electromechanical efficiency of pure refrigerant R134a.

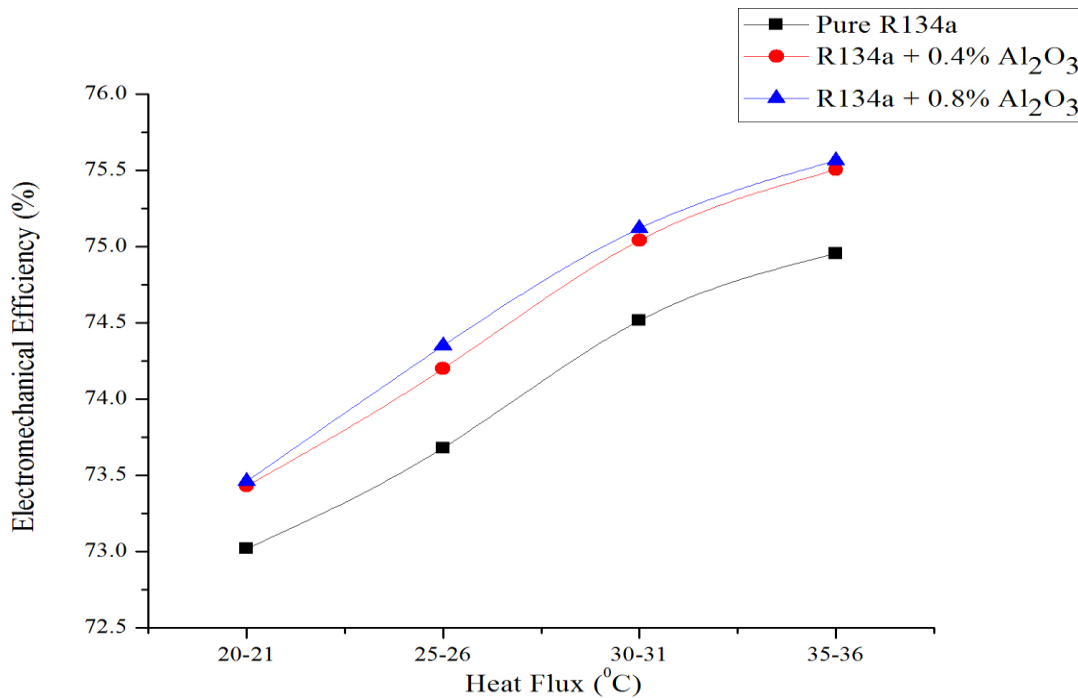


Figure 5.17: Electromechanical Efficiency comparison for at 6 LPH volume flow rate and heat flux at 20-21°C, 25-26 °C, 30-31°C and 35-36°C

As Figure 5.15, Figure 5.16 and Figure 5.17 shows that by using nanorefrigerant (R134a + 0.4 %  $\text{Al}_2\text{O}_3$  and R134a + 0.8 %  $\text{Al}_2\text{O}_3$ ) the electromechanical efficiency is improved in every case of heat flux (20-21, 25-26, 30-31, 35-36). Experimental results show that by using nanorefrigerant the power consumption is increasing due to increment of pressure ratio between compressor discharge and suction. In other hand energy gain (in KW) by the refrigerant/nanorefrigerant is also increasing this may be due to improvement in the isobaric specific heat capacity and density of nanorefrigerant.

### **5.3.2 Electromechanical Efficiency Comparison According to Constant Heat Flux**

To comparison according to constant heat flux first calculation is done on 20-21<sup>0</sup>C at 6LPH, 8LPH and 10LPH volume flow rate. Firstly Figure 5.18 show that with pure R134a at 6LPH electromechanical efficiency is found to be 65.39 % whereas at 8 LPH and 10LPH is 65.95 % and 66.28 % respectively. Therefore it is calculated that, electromechanical efficiency is improved by 0.87 % at 8LPH and at 10LPH electromechanical efficiency is improved by 1.37 % when compared to electromechanical efficiency at 6 LPH.

Similarly calculation is done with R134a + 0.4 %  $\text{Al}_2\text{O}_3$  and R134a + 0.8 %  $\text{Al}_2\text{O}_3$  at constant heat flux 20-21<sup>0</sup>C. The results shows that with R134a + 0.4 %  $\text{Al}_2\text{O}_3$  at 6LPH electromechanical efficiency is found to be 66.23 % whereas at 8 LPH and 10LPH is 67.04 % and 67.33 % respectively. Therefore it is calculated that, electromechanical efficiency is improved by 1.22 % at 8LPH and at 10LPH electromechanical efficiency is improved by 1.66 % when compared to electromechanical efficiency at 6 LPH.

Now with R134a + 0.8 %  $\text{Al}_2\text{O}_3$  at 6LPH electromechanical efficiency is found to be 66.45 % whereas at 8 LPH and 10LPH is 67.32 % and 67.69 % respectively. Therefore it is calculated that, electromechanical efficiency is improved by 1.31 % at 8LPH and at 10LPH electromechanical efficiency is improved by 1.87 % when compared to electromechanical efficiency at 6 LPH.

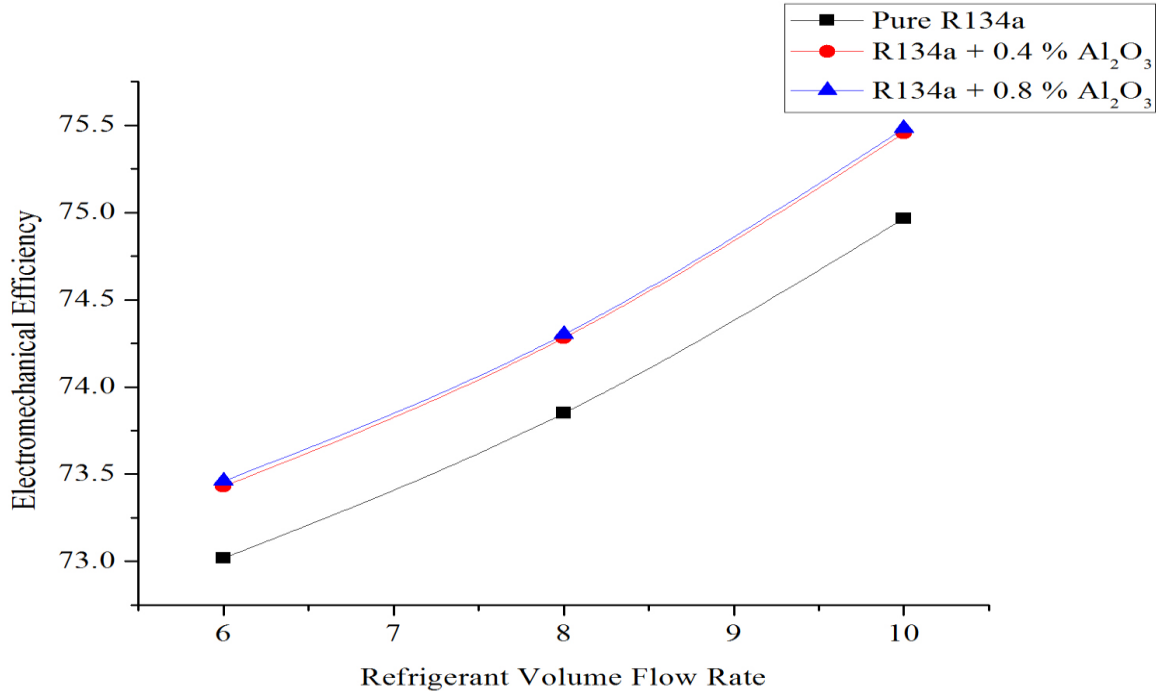


Figure 5.18: Electromechanical Efficiency comparison for heat flux at 20-21<sup>0</sup>C and volume flow rate 6LPH, 8LPH and 10 LPH

Now comparison according to constant heat flux first calculation is done on 25-26<sup>0</sup>C at 6LPH, 8LPH and 10LPH volume flow rate. Firstly Figure 5.19 show that with pure R134a at 6LPH electromechanical efficiency is found to be 66.37 % whereas at 8 LPH and 10LPH is 66.72 % and 67.08 % respectively. Therefore it is calculated that, electromechanical efficiency is improved by 0.52 % at 8LPH and at 10LPH electromechanical efficiency is improved by 1.07 % when compared to electromechanical efficiency at 6 LPH.

Similarly calculation is done with R134a + 0.4 % Al<sub>2</sub>O<sub>3</sub> and R134a + 0.8 % Al<sub>2</sub>O<sub>3</sub> at constant heat flux 25-26<sup>0</sup>C. The results shows that with R134a + 0.4 % Al<sub>2</sub>O<sub>3</sub> at 6LPH electromechanical efficiency is found to be 67.56 % whereas at 8 LPH and 10LPH is 68.29 % and 68.63 % respectively. Therefore it is found that, electromechanical efficiency is improved by 1.08 % at 8LPH and at 10LPH electromechanical efficiency is improved by 1.58 % when compared to electromechanical efficiency at 6 LPH.

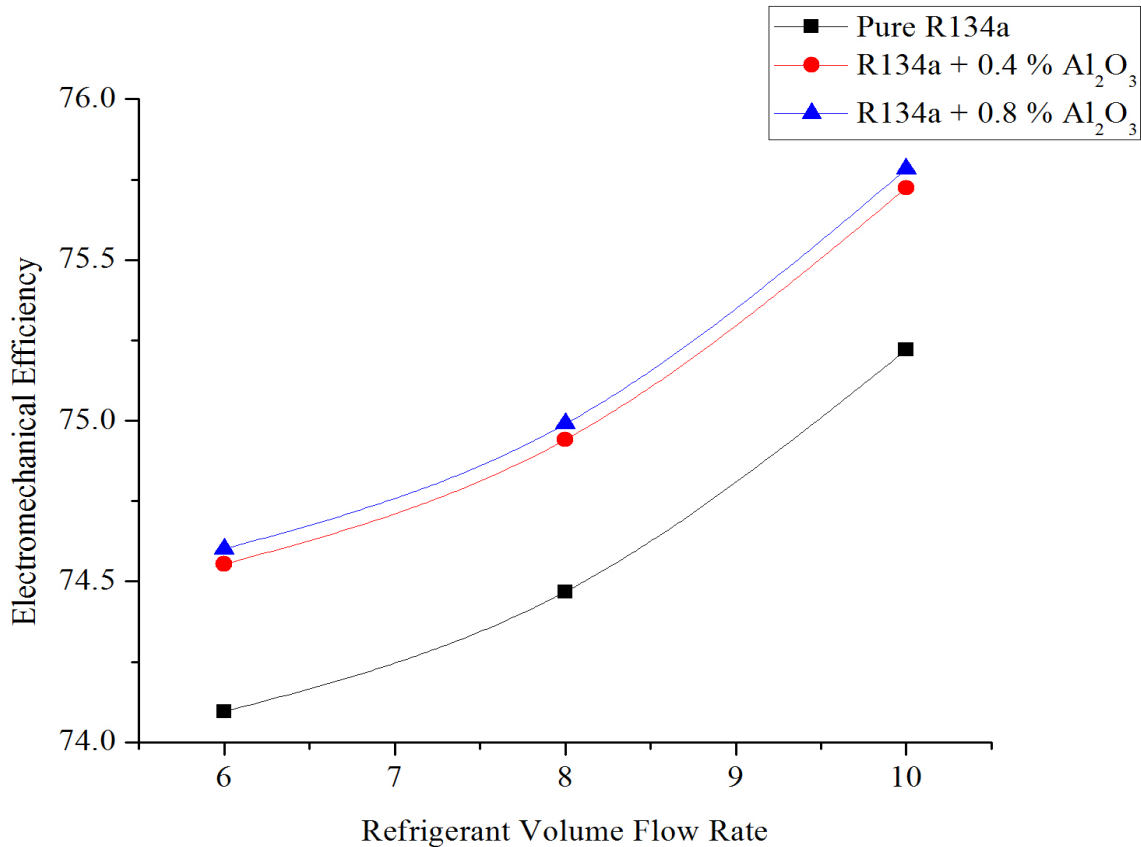


Figure 5.19: Electromechanical Efficiency comparison for heat flux at 25-26<sup>0</sup>C and volume flow rate 6LPH, 8LPH and 10 LPH

Now with R134a + 0.8 % Al<sub>2</sub>O<sub>3</sub> at 6LPH C.O.P. is found to be 67.76 % whereas at 8 LPH and 10LPH is 68.09 % and 68.63 % respectively. Therefore it is calculated that, electromechanical efficiency is improved by 0.49 % at 8LPH and at 10LPH electromechanical efficiency is improved by 1.28 % when compared to electromechanical efficiency at 6 LPH.

Now comparison according to constant heat flux first calculation is done on 30-31<sup>0</sup>C at 6LPH, 8LPH and 10LPH volume flow rate. Firstly Figure 5.20 show that with pure R134a at 6LPH electromechanical efficiency is found to be 67.58 % whereas at 8 LPH and 10LPH is 67.82 % and 69.04 % respectively. Therefore it is calculated that, electromechanical efficiency is improved by 0.36 % at 8LPH and at 10LPH electromechanical efficiency is improved by 2.17 % when compared to electromechanical efficiency at 6 LPH.

Similarly calculation is done with R134a + 0.4 %  $\text{Al}_2\text{O}_3$  and R134a + 0.8 %  $\text{Al}_2\text{O}_3$  at constant heat flux 30-31<sup>0</sup>C. The results shows that with R134a + 0.4 %  $\text{Al}_2\text{O}_3$  at 6LPH electromechanical efficiency is found to be 69.43 % whereas at 8 LPH and 10LPH is 69.76 % and 71.04 % respectively. Therefore it is found that, electromechanical efficiency is improved by 0.48 % at 8LPH and at 10LPH electromechanical efficiency is improved by 2.32 % when compared to electromechanical efficiency at 6 LPH.

Now with R134a + 0.8 %  $\text{Al}_2\text{O}_3$  at 6LPH electromechanical efficiency is found to be 69.55 % whereas at 8 LPH and 10LPH is 70.36 % and 71.66 % respectively. Therefore it is calculated that, electromechanical efficiency is improved by 1.16 % at 8LPH and at 10LPH electromechanical efficiency is improved by 3.03 % when compared to electromechanical efficiency at 6 LPH.

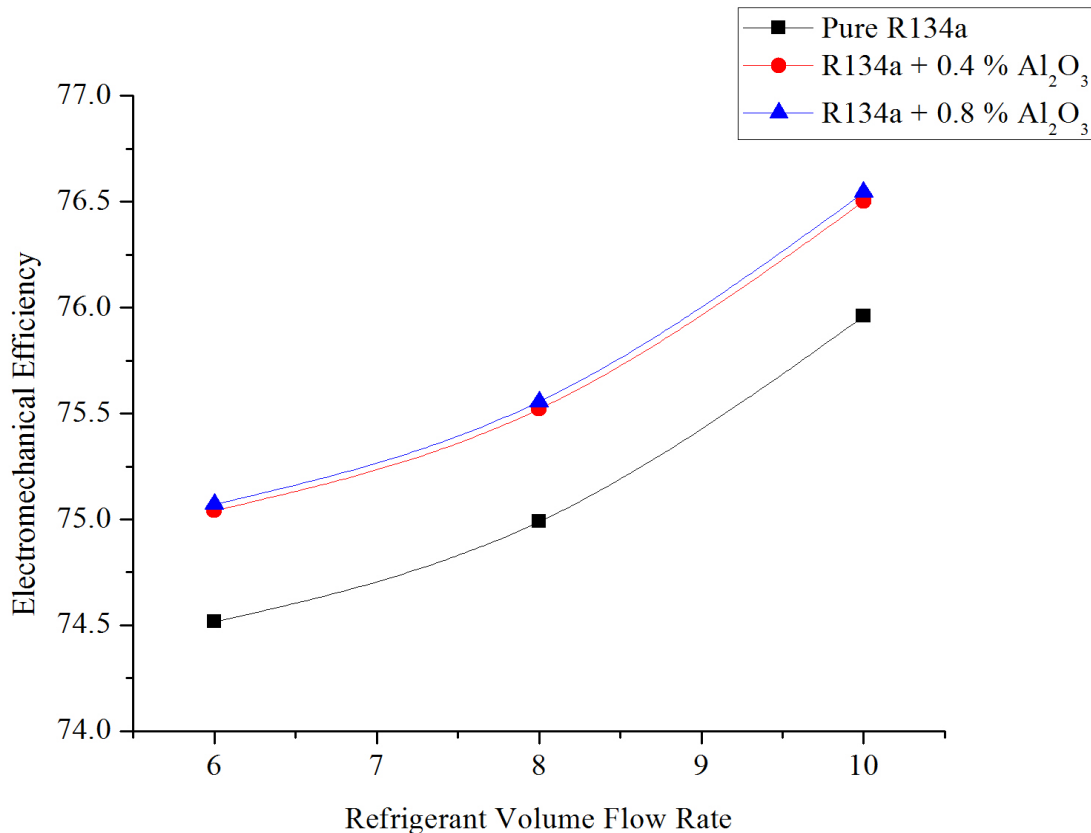


Figure 5.20: Electromechanical Efficiency comparison for heat flux at 30-31<sup>0</sup>C and volume flow rate 6LPH, 8LPH and 10 LPH

Now comparison according to constant heat flux first calculation is done on 35-36<sup>0</sup>C at 6LPH, 8LPH and 10LPH volume flow rate. Firstly Figure 5.21 show that with pure R134a at 6LPH electromechanical efficiency is found to be 69.46 % whereas at 8 LPH and 10LPH is 69.89 % and 70.41 % respectively. Therefore it is calculated that, electromechanical efficiency is improved by 0.61 % at 8LPH and at 10LPH electromechanical efficiency is improved by 1.36 % when compared to electromechanical efficiency at 6 LPH.

Similarly calculation is done with R134a + 0.4 % Al<sub>2</sub>O<sub>3</sub> and R134a + 0.4 % Al<sub>2</sub>O<sub>3</sub> at constant heat flux 35-36<sup>0</sup>C. The results shows that with R134a + 0.4 % Al<sub>2</sub>O<sub>3</sub> at 6LPH electromechanical efficiency is found to be 71.60 % whereas at 8 LPH and 10LPH is 72.00 % and 72.73 % respectively. Therefore it is found that, electromechanical efficiency is improved by 0.55 % at 8LPH and at 10LPH electromechanical efficiency is improved by 1.57 % when compared to electromechanical efficiency at 6 LPH.

Now with R134a + 0.4 % Al<sub>2</sub>O<sub>3</sub> at 6LPH electromechanical efficiency is found to be 67.05 whereas at 8 LPH and 10LPH is 72.58 % and 73.20 % respectively. Therefore it is calculated that, electromechanical efficiency is improved by 0.73 % at 8LPH and at 10LPH electromechanical efficiency is improved by 1.60 % when compared to electromechanical efficiency at 6 LPH.

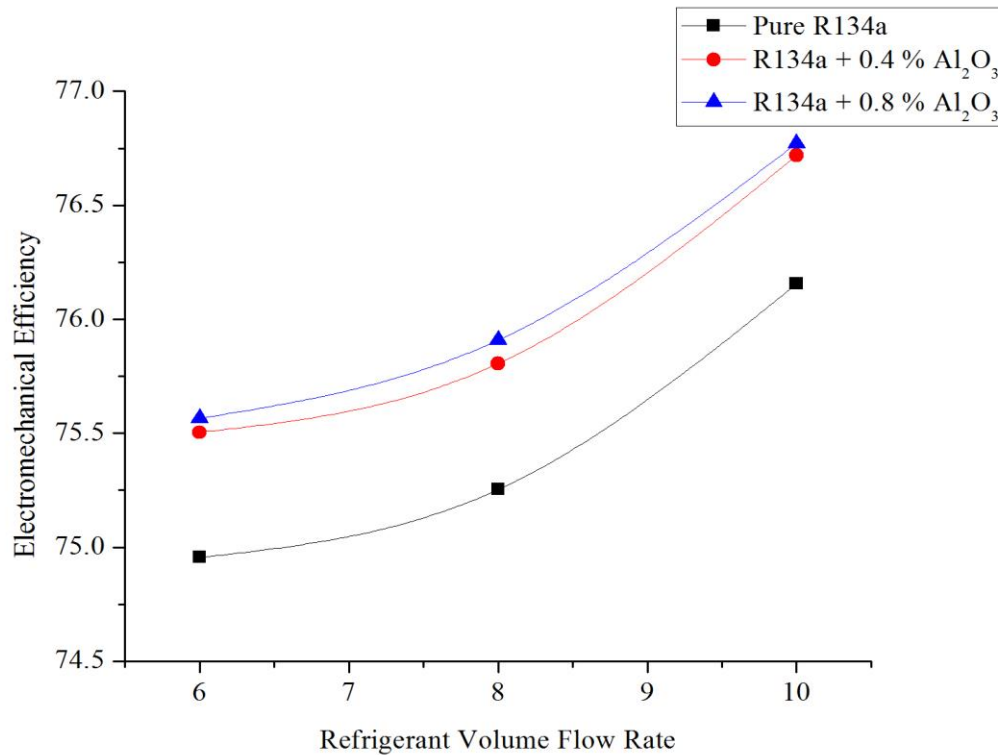


Figure 5.21: Electromechanical Efficiency comparison for heat flux at 35-36<sup>0</sup>C and volume flow rate 6LPH, 8LPH and 10 LPH

As Figure 5.18, Figure 5.19, Figure 5.20 and Figure 5.21 shows that by using nanorefrigerant (R134a + 0.4 % Al<sub>2</sub>O<sub>3</sub> and R134a + 0.8 % Al<sub>2</sub>O<sub>3</sub>) the electromechanical efficiency is improved and as volume flow rate increases the electromechanical efficiency is found to be improved. By increase in volume flow rate both actual specific enthalpy change as well as power consumption by compressor increases but increment in actual specific enthalpy change is more than the increment in power consumption by compressor due to increase in mass flow so, this may affect improvement in electromechanical efficiency with increment in volume flow rate 6LPH to 10LPH. Hence the reciprocating refrigerant compressor works better at higher volume flow rate.

#### 5.4 Overall efficiency

The overall efficiency defines as the energy gain by the refrigerant adiabatically how much resembles the electrical power input to compressor. The overall efficiency is combination

product of adiabatic efficiency and electromechanical efficiency. The overall efficiency calculates as the ratio energy gain (in KW) ideally to electrical power input to compressor which can be measured by energy meter. The overall efficiency for a compression process can be calculated with the equation

$$\text{Overall Efficiency } (\eta_o) = \frac{\dot{m}_2 h_2 - \dot{m}_1 h_1}{W_{ele}} \quad (9)$$

Overall efficiency can be found by equation

$$\text{Overall Efficiency } (\eta_o) = \eta_{adia} \cdot \eta_{eleme} \quad (10)$$

### 5.5.1 Overall Efficiency Comparison According to Constant Volume Flow Rate

Firstly the experiment is performed with 10 LPH volume flow rate of refrigerant maintaining constant evaporator load temperature around 20-21°C. As Figure 5.22 shows, the overall efficiency with pure R134a is found to be 49.67 % whereas with R134a + 0.4 % Al<sub>2</sub>O<sub>3</sub> and R134a + 0.8 % Al<sub>2</sub>O<sub>3</sub>, overall efficiency is 50.81 % and 51.09 % respectively. Therefore it is found that, by using R134a + 0.4 % Al<sub>2</sub>O<sub>3</sub> nanorefrigerant sample overall efficiency is improved by 2.24 % and with R134a + 0.8 % Al<sub>2</sub>O<sub>3</sub> overall efficiency is improved by 2.83 % when compared to overall efficiency of pure refrigerant R134a.

Similarly readings are taken at heat flux 25-26°C, 30-35°C, and 35-36 °C at same flow rate. The C.O.P at 25-26°C heat flux with pure R134a is calculated to be 50.46 % whereas with R134a + 0.4 % Al<sub>2</sub>O<sub>3</sub> and R134a + 0.8 % Al<sub>2</sub>O<sub>3</sub>, overall efficiency is 51.97 % and 52.01 % respectively. Therefore it is found that, by using R134a + 0.4 % Al<sub>2</sub>O<sub>3</sub> nanorefrigerant sample overall efficiency is improved by 2.98 % and with R134a + 0.8 % Al<sub>2</sub>O<sub>3</sub> overall efficiency is improved by 3.06 % when compared to overall efficiency of pure refrigerant R134a.

The C.O.P at 30-31°C heat flux with pure R134a is calculated to be 52.43 % whereas with R134a + 0.4 % Al<sub>2</sub>O<sub>3</sub> and R134a + 0.8 % Al<sub>2</sub>O<sub>3</sub>, overall efficiency is 55.35 % and 55.85 % respectively. Therefore it is found that, by using R134a + 0.4 % Al<sub>2</sub>O<sub>3</sub> nanorefrigerant sample overall efficiency is improved by 3.63 % and with R134a + 0.8 % Al<sub>2</sub>O<sub>3</sub> overall efficiency is improved by 5.59 % when compared to overall efficiency of pure refrigerant R134a.

The C.O.P at 35-36°C heat flux with pure R134a is calculated to be 53.62 % whereas with R134a + 0.4 % Al<sub>2</sub>O<sub>3</sub> and R134a + 0.8 % Al<sub>2</sub>O<sub>3</sub>, overall efficiency is 55.79 % and 56.21 % respectively.

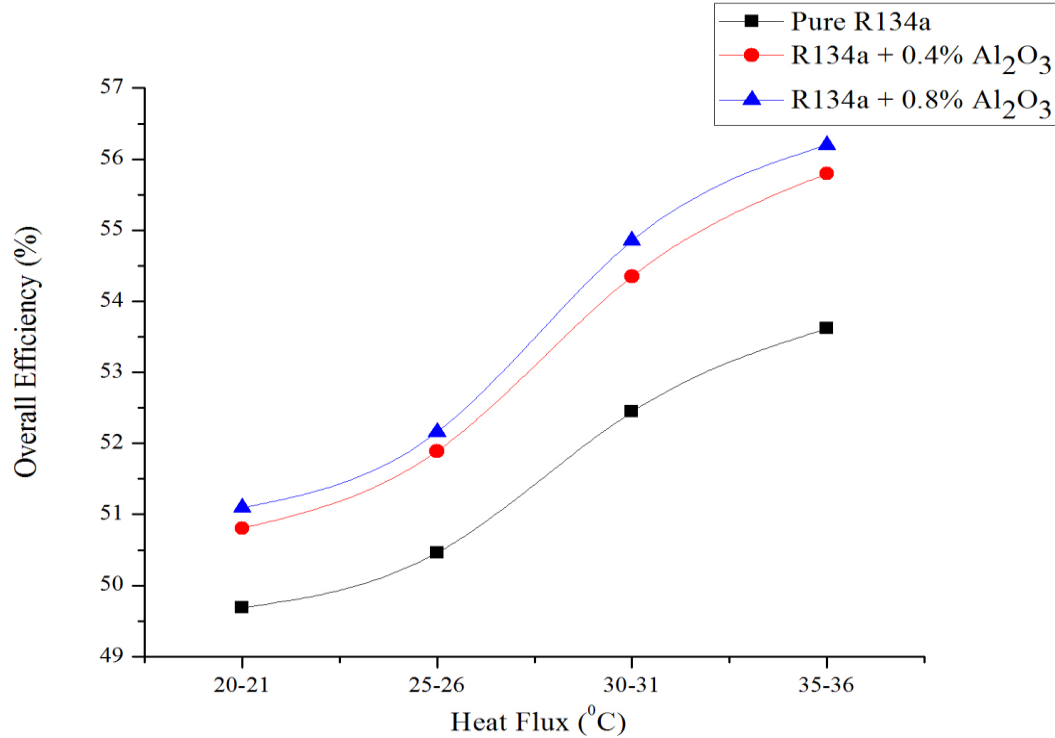


Figure 5.22: Overall Efficiency comparison for at 10 LPH volume flow rate and heat flux at 20-21°C, 25-26°C, 30-31°C and 35-36°C

Therefore it is found that, by using R134a + 0.4 % Al<sub>2</sub>O<sub>3</sub> nanorefrigerant sample overall efficiency is improved by 5.06 % and with R134a + 0.8 % Al<sub>2</sub>O<sub>3</sub> overall efficiency is improved by 5.81 % when compared to overall efficiency of pure refrigerant R134a.

After 10 LPH volume flow rate similar experiment is performed with 8 LPH volume flow rate of refrigerant maintaining constant evaporator load temperature around 20-21°C. As Figure 5.23 shows, the overall efficiency with pure R134a is found to be 48.71 % whereas with R134a+ 0.4 % Al<sub>2</sub>O<sub>3</sub> and R134a + 0.8 % Al<sub>2</sub>O<sub>3</sub>, overall efficiency is 49.79 % and 50.47 % respectively. Therefore it is found that, by using R134a + 0.4 % Al<sub>2</sub>O<sub>3</sub> nanorefrigerant sample overall efficiency is improved by 2.19 % and with R134a + 0.8 % Al<sub>2</sub>O<sub>3</sub> overall efficiency is improved by 3.53 % when compared to overall efficiency of pure refrigerant R134a.

Similarly readings are taken at heat flux 25-26°C, 30-35°C, and 35-36 °C at same flow rate. The overall efficiency at 25-26°C heat flux with pure R134a is calculated to be 49.68 % whereas with R134a + 0.4 % Al<sub>2</sub>O<sub>3</sub> and R134a + 0.8 % Al<sub>2</sub>O<sub>3</sub>, overall efficiency is 51.17 % and 51.06 % respectively. Therefore it is found that, by using R134a + 0.4 % Al<sub>2</sub>O<sub>3</sub> nanorefrigerant sample overall efficiency is improved by 3.00 % and with R134a + 0.8 % Al<sub>2</sub>O<sub>3</sub> overall efficiency is improved by 2.77 % when compared to overall efficiency of pure refrigerant R134a.

The overall efficiency at 30-31°C heat flux with pure R134a is calculated to be 50.85 % whereas with R134a + 0.4 % Al<sub>2</sub>O<sub>3</sub> and R134a + 0.8 % Al<sub>2</sub>O<sub>3</sub>, overall efficiency is 52.69 % and 53.16 % respectively. Therefore it is found that, by using R134a + 0.4 % Al<sub>2</sub>O<sub>3</sub> nanorefrigerant sample overall efficiency is improved by 3.59 % and with R134a + 0.4 % Al<sub>2</sub>O<sub>3</sub> overall efficiency is improved by 5.53 % when compared to overall efficiency of pure refrigerant R134a.

The overall efficiency at 35-36°C heat flux with pure R134a is calculated to be 52.49 % whereas with R134a + 0.4 % Al<sub>2</sub>O<sub>3</sub> and R134a + 0.8 % Al<sub>2</sub>O<sub>3</sub>, overall efficiency is 55.48 % and 55.98 % respectively. Therefore it is found that, by using R134a + 0.4 % Al<sub>2</sub>O<sub>3</sub> nanorefrigerant sample overall efficiency is improved by 3.79 % and with R134a + 0.8 % Al<sub>2</sub>O<sub>3</sub> overall efficiency is improved by 5.75 % when compared to overall efficiency of pure refrigerant R134a.

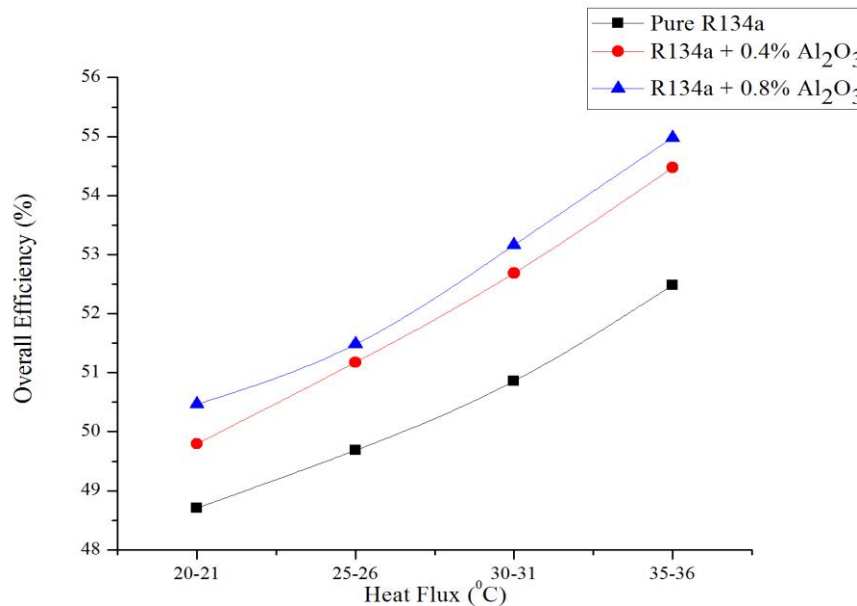


Figure 5.23: Overall Efficiency comparison for at 8 LPH volume flow rate and heat flux at 20-21°C, 25-26 °C, 30-31°C and 35-36°C

After 8 LPH volume flow rate similar experiment is performed with 6 LPH volume flow rate of refrigerant maintaining constant evaporator load temperature around 20-21°C. As Figure 5.24 shows, the overall efficiency with pure R134a is found to be 47.75 % whereas with R134a+ 0.4 % Al<sub>2</sub>O<sub>3</sub> and R134a + 0.8 % Al<sub>2</sub>O<sub>3</sub>, overall efficiency is 48.64 % and 48.81 % respectively. Therefore it is found that, by using R134a + 0.4 % Al<sub>2</sub>O<sub>3</sub> nanorefrigerant sample overall efficiency is improved by 1.86 % and with R134a + 0.8 % Al<sub>2</sub>O<sub>3</sub> overall efficiency is improved by 2.24 % when compared to overall efficiency of pure refrigerant R134a.

Similarly readings are taken at heat flux 25-26°C, 30-35°C, and 35-36 °C at same flow rate. The overall efficiency at 25-26°C heat flux with pure R134a is calculated to be 49.18 % whereas with R134a + 0.4 % Al<sub>2</sub>O<sub>3</sub> and R134a + 0.8 % Al<sub>2</sub>O<sub>3</sub>, overall efficiency is 50.37 % and 50.55 % respectively. Therefore it is found that, by using R134a + 0.4 % Al<sub>2</sub>O<sub>3</sub> nanorefrigerant sample overall efficiency is improved by 2.41 % and with R134a + 0.8 % Al<sub>2</sub>O<sub>3</sub> overall efficiency is improved by 2.96 % when compared to overall efficiency of pure refrigerant R134a.

The overall efficiency at 30-31°C heat flux with pure R134a is calculated to be 50.36 % whereas with R134a + 0.4 % Al<sub>2</sub>O<sub>3</sub> and R134a + 0.8 % Al<sub>2</sub>O<sub>3</sub>, overall efficiency is 52.10 % and 52.21 % respectively. Therefore it is found that, by using R134a + 0.4 % Al<sub>2</sub>O<sub>3</sub> nanorefrigerant sample overall efficiency is improved by 3.47 % and with R134a + 0.8 % Al<sub>2</sub>O<sub>3</sub> overall efficiency is improved by 3.68 % when compared to overall efficiency of pure refrigerant R134a.

The overall efficiency at 35-36°C heat flux with pure R134a is calculated to be 52.07 % whereas with R134a + 0.4 % Al<sub>2</sub>O<sub>3</sub> and R134a + 0.8 % Al<sub>2</sub>O<sub>3</sub>, overall efficiency is 55.06 % and 55.44 % respectively. Therefore it is found that, by using R134a + 0.4 % Al<sub>2</sub>O<sub>3</sub> nanorefrigerant sample overall efficiency is improved by 3.86 % and with R134a + 0.8 % Al<sub>2</sub>O<sub>3</sub> overall efficiency is improved by 5.58 % when compared to overall efficiency of pure refrigerant R134a.

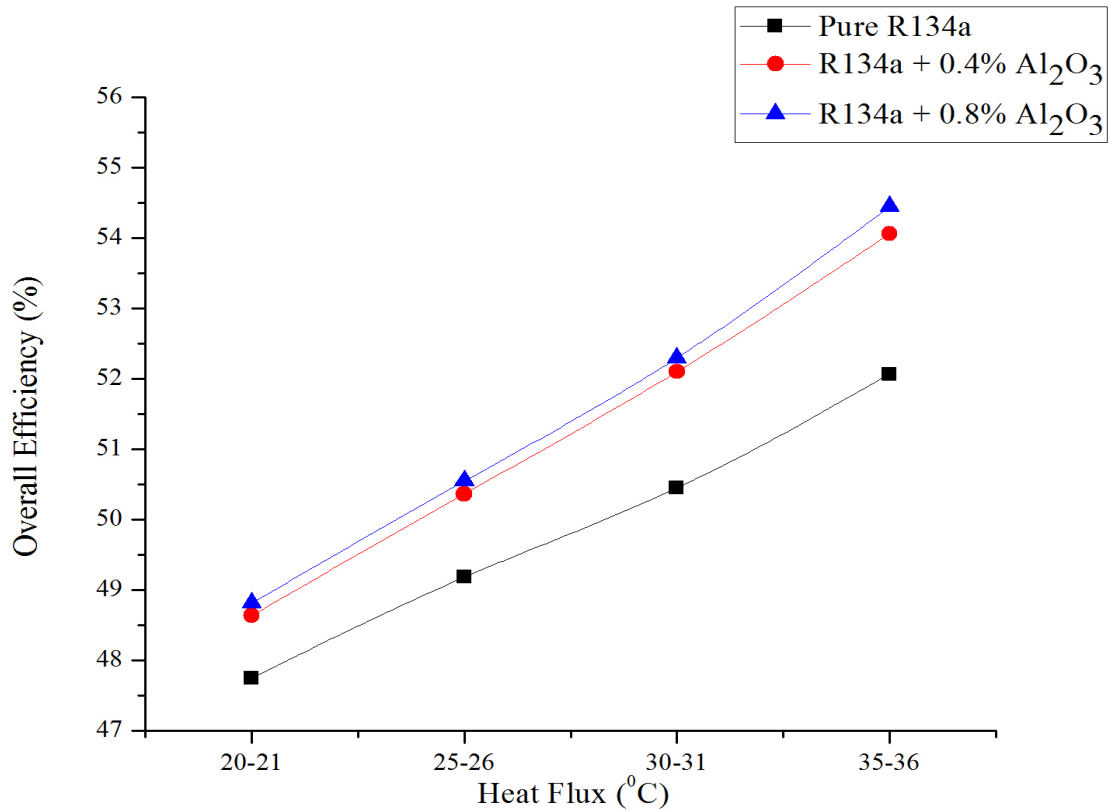


Figure 5.24: Overall Efficiency comparison for at 6 LPH volume flow rate and heat flux at 20-21<sup>0</sup>C, 25-26 <sup>0</sup>C, 30-31<sup>0</sup>C and 35-36<sup>0</sup>C

As Figure 5.22, Figure 5.23 and Figure 5.24 shows that by using nanorefrigerant (R134a + 0.4 % Al<sub>2</sub>O<sub>3</sub> and R134a + 0.8 % Al<sub>2</sub>O<sub>3</sub>) the overall efficiency is improved in every case of heat flux (20-21, 25-26, 30-31, 35-36). As discuss before by using nanorefrigerant the adiabatic efficiency and the electromechanical efficiency both improve so, the overall efficiency also may increase.

### 5.5.2 Overall Efficiency Comparison According to Constant Heat Flux

To comparison according to constant heat flux first calculation is done on 20-21<sup>0</sup>C at 6LPH, 8LPH and 10LPH volume flow rate. Firstly Figure 5.25 show that with pure R134a at 6LPH overall efficiency is found to be 47.75 % whereas at 8 LPH and 10LPH is 48.71 % and 49.69 % respectively. Therefore it is calculated that, overall efficiency is improved by 2.02 % at 8LPH

and at 10LPH overall efficiency is improved by 5.07 % when compared to overall efficiency at 6 LPH.

Similarly calculation is done with R134a + 0.4 %  $\text{Al}_2\text{O}_3$  and R134a + 0.8 %  $\text{Al}_2\text{O}_3$  at constant heat flux 20-21<sup>0</sup>C. The results shows that with R134a + 0.4 %  $\text{Al}_2\text{O}_3$  at 6LPH overall efficiency is found to be 48.64 % whereas at 8 LPH and 10LPH is 49.80 % and 50.81 % respectively. Therefore it is calculated that, overall efficiency is improved by 2.39 % at 8LPH and at 10LPH overall efficiency is improved by 5.46 % when compared to overall efficiency at 6 LPH.

Now with R134a + 0.8 %  $\text{Al}_2\text{O}_3$  at 6LPH overall efficiency is found to be 48.81 % whereas at 8 LPH and 10LPH is 50.47 % and 51.09 % respectively. Therefore it is calculated that, overall efficiency is improved by 3.38 % at 8LPH and at 10LPH overall efficiency is improved by 5.67 % when compared to overall efficiency at 6 LPH.

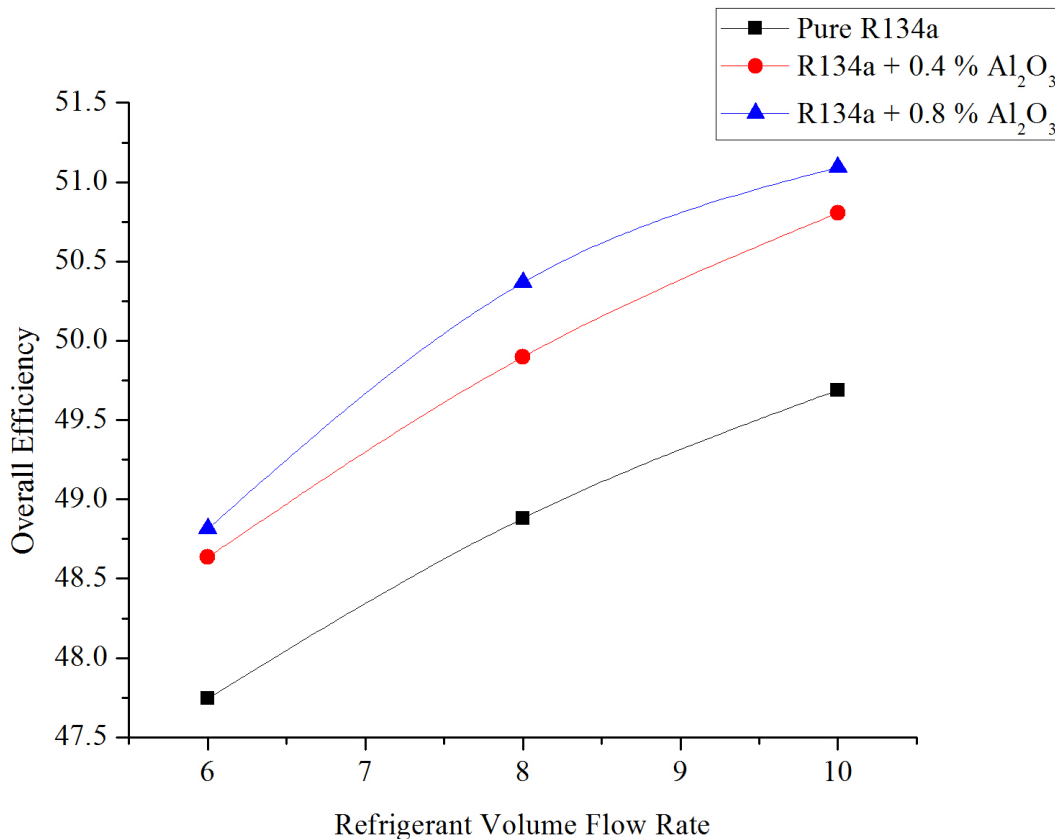


Figure 5.25: Overall Efficiency comparison for heat flux at 20-21<sup>0</sup>C and volume flow rate 6LPH, 8LPH and 10 LPH

Now comparison according to constant heat flux first calculation is done on 25-26<sup>0</sup>C at 6LPH, 8LPH and 10LPH volume flow rate. Firstly Figure 5.26 show that with pure R134a at 6LPH overall efficiency is found to be 49.18 % whereas at 8 LPH and 10LPH is 49.68 % and 50.46 % respectively. Therefore it is calculated that, overall efficiency is improved by 1.03 % at 8LPH and at 10LPH overall efficiency is improved by 2.60 % when compared to overall efficiency at 6 LPH.

Similarly calculation is done with R134a + 0.4 % Al<sub>2</sub>O<sub>3</sub> and R134a + 0.8 % Al<sub>2</sub>O<sub>3</sub> at constant heat flux 25-26<sup>0</sup>C. The results shows that with R134a + 0.4 % Al<sub>2</sub>O<sub>3</sub> at 6LPH overall efficiency is found to be 50.37 % whereas at 8 LPH and 10LPH is 51.18 % and 51.97 % respectively. Therefore it is found that, overall efficiency is improved by 1.61 % at 8LPH and at 10LPH overall efficiency is improved by 3.18 % when compared to overall efficiency at 6 LPH.

Now with R134a + 0.8 % Al<sub>2</sub>O<sub>3</sub> at 6LPH C.O.P. is found to be 50.55 % whereas at 8 LPH and 10LPH is 51.06 % and 52.01 % respectively. Therefore it is calculated that, overall efficiency is improved by 1.01 % at 8LPH and at 10LPH overall efficiency is improved by 2.89 % when compared to overall efficiency at 6 LPH.

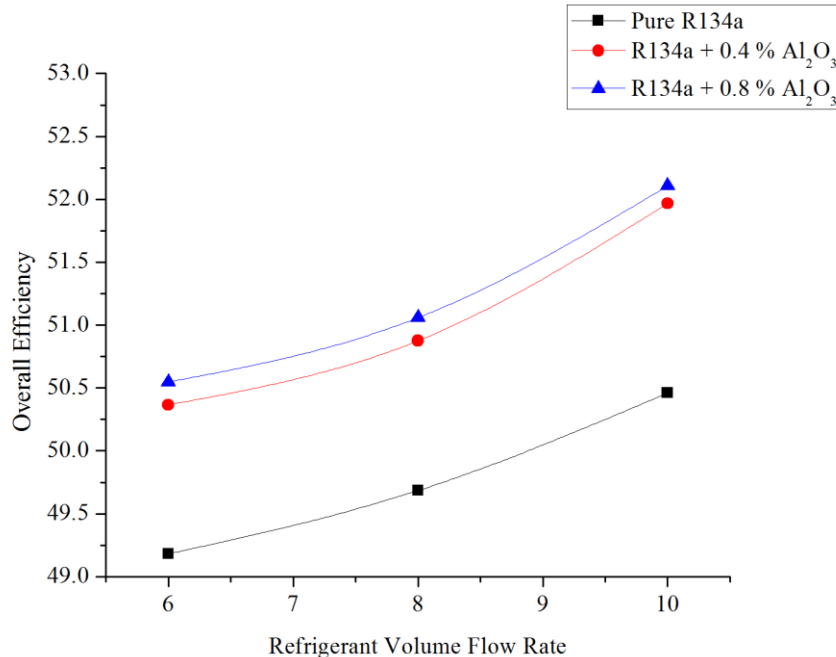


Figure 5.26: Overall Efficiency comparison for heat flux at 25-26<sup>0</sup>C and volume flow rate 6LPH, 8LPH and 10 LPH

Now comparison according to constant heat flux first calculation is done on 30-31<sup>0</sup>C at 6LPH, 8LPH and 10LPH volume flow rate. Firstly Figure 5.27 show that with pure R134a at 6LPH overall efficiency is found to be 50.36 % whereas at 8 LPH and 10LPH is 50.86 % and 52.44 % respectively. Therefore it is calculated that, overall efficiency is improved by 1.00 % at 8LPH and at 10LPH overall efficiency is improved by 5.15 % when compared to overall efficiency at 6 LPH.

Similarly calculation is done with R134a + 0.4 % Al<sub>2</sub>O<sub>3</sub> and R134a + 0.8 % Al<sub>2</sub>O<sub>3</sub> at constant heat flux 30-31<sup>0</sup>C. The results shows that with R134a + 0.4 % Al<sub>2</sub>O<sub>3</sub> at 6LPH overall efficiency is found to be 52.10 % whereas at 8 LPH and 10LPH is 52.69 % and 55.35 % respectively. Therefore it is found that, overall efficiency is improved by 1.12 % at 8LPH and at 10LPH overall efficiency is improved by 5.31 % when compared to overall efficiency at 6 LPH.

Now with R134a + 0.8 % Al<sub>2</sub>O<sub>3</sub> at 6LPH overall efficiency is found to be 52.21 % whereas at 8 LPH and 10LPH is 53.16 % and 55.85 % respectively. Therefore it is calculated that, overall efficiency is improved by 1.82 % at 8LPH and at 10LPH overall efficiency is improved by 5.05 % when compared to overall efficiency at 6 LPH.

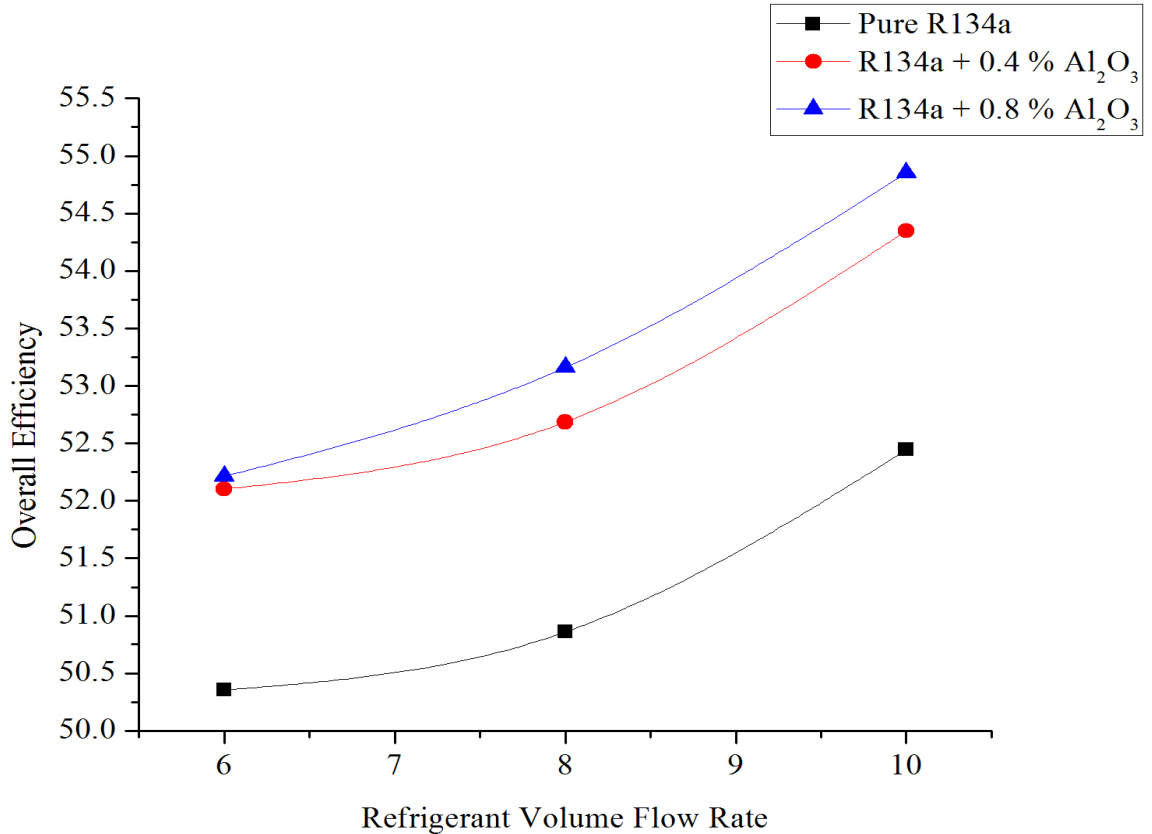


Figure 5.27: Overall Efficiency comparison for heat flux at 30-31<sup>0</sup>C and volume flow rate 6LPH, 8LPH and 10 LPH

Now comparison according to constant heat flux first calculation is done on 35-36<sup>0</sup>C at 6LPH, 8LPH and 10LPH volume flow rate. Firstly Figure 5.28 show that with pure R134a at 6LPH overall efficiency is found to be 52.07 % whereas at 8 LPH and 10LPH is 52.49 % and 53.62 % respectively. Therefore it is calculated that, overall efficiency is improved by 0.81 % at 8LPH and at 10LPH overall efficiency is improved by 2.98 % when compared to overall efficiency at 6 LPH.

Similarly calculation is done with R134a + 0.4 % Al<sub>2</sub>O<sub>3</sub> and R134a + 0.4 % Al<sub>2</sub>O<sub>3</sub> at constant heat flux 35-36<sup>0</sup>C. The results shows that with R134a + 0.4 % Al<sub>2</sub>O<sub>3</sub> at 6LPH overall efficiency is found to be 55.06 % whereas at 8 LPH and 10LPH is 55.48 % and 55.79 % respectively. Therefore it is found that, overall efficiency is improved by 0.85 % at 8LPH and at 10LPH overall efficiency is improved by 3.56 % when compared to overall efficiency at 6 LPH.

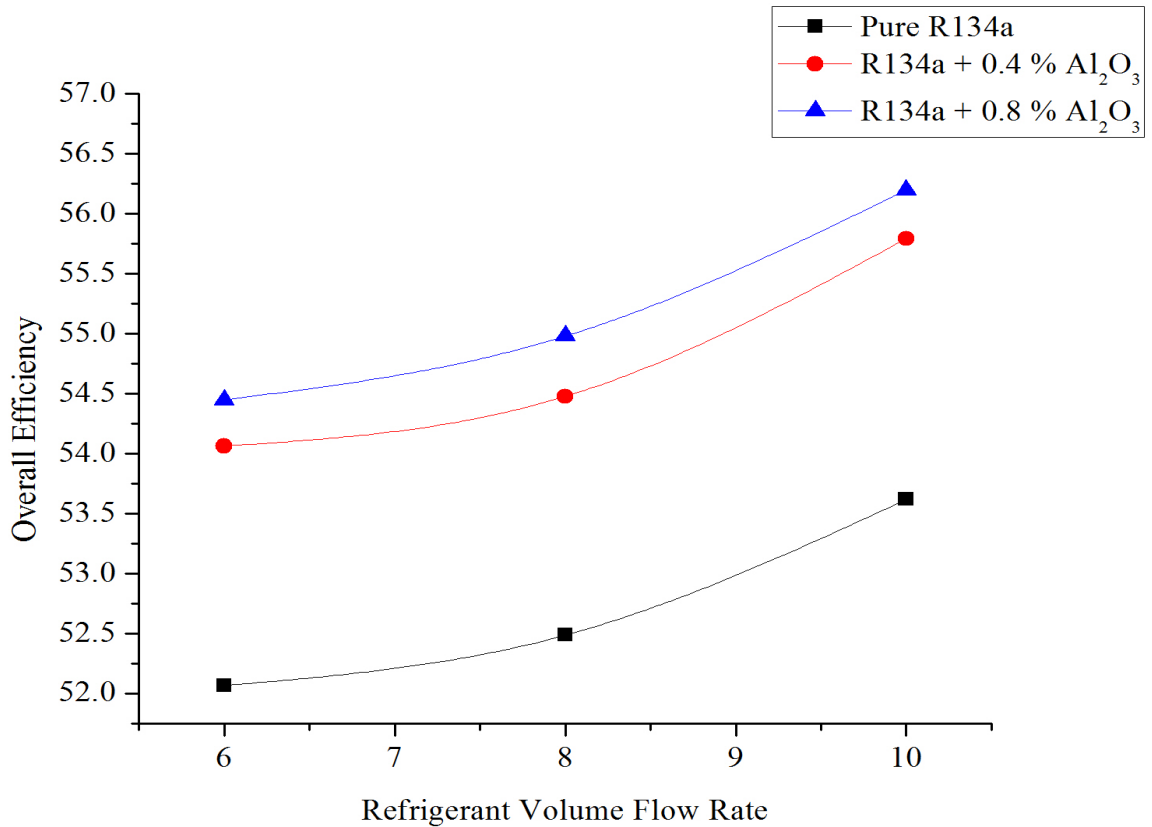


Figure 5.28: Overall Efficiency comparison for heat flux at 35-36<sup>0</sup>C and volume flow rate 6LPH, 8LPH and 10 LPH

Now with R134a + 0.4 % Al<sub>2</sub>O<sub>3</sub> at 6LPH overall efficiency is found to be 55.45 % whereas at 8 LPH and 10LPH is 55.98 % and 56.20 % respectively. Therefore it is calculated that, overall efficiency is improved by 0.98 % at 8LPH and at 10LPH overall efficiency is improved by 3.22 % when compared to overall efficiency at 6 LPH.

As Figure 5.25, Figure 5.26, Figure 5.27 and Figure 5.28 show that by using nanorefrigerant (R134a + 0.4 % Al<sub>2</sub>O<sub>3</sub> and R134a + 0.8 % Al<sub>2</sub>O<sub>3</sub>) the overall efficiency is improved and as volume flow rate increases the overall efficiency is found to be improved. As discuss before by using nanorefrigerant the adiabatic efficiency and the electromechanical efficiency both improve so, the overall efficiency also may increase.

# Chapter - 6

## Conclusions and Future Scope

---

### 6.1 Conclusions

In this study the performance of domestic refrigerator based experimental test setup has been investigated by using pure refrigerant R134 and nanorefrigerant (R134a + Al<sub>2</sub>O<sub>3</sub>). Experimental facility is developed in our refrigeration and air conditioning laboratory. Results show that the use of nanorefrigerant (R134a + Al<sub>2</sub>O<sub>3</sub>) instead of pure refrigerant R134a is advantageous. It has been observed that there is a significant improvement in the performance of the system when nanoparticles are used along with conventional refrigerant (R134a) within certain limit. Following conclusions are derived from this experimental study:-

(i) Coefficient of performance (COP) of vapour compression system is found to be improved by dispersing Al<sub>2</sub>O<sub>3</sub> nanoparticles in R134a refrigerant. This improvement is maximum (1.62 % to 5.45 %) with 0.8 % mass fraction of Al<sub>2</sub>O<sub>3</sub> in refrigerant for all volume flow rates and evaporator heat fluxes. Higher heat flux results increase (2.02 % to 6.78 %) in COP of the system at all refrigerant volume flow rates and also at pure R134a and nanorefrigerant (R134a + Al<sub>2</sub>O<sub>3</sub>).

(ii) The coefficient of performance (COP) of vapour compression system is found to be decreasing with increase in volume flow rate (from 6LPH to 10LPH) for both pure refrigerant and nanorefrigerant, hence vapour compression refrigeration system operates more efficiently at lower volume flow rate.

(iii) Adiabatic efficiency of reciprocating refrigerant compressor is found to be improved by dispersing Al<sub>2</sub>O<sub>3</sub> nanoparticles in R134a refrigerant. This improvement is maximum (1.29 % to 3.98 %) with 0.8 % mass fraction of Al<sub>2</sub>O<sub>3</sub> in refrigerant for all volume flow rates and evaporator heat fluxes compare to 0.4 % mass fraction of Al<sub>2</sub>O<sub>3</sub> and pure R134a. Higher heat flux results increase (1.21 % to 4.45 %) in adiabatic efficiency of the system at all refrigerant volume flow rates and also at pure R134a and nanorefrigerant (R134a + Al<sub>2</sub>O<sub>3</sub>). Experimental results show that the reciprocating compressor operates adiabatically more efficiently at higher heat flux.

(iv) The adiabatic efficiency of reciprocating refrigerant compressor is found to be improved(1.29 % to 3.98 %) with increase in volume flow rate (from 6LPH to 10LPH) for both pure refrigerant and nanorefrigerant, hence The adiabatic efficiency of reciprocating refrigerant compressor more when it operates at higher volume flow rate.

(v) Electromechanical efficiency of reciprocating refrigerant compressor is found to be marginally improved by dispersing  $\text{Al}_2\text{O}_3$  nanoparticles in R134a refrigerant. This improvement is maximum (0.56 % to .85 %) with 0.8 % mass fraction of  $\text{Al}_2\text{O}_3$  in refrigerant for all volume flow rates and evaporator heat fluxes compare to 0.4 % mass fraction of  $\text{Al}_2\text{O}_3$  and pure R134a. Higher heat flux results increase (0.3 % to 1.72 %) in electromechanical efficiency of the system at all refrigerant volume flow rates and also at pure R134a and nanorefrigerant ( $\text{R134a} + \text{Al}_2\text{O}_3$ ). Experimental results show that the reciprocating compressor operates mechanically and electrically more efficiently at higher heat flux.

(vi) The Electromechanical efficiency of reciprocating refrigerant compressor is found to be improved(0.36 % to 3.03 %) with increase in volume flow rate (from 6LPH to 10LPH) for both pure refrigerant and nanorefrigerant, hence The electromechanical efficiency of reciprocating refrigerant compressor more when it operates at higher volume flow rate.

(vii) Overall efficiency of reciprocating refrigerant compressor is found to be improved by dispersing  $\text{Al}_2\text{O}_3$  nanoparticles in R134a refrigerant. This improvement is maximum (1.86 to 5.87 %) with 0.8 % mass fraction of  $\text{Al}_2\text{O}_3$  in refrigerant for all volume flow rates and evaporator heat fluxes compare to 0.4 % mass fraction of  $\text{Al}_2\text{O}_3$  and pure R134a. Higher heat flux results increase (0.3 % to 1.72 %) in Overall efficiency of the system at all refrigerant volume flow rates and also at pure R134a and nanorefrigerant ( $\text{R134a} + \text{Al}_2\text{O}_3$ ). Experimental results show that the reciprocating compressor operates totally more efficiently at higher heat flux.

(vii) Overall efficiency of reciprocating refrigerant compressor is found to be improved(0.81 % to 4.67 %) with increase in volume flow rate (from 6LPH to 10LPH) for both pure refrigerant and nanorefrigerant, hence The overall efficiency of reciprocating refrigerant compressor more when it operates at higher volume flow rate.

(ix) System works normally with nanorefrigerant.

So from above conclusions it can be concluded that the use of R134a based nanofluid with 0.8 %  $\text{Al}_2\text{O}_3$  is beneficial in order to improve system performance and efficiencies of reciprocating refrigerant compressor. However the performance in long run is point of attention and requires further research.

## 6.2 Challenges with Nanofluids

The use of nanofluids in wide variety of applications appears promising. But the development in this field is hindered by certain points that include lack of agreement on results presented by various researchers, lack of theoretical appreciation of the reasons responsible for properties enhancement. Therefore, there are certain important issues that may receive greater attention in near future. Some major challenges includes:-

**(i) Long term stability of nanoparticles dispersion** - Preparation of homogeneous nanofluid remains a challenge as the nanoparticles always form clusters due to very strong interactions. However to have stable suspensions, therefore me physical and chemical methods have been introduced that include use of surfactant, modification of particle surface or apply strong opposite forces on suspended particles. Further the heat exchanger operates under laminar conditions, the use of nanofluids is found effective, but at same time high price and instability potential are also requires attention. Moreover, the long term stability of nanoparticles in base fluid is one of the very basic requirements of nanofluids applications. Despite to other common base fluids like ethylene glycol and water, the rapid agglomeration and settling of common nanoparticles has been found in refrigerants.

**(ii) Higher viscosity** - The viscosity of nanofluids normally increasing with increase particle concentration. In some investigations it has been reported that the nanofluid viscosity increasing rapidly with increased volume percentages of nanoparticles. The increased viscosity consumes more power to run the system.

**(iii) Lower specific heat** - Some investigations also found that nanofluids specific heat is lower than base fluid. It has been presented that ethylene glycol + CuO, ethylene glycol +  $\text{SiO}_2$  nanofluids and ethylene glycol +  $\text{Al}_2\text{O}_3$  nanofluids have lower specific heat as compared to base

fluids. An ideal refrigerant should always possess high specific heat in order to remove more heat from refrigerating space.

**(iv) High cost of Nanofluids** - Higher cost of production of nanofluids is among the main reasons that restrict their application in industry. Nanofluids can be produced by either one-step or two-step methods and both methods require sophisticated and advanced instruments. Hence high cost associated with nanofluids is also one of the major implications for its applications.

**(v) Fouling** - Although many nanofluids have been applied with single phase heat transfer application are found effective with enhancement in heat transfer characteristics. But when nanoparticles were applied in the boiling heat transfer applications, it has been pointed out that they caused fouling on heat transfer surface, hence result decrease in the heat transfer coefficient Praveen K. et al. [2009].

### **6.3 Future Scope**

The results show that nanofluids have notable potential to improve performance characteristics of reciprocating refrigerant compressor. However, it is unclear why there insignificant decrease in both discharge pressure and suction pressure is observed with significant increase mass fraction of nanoparticle. Moreover, challenges with particle circulation, dispersion and its effects on the cylinder walls, inlet valve and outlet valve of the compressor of refrigeration system have not been addressed. However, the present investigations are compelling that the further research should be undertaken. Future research is required to investigate the influence of the particle material, size, shape and concentration on compressor performance, long term stability of nanoparticles in refrigerant and effect of nanoparticles on various like volumetric efficiency, vibration and erosion on the walls of refrigeration compression system. Experimental results on the fundamental properties such as specific heat, density and viscosity of nanorefrigerants are limited in the literature therefore there are potentials to explore research to determine these properties experimentally also.

## References

- Apra C., Greco A. (2003) Performance evaluation of R22 and R407C in a vapour compression plant with reciprocating compressor. *Applied thermal engineering*, 23: 215-227.
- Baskaran A., Mathews P. K. (2012) A performance comparison of vapour compression refrigeration system using eco-friendly refrigerants of low global warming potential. *International Journal of Scientific and Research Publications*, 2(9): 1-8.
- Bi S., Shi L., Zhang L. (2008) Application of nanoparticles in domestic refrigerators, *International Compressor Engineering Conference*, Purdue University.
- Jwo T., Ting C. C., Wang W. U. (2008) Efficiency analysis of home refrigerators by replacing hydrocarbon refrigerants. *Applied Thermal Engineering*, 42(5): 697-701.
- Choi S.U.S. (2001) Enhancing thermal conductivity of fluids with nanoparticles. *ASME FED* 231, 66(2): 99–103.
- Coumaressin T., Palaniradja K. (2014) Performance analysis of a refrigeration system using nanofluid. *International Journal of Advanced Mechanical Engineering*, 28(1): 1834-1843.
- Dutta A. K., Aritome K. (2000) Performance Characteristics of Air-Conditioner Under Tropical Ambient Condition. *International Compressor Engineering Conference*, Purdue University.
- Gond R. K., Chaudhary R. P., Khan M. A., Jain G. (2016) Performance and exergy analysis of vapour compression refrigeration system using various alternative of R134a. *International Research Journal of Engineering and Technology (IRJET)*, 03(05): 2395 - 0056.
- Grace I., Datta D., Tassou S. A. (2002) Comparison of hermetic scroll and reciprocating compressors operating under varying refrigerant charge and load. *International Compressor Engineering Conference*, Purdue University.

- Grolier P. (2002) A method to estimate the performance of reciprocating compressors. *International Compressor Engineering Conference*, Purdue University.
- Hafez E.A., Taher S.H., Torki A.H.M., Hamad S.S. (2011) Heat transfer analysis of vapor compression system using nano Cuo-R134a. *International Conference on Advanced Materials Engineering IPCSIT*, 15(1): 150-173.
- Hao P., Guoliang D., Haitao H., Weiting J., Dawei Z., Kaijiang W. (2010) Nucleate pool boiling heat transfer characteristics of refrigerant/oil mixture with diamond nanoparticles. *International Journal of refrigeration*, 33: 347–58.
- Hao P., Guoliang D., Weitin J., Haitao H., Yifeng G. (2009) Heat transfer characteristics of refrigerant-based nanofluid flow boiling inside a horizontal smooth tube. *International Journal of Refrigeration*, 32: 1259–70.
- <http://en.wikipedia.org/wiki/1,1,1,2-Tetrafluoroethane>
- [http://en.wikipedia.org/wiki/Transmission\\_electron\\_microscopy](http://en.wikipedia.org/wiki/Transmission_electron_microscopy)
- [http://en.wikipedia.org/wiki/X-ray\\_Diffraction](http://en.wikipedia.org/wiki/X-ray_Diffraction)
- <http://www.refrigeration.com/learn-refrigeration/refrigeration-repairs/using-flare-fittings>
- Jwo C.S., Jeng L.Y., Teng T.P., Chang H. (2009) Effect of nano lubricant on the performance of Hydrocarbon refrigerant system. *J. Vac. Sci. Techno.*, 27(3): 1473-1477.
- Kedzierski M.A., Gong M. (2009) Effect of CuO nanolubricant on R134a pool boiling heat transfer with extensive measurement and analysis details. *National Institute of Standards and Technology*, 28(2): 410-431.
- Kilicarslan A., Müller N. (2005) A comparative study of water as a refrigerant with some current refrigerants. *International journal of energy research*, 29(11): 947-959.
- Kumar S.D., Elansezhian R. (2012) Experimental study on Al<sub>2</sub>O<sub>3</sub>-R134a nano refrigerant in refrigeration system. *International Journal of Modern Engineering Research*, 2(5): 3927-3929.

- Kurtulus O., Yang B., Lumpkin D., Groll E. A., Jestings L., Conde R. (2014) Performance and Operating Characteristics of a Novel Positive-Displacement Oil-Free CO<sub>2</sub> Compressor. *International Compressor Engineering Conference*, Purdue University
- Praveen K., Namburu DK., Das KM., Ravikanth SV. (2009) Numerical study of turbulent flow and heat transfer characteristics of nanofluids considering variable properties. *International Journal of Thermal Sciences*, 48: 290–302.
- Pandeya P. N., Soedel W. (1978) A generalized approach towards compressor performance analysis. *International Compressor Engineering Conference*, Purdue University
- Sauls J. R. (1982) Performance characteristics of fixed volume ratio compressors. *International Compressor Engineering Conference*, Purdue University.
- Subramani N., Prakash M. J., (2011) Experimental studies on a vapour compression system using nanorefrigerants. *International Journal of Engineering, Science and Technology*, 3(9): 95-102.
- Wang X., Xu X., Choi S.U.S. (1999) Thermal conductivity of nanoparticlefluid mixture. *J. Thermal Physics Heat Transfer*, 13(2): 474.
- Xiaoke L., Changjun Z., Xinyu V., Wenliang L. (2015) Stability and enhanced thermal conductivity of ethylene glycol-based SiC nanofluids. *International Journal of Heat and Mass Transfer*, 89(4): 613-619.
- Praveen K., Namburu K., Das M., Ravikanth V. (2009), Numerical study of turbulent flow and heat transfer characteristics of nanofluids considering variable properties *International Journal of Thermal Sciences*,48: 290–302.